

ENCLOSURE 6

WCAP-17028-NP Revision 6 "Evaluation of Debris-Loading Head-Loss Tests for AP1000™ Fuel Assemblies During Loss of Coolant Accidents"

Westinghouse Non-Proprietary Class 3

WCAP-17028-NP
APP-MY03-T2C-004
Revision 6

June 2010

Evaluation of Debris-Loading Head-Loss Tests for AP1000™ Fuel Assemblies During Loss of Coolant Accidents



Westinghouse

WCAP-17028-NP
APP-MY03-T2C-004
Revision 6

Evaluation of Debris-Loading Head-Loss Tests for AP1000™ Fuel Assemblies During Loss of Coolant Accidents

K. L. Ruth*
S. L. Baier*
Systems & Equipment Engineering I

T. L. Schulz
Y. J. Song
J. P. Pezze
AP1000 Nuclear Systems Engineering

G. Scaddozzo
Ansaldo Nucleare

W. A. Byers
Materials Center of Excellence

June 2010

Approved: **Timothy D. Croyle, Manager***
Systems & Equipment Engineering I

*Electronically approved records are authenticated in the electronic document management system.

Westinghouse Electric Company LLC
P.O. Box 355
Pittsburgh, PA 15230-0355

©2010 Westinghouse Electric Company LLC
All Rights Reserved

RECORD OF REVISIONS

Revision	Date	Description
0	February 2008	Original
1	July 2009	Revision bars are not included in this document because this revision supersedes the original document in its entirety.
2	September 2009	This revision provides clarification on the licensing basis debris load and limiting case. Identified errors in Tables 4-2, 5-1, 6-3 and 9-1 have been corrected. Revision bars are provided for all changes to this revision.
3	December 2009	<p>This revision contains sixteen FA tests that supplement the information provided in all previous revisions of WCAP-17028-P.</p> <p>This revision confirms the licensing basis for the reasonable assurance of LTCC under core debris loading conditions for the AP1000.</p> <p>This revision supersedes all previous revisions.</p> <p>Executive Summary: Minor editorial revisions</p> <p>Section 1: Minor editorial revisions</p> <p>Section 2: Minor editorial revisions</p> <p>Section 3: Minor editorial revisions</p> <p>Section 4: Minor editorial revisions</p> <p>Section 5: New Section</p> <p>Section 6: Major Revision</p> <p>Section 7: Major Revision</p> <p>Section 8: Major Revision</p> <p>Section 9: Major Revision</p> <p>Section 10: Minor editorial revisions</p> <p>Section 11: Minor editorial revisions</p> <p>Appendix A: No Change</p> <p>Appendix B: No Change</p> <p>Appendix C: Updated</p> <p>Appendix D: New</p> <p>Appendix E: New</p>

RECORD OF REVISIONS (cont.)

Revision	Date	Description
4	February 2010	<p>This revision contains nine new FA tests plus the existing sixteen FA tests from Revision 3 that supplement the information provided in all previous revisions of WCAP-17028-P.</p> <p>This revision confirms the licensing basis for the reasonable assurance of LTCC under debris loading conditions of the AP1000.</p> <p>This revision supersedes all previous revisions.</p> <p>Executive Summary: Minor editorial revisions</p> <p>Section 1: Minor editorial revisions</p> <p>Section 2: Minor editorial revisions</p> <p>Section 3: Minor editorial revisions</p> <p>Section 4: Major Revision</p> <p>Section 5: Major Revision</p> <p>Section 6: Minor Revision</p> <p>Section 7: Major Revision</p> <p>Section 8: Major Revision</p> <p>Section 9: Major Revision</p> <p>Section 10: Minor editorial revisions</p> <p>Section 11: Minor editorial revisions</p> <p>Appendix A: No Change</p> <p>Appendix B: No Change</p> <p>Appendix C: Updated</p> <p>Appendix D: No Change</p> <p>Appendix E: No Change</p> <p>Revision bars are not included in this revision of WCAP-17028-P since changes were excessive.</p>
5	March 2010	<p>The purpose of this revision is to correct editorial discrepancies between WCAP-17028-P Revision 4 and WCAP-17028-NP Revision 4.</p> <p>The technical content in this document has not changed from Revision 4. Revision bars are not included since changes were only editorial and minor.</p>

RECORD OF REVISIONS (cont.)

Revision	Date	Description
6	See EDMS	<p>The purpose of this revision is to address RAI-SRP6 2.2-SPCV-25-P Rev 1 concerning the additional 20 lbm of particulate added to the AP1000 Licensing Basis Debris Load. Note that, Table 6-1 in this Revision is more current than Table 6-1 in RAI-SRP6 2.2-SPCV-25-P Rev 1.</p> <p>The following sections were updated and include revision bars:</p> <p>Section 1</p> <p>Section 4.1, Table 4-2</p> <p>Section 5, 5.1, 5.2 and 5.8</p> <p>Section 6, Table 6-1</p> <p>Section 7, Table 7-4</p> <p>Section 8.37, 8.38, 8.39, 8.39.2, Figure 8-109 and Figure 8-111</p> <p>Section 9.1.3, Section 9.1.7 and Table 9-2</p> <p>All changes made to this document include revision bars except for typographical errors. Typographical errors were acknowledged and corrected.</p>

ACKNOWLEDGEMENTS

The support of the Science and Technology Center technicians Allan Neville, Michael Peck, Robert Rees, and Michael Ruffner is gratefully acknowledged.

TABLE OF CONTENTS

RECORD OF REVISIONS	iii
ACKNOWLEDGEMENTS	vi
LIST OF TABLES	xi
LIST OF FIGURES	xiii
LIST OF ACRONYMS, ABBREVIATIONS, AND TRADEMARKS	xix
EXECUTIVE SUMMARY	xxi
1 BACKGROUND	1-1
2 OBJECTIVE	2-1
3 APPROACH	3-1
4 DESCRIPTION OF EXPERIMENTAL APPARATUS	4-1
4.1 COMPONENTS USED IN HEAD-LOSS TESTING	4-1
4.1.1 Physical Components	4-1
5 ACCEPTANCE CRITERION	5-1
5.1 ACCEPTANCE CRITERIA FOR SEQUENTIAL AND CONCURRENT DEBRIS ADDITIONS FOR COLD-LEG TESTS	5-2
5.1.1 Sequential and Concurrent Debris Additions Acceptance Criteria (First Acceptance Criteria)	5-3
5.1.2 Concurrent Debris Additions Acceptance Criteria (Second Acceptance Criteria)	5-4
5.2 DP/FLOW DEPENDENCE RELATIONSHIP	5-5
6 DEBRIS PREPARATION	6-1
6.1 PARTICULATE	6-1
6.2 FIBERS	6-1
6.3 CHEMICAL PRECIPITATES	6-2
6.4 DEBRIS LOADS	6-2
7 TEST MATRIX AND INITIAL CONDITIONS	7-1
8 TEST RESULTS	8-1
8.1 SUMMARY OF AP1000 FA TESTING	8-1
8.2 TEST #1 (CIBAP01)	8-6
8.3 TEST #2 (CIBAP02)	8-8
8.4 TEST #3 (CIBAP03)	8-10
8.5 TEST #4 (CIBAP04)	8-12
8.6 TEST #5 (CIBAP05)	8-14

TABLE OF CONTENTS (cont.)

8.7	TEST #6 (CIBAP06).....	8-16
8.8	TEST #8 (CIBAP08).....	8-18
8.9	TEST #9 (CIBAP09).....	8-20
8.10	TEST #10 (CIBAP10).....	8-22
8.11	TEST #11 (CIBAP11).....	8-24
8.12	TEST #13 (CIBAP13).....	8-26
8.13	TEST #14 (CIBAP14).....	8-29
8.14	TEST #15 (CIBAP15).....	8-31
8.15	TEST #16 (CIBAP16).....	8-33
8.16	TEST #17 (CIBAP17).....	8-39
8.17	TEST #18 (CIBAP18).....	8-42
8.18	TEST #19 (CIBAP19).....	8-44
8.19	TEST #20 (CIBAP20).....	8-46
8.20	TEST #21 (CIBAP21).....	8-48
8.21	TEST #22 (CIBAP22).....	8-50
8.22	TEST #23 (CIBAP23).....	8-52
8.23	TEST #24 (CIBAP24).....	8-54
	8.23.1 Varying Initial Flow Rates.....	8-55
8.24	TEST #25 (CIBAP25).....	8-61
8.25	TEST #26 (CIBAP26).....	8-63
8.26	TEST #27 (CIBAP27).....	8-65
8.27	TEST #28 (CIBAP28).....	8-72
8.28	TEST #29 (CIBAP29).....	8-74
8.29	TEST #30 (CIBAP30).....	8-76
8.30	TEST #31 (CIBAP31).....	8-82
8.31	TEST #32 (CIBAP32).....	8-84
8.32	TEST #33 (CIBAP33).....	8-86
8.33	TEST #34 (CIBAP34).....	8-88
8.34	TEST #35 (CIBAP35).....	8-93
8.35	TEST #36 (CIBAP36).....	8-95
8.36	TEST #37 (CIBAP37).....	8-100
8.37	TEST #38 (CIBAP38).....	8-102
8.38	TEST #39 (CIBAP39).....	8-110
8.39	PRESSURE DIFFERENTIAL WITH FLOW.....	8-115
	8.39.1 Variation of dP with Variation of Flow and End-of-Test Data.....	8-115
	8.39.2 Bed Stability During Flow Sweeps.....	8-120
	8.39.3 Basis for the Developed Correlation	8-122
8.40	INVALIDATED TESTS	8-132
9	CONCLUSIONS	9-1
9.1	TEST PROGRAM SUMMARY	9-1
	9.1.1 Latent Fiber Length	9-5
	9.1.2 Chemical Addition Rate.....	9-7
	9.1.3 Debris Quantities	9-8

TABLE OF CONTENTS (cont.)

9.1.4	Flow Variations.....	9-10
9.1.5	Debris Addition Sequence	9-11
9.1.6	Coolant Chemistry and Temperature	9-12
9.1.7	Effect of Debris Addition with Different Break Scenarios (Hot-Leg vs. Cold-Leg)	9-14
9.2	APPLICABILITY OF TESTING TO AP1000 DESIGN.....	9-16
10	SUMMARY	10-1
11	REFERENCES	11-1
APPENDIX A	APP-FA01-T1P-001 REVISION 0: TEST PLAN FOR AP1000 DEBRIS LOADING HEAD-LOSS ACROSS FA	A-1
APPENDIX B	APP-FA01-T1P-001 REVISION 1: TEST PLAN FOR AP1000 DEBRIS LOADING HEAD-LOSS ACROSS FA	B-1
APPENDIX C	TEST PROCEDURES FOR AP1000 DEBRIS LOADING HEAD-LOSS ACROSS FA	C-1
APPENDIX D	DEBRIS PREPARATION.....	D-1
APPENDIX E	TEST FACILITY OVERVIEW	E-1

LIST OF TABLES

Table 4-1	Instrumentation for Debris Loading Head-loss Testing	4-8
Table 4-2	AP1000 Licensing Basis Latent Debris Load	4-10
Table 5-1	Values of the Exponent 'b' to be used in Equation (5.1.1)	5-3
Table 5-2	Exponent 'b' Obtained by Best Fit of the Experimental Data from the Tests Performed with Oscillating Flow Rates and Sequential Additions (P/F/C)	5-7
Table 5-3	Exponent 'b' Obtained by Best Fit of the Experimental Data from the Tests Performed with Sequential Debris Additions (P/F/C) from Section 5.1.1	5-7
Table 5-4	Exponent 'b' Obtained by Best Fit of the Experimental Data from the Tests Performed with Coincident Debris Additions from Section 5.1.2	5-7
Table 6-1	Original vs. Current AP1000 Post-LOCA Debris Load Design Basis	6-3
Table 7-1	Initial Conditions of AP1000 FA Head-Loss Tests CIBAP01 through CIBAP10	7-3
Table 7-2	Initial Conditions of AP1000 FA Head-Loss Tests CIBAP11 through CIBAP20	7-4
Table 7-3	Initial Conditions of AP1000 FA Head-Loss Tests CIBAP21 through CIBAP30	7-5
Table 7-4	Initial conditions of AP1000 FA Head-Loss Tests CIBAP31 through CIBAP39	7-6
Table 8-1	Summary of AP1000 Fuel Assemblies Head-Loss Tests	8-3
Table 8-2	Fibrous Debris Mix Used in Test CIBAP11	8-24
Table 8-3	Sensitivity Analysis on the Exponent for Type 2 Tests	8-126
Table 8-4	Probability to Exceed Acceptance Criteria, 95% UB Standard Deviation	8-126
Table 8-5	Test Results and dP Adjusted at 5.3 gpm for Comparison Against the Second Acceptance Criterion	8-130
Table 9-1	AP1000 Fuel Debris Tests Scaled Results	9-2
Table 9-2	Scaled Maximum dP at Flow Prior to 9 Hours for Concurrent Addition Tests	9-4

LIST OF FIGURES

Figure 4-1	Schematic of the Test Loop (Cold-leg Break).....	4-3
Figure 4-2	Schematic of the Test Loop (Hot-Leg Break).....	4-4
Figure 4-3	Schematic of Test Loop (Heated Test).....	4-5
Figure 4-4	Schematic of Test Loop (Boiling Simulation)	4-6
Figure 5-1	Values of the Exponent ‘b’ for the Fully Formed Debris Bed, Estimated in Test CIBAP 08 through CIBAP 11 and CIBAP 18 through CIBAP 34 by a Best Fit of the Experimental Data	5-9
Figure 5-2	Distribution of the Exponent for the Fully Formed Debris Bed Estimated in Test CIBAP 08 through CIBAP 11 and CIBAP 18 through CIBAP 34.....	5-9
Figure 5-3	Coefficient “R” Values for the Fully Formed Debris Bed Estimated in Test CIBAP 08 through CIBAP 11 and CIBAP 18 through CIBAP 34 by a Best Fit of the Experimental Data	5-10
Figure 5-4	Distribution of the Resistance Coefficient for the Fully Formed Debris Bed Estimated in Test CIBAP 08 through CIBAP 11 and CIBAP 18 through CIBAP 34	5-10
Figure 8-1	Head-Loss and Flow Rate History for Test CIBAP01	8-7
Figure 8-2	Head-Loss and Flow Rate History for Test CIBAP02	8-9
Figure 8-3	Head-Loss and Flow Rate History for Test CIBAP03	8-11
Figure 8-4	Head-Loss and Flow Rate History for Test CIBAP04	8-13
Figure 8-5	Head-Loss and Flow Rate History for Test CIBAP05	8-15
Figure 8-6	Head-Loss and Flow Rate History for Test CIBAP06	8-17
Figure 8-7	Head-Loss and Flow Rate History for Test CIBAP08	8-19
Figure 8-8	Head-Loss and Flow Rate History for Test CIBAP09	8-21
Figure 8-9	Head-Loss and Flow Rate History for Test CIBAP10	8-23
Figure 8-10	Head-Loss and Flow Rate History for Test CIBAP11	8-25
Figure 8-11	Head-Loss and Flow Rate History for Test CIBAP13	8-27
Figure 8-12	Concentration of Chemical Debris with Time	8-28
Figure 8-13	Head-Loss and Flow Rate History for Test CIBAP14	8-30
Figure 8-14	Head-Loss and Flow Rate History for Test CIBAP15	8-32
Figure 8-15	Head-Loss and Flow Rate History for Test CIBAP16	8-34
Figure 8-16	Debris Load For Test CIBAP16.....	8-35
Figure 8-17	Clean Assembly For Test CIBAP16.....	8-35

LIST OF FIGURES (cont.)

Figure 8-18	Addition of Particulates for Test CIBAP16	8-36
Figure 8-19	Accumulation of Fiber at Bottom Nozzle and P-Grid for Test CIBAP16	8-36
Figure 8-20	Debris Bed After Chemical Introduction For Test CIBAP16	8-37
Figure 8-21	Debris Bed After the Second Chemical Introduction For Test CIBAP16.....	8-37
Figure 8-22	Debris Bed After The Third Chemical Introduction For Test CIBAP16	8-38
Figure 8-23	Debris Bed After Final Chemical Introduction For Test CIBAP16	8-38
Figure 8-24	Head-Loss and Flow Rate History for Test CIBAP17	8-40
Figure 8-25	Schematic of The Test Loop Configuration For CIBAP17.....	8-41
Figure 8-26	Head-Loss and Flow Rate History for Test CIBAP18	8-43
Figure 8-27	Head-Loss and Flow Rate History for Test CIBAP19	8-45
Figure 8-28	Head-Loss and Flow Rate History for Test CIBAP20	8-47
Figure 8-29	Head-Loss and Flow Rate History for Test CIBAP21	8-49
Figure 8-30	Head-Loss and Flow Rate History for Test CIBAP22	8-51
Figure 8-31	Head-Loss and Flow Rate History for Test CIBAP23	8-53
Figure 8-32	Head-Loss and Flow Rate History for Test CIBAP24	8-55
Figure 8-33	Flow Versus dP During Test CIBAP24	8-56
Figure 8-34	Accumulation of Debris at the Bottom of the P-Grid After Second Concurrent Debris Addition in Test CIBAP24	8-57
Figure 8-35	Accumulation of Debris at the Bottom of the P-Grid After Third Concurrent Debris Addition in Test CIBAP24	8-57
Figure 8-36	Accumulation of Debris at the Bottom of the P-Grid After Fourth Concurrent Debris Addition in Test CIBAP24	8-58
Figure 8-37	Accumulation of Debris Around the Edge of the Bottom Nozzle After Seventh Concurrent Debris Addition in Test CIBAP24.....	8-58
Figure 8-38	Accumulation of Debris in the Middle of the First Grid Above the P-Grid After the Ninth Addition in Test CIBAP24	8-59
Figure 8-39	Accumulation of Debris Around the Bottom of the Second Spacer Grid After the Ninth Addition in Test CIBAP24	8-59
Figure 8-40	Accumulation of Debris Around the Bottom Nozzle and P-Grid at the End of Test CIBAP24 Prior to Flow Sweeps	8-60
Figure 8-41	Head-Loss and Flow Rate History for Test CIBAP25	8-62
Figure 8-42	Head-Loss and Flow Rate History for Test CIBAP26	8-64

LIST OF FIGURES (cont.)

Figure 8-43	Head-Loss and Flow Rate History for Test CIBAP27	8-66
Figure 8-44	Flow Versus dP during Test CIBAP27	8-67
Figure 8-45	Accumulation of Debris Around the Bottom Nozzle and P-Grid after the Third Concurrent Addition in Test CIBAP27	8-67
Figure 8-46	Accumulation of Debris Around the Bottom Nozzle and P-Grid at the Fourth Concurrent Addition in Test CIBAP27.....	8-68
Figure 8-47	Accumulation of Debris Around the Bottom Nozzle and P-Grid at the Fifth Concurrent Addition in Test CIBAP27	8-68
Figure 8-48	Accumulation of Debris Around the Bottom Nozzle and P-Grid 30 Minutes into the Fifth Concurrent Addition in Test CIBAP27	8-69
Figure 8-49	Accumulation of Debris Around the Bottom Nozzle and P-Grid 30 Minutes into the Ninth Chemical Addition in Test CIBAP27.....	8-69
Figure 8-50	Accumulation of Debris Around the Bottom Nozzle and P-Grid at the Time of the Tenth Chemical Addition in Test CIBAP27	8-70
Figure 8-51	Accumulation of Debris Around the Bottom Nozzle and P-Grid 30 Minutes into the Twelfth Chemical Addition in Test CIBAP27.....	8-70
Figure 8-52	Accumulation of Debris Around the Bottom Nozzle and P-Grid 15 Minutes After the Fourteenth Chemical Addition in Test CIBAP27.....	8-71
Figure 8-53	Accumulation of Debris Around the Bottom Nozzle and P-Grid Prior to Flow Sweeps in CIBAP27	8-71
Figure 8-54	Head-Loss and Flow Rate History for Test CIBAP28	8-73
Figure 8-55	Head-Loss and Flow Rate History for Test CIBAP29	8-75
Figure 8-56	Head-Loss and Flow Rate History for Test CIBAP30	8-77
Figure 8-57	Accumulation of Debris at the Bottom Nozzle and P-Grid 30 Minutes After the Third Concurrent Addition in Test CIBAP30	8-78
Figure 8-58	Accumulation of Debris at the Bottom Nozzle and P-Grid 30 Minutes After the Fourth Concurrent Addition in Test CIBAP30.....	8-78
Figure 8-59	Accumulation of Debris at the Bottom Nozzle and P-Grid 30 Minutes After the Fifth Concurrent Addition in Test CIBAP30	8-79
Figure 8-60	Accumulation of Debris at the Bottom Nozzle and P-Grid 30 Minutes After the Ninth Chemical Addition in Test CIBAP30.....	8-79
Figure 8-61	Accumulation of Debris at the Bottom Nozzle and P-Grid 30 Minutes After the Twelfth Chemical Addition in Test CIBAP30	8-80

LIST OF FIGURES (cont.)

Figure 8-62	Accumulation of Debris at the Bottom Nozzle and P-Grid 30 Minutes After the Seventeenth Chemical Addition in Test CIBAP30	8-80
Figure 8-63	Accumulation of Debris at the Bottom Nozzle and P-Grid Near the End of the Flow Sweeps in Test CIBAP30.....	8-81
Figure 8-64	Head-loss and Flow Rate History for Test CIBAP31	8-83
Figure 8-65	Head-loss and Flow Rate History for Test CIBAP32	8-85
Figure 8-66	Head-loss and Flow Rate History for Test CIBAP33	8-87
Figure 8-67	Head-loss and Flow Rate History for Test CIBAP34	8-89
Figure 8-68	Accumulation of Debris at the Bottom Nozzle and P-Grid Right before the Fourth Addition in Test CIBAP34	8-90
Figure 8-69	Accumulation of Debris at the Bottom Nozzle and P-Grid 30 Minutes after the Fourth Concurrent Addition in Test CIBAP34.....	8-90
Figure 8-70	Accumulation of Debris at the Bottom Nozzle and P-Grid 30 Minutes after the Ninth Chemical Addition in Test CIBAP34.....	8-91
Figure 8-71	Accumulation of Debris at the Bottom Nozzle and P-Grid 30 Minutes after the Twelfth Chemical Addition in Test CIBAP34	8-91
Figure 8-72	Accumulation of Debris at the Bottom Nozzle and P-Grid 30 Minutes after the Last Chemical Addition in Test CIBAP34.....	8-92
Figure 8-73	Head-loss and Flow Rate History from Test CIBAP35	8-94
Figure 8-74	Head-loss and Flow Rate History for Test CIBAP36	8-96
Figure 8-75	Accumulation of Debris at the p-grid 30 Minutes after the Third Concurrent Addition in Test CIBAP36.....	8-97
Figure 8-76	Accumulation of Debris at the p-grid 30 Minutes after the Ninth Chemical Addition in Test CIBAP36.....	8-97
Figure 8-77	Accumulation of Debris at the p-grid 30 Minutes after the Fifteenth Chemical Addition in Test CIBAP36.....	8-98
Figure 8-78	Accumulation of Debris at the Third Grid 30 Minutes after Fifteenth Chemical in Test CIBAP36	8-98
Figure 8-79	Accumulation of Debris at the p-grid at the End of the Test CIBAP36	8-99
Figure 8-80	Data Plot from Test CIBAP37 Baseline dP Corrected to Zero	8-101
Figure 8-81	Data Plot from Test CIBAP38 Baseline dP Corrected to Zero	8-103
Figure 8-82	Photograph of the Top-Grid 59 Minutes after the First Concurrent Addition in Test CIBAP38	8-104

LIST OF FIGURES (cont.)

Figure 8-83	Photograph of the Top-Grid after Stable Air and Water Flow are Achieved in Test CIBAP38.....	8-104
Figure 8-84	Photograph of the Top Grid Seconds before Simulating Boiling Began	8-105
Figure 8-85	Photograph of the Top Grid 6 Seconds after Simulated Boiling Began.....	8-105
Figure 8-86	Photograph of the Top Grid 12 Seconds after Simulated Boiling Began.....	8-106
Figure 8-87	Photograph of the Top Grid 19 Seconds after Simulated Boiling Began.....	8-106
Figure 8-88	Photograph of the Top Grid 24 Seconds after Simulated Boiling Began.....	8-107
Figure 8-89	Photograph of a Spacer 51 Minutes after First Addition (SiC) During Up-flow in Test CIBAP38	8-107
Figure 8-90	Photograph of the Top-Grids 51 Minutes after First Addition (SiC) During Up-flow in Test CIBAP38.....	8-108
Figure 8-91	Photograph of the Top-Grid 51 Minutes after First Addition (SiC) During Up-flow in Test CIBAP38.....	8-108
Figure 8-92	Photograph of the p-grid after Flow Sweeps in Test CIBAP38	8-109
Figure 8-93	Data Plot from Test CIBAP39 Baseline dP Corrected to Zero	8-111
Figure 8-94	Photograph of the Spacer Grid 34 Minutes after the First Concurrent Addition in Test CIBAP39	8-112
Figure 8-95	Photograph of the Spacer Grid 34 Minutes after the Second Concurrent Addition in Test CIBAP39	8-112
Figure 8-96	Photograph of the Spacer Grid 30 Minutes during Water and Air Flow Stabilization for 60 Minutes after the Last Chemical Addition	8-113
Figure 8-97	Photograph during Water and Air Flow Stabilization for 60 Minutes after the Last Chemical Addition	8-113
Figure 8-98	Photograph of the Top-Grid during Water and Air Flow Stabilization for 60 Minutes after the Last Chemical Addition	8-114
Figure 8-99	Photograph of the Spacer Grid during the Last Flow Profile in Test CIBAP39	8-114
Figure 8-100	dP Versus Flow For Test CIBAP09.....	8-116
Figure 8-101	dP Versus Flow For Test CIBAP11	8-117
Figure 8-102	dP First and Last Flow Cycle in Test CIBAP 11	8-117
Figure 8-103	dP Versus Flow For Test CIBAP20.....	8-118
Figure 8-104	dP Versus Flow For Test CIBAP21	8-118
Figure 8-105	dP Versus Flow For Test CIBAP25.....	8-119

LIST OF FIGURES (cont.)

Figure 8-106	dP Versus Flow For Test CIBAP26.....	8-119
Figure 8-107	dP Versus Flow For Test CIBAP30.....	8-120
Figure 8-108	dP Versus Flow for Test CIBAP20.....	8-121
Figure 8-109	dP Versus Flow during the First and the Last Part of the Flow Sweeps in Test CIBAP18	8-122
Figure 8-110	Evolution of the dP-Flow Relationship during Test CIBAP 34	8-127
Figure 8-111	Evolution of the Exponent and Coefficient Characterizing the dp-Flow Relationship during Test CIBAP 34.....	8-127
Figure 8-112	Comparison Between the Measured DP and the DP Adjusted at [] ^{a,c} gpm for Test CIBAP 34	8-128
Figure 8-113	Comparison Between the Measured DP And the DP adjusted at [] ^{a,c} gpm for Test CIBAP 30	8-128
Figure 9-1	AP1000 Fuel Debris Tests Scaled Results	9-4
Figure 9-2	Fibers Photographed Near the End of Test CIBAP11	9-6
Figure 9-3	Resident Fibers Collected from Plant B Described in NUREG/CR 6877	9-7
Figure 9-4	Comparison of Tests at [] ^{a,c} with Boric Acid and TSP to Room Temperature Water Tests	9-13
Figure 9-5	AP1000 FA Schematic	9-16

LIST OF ACRONYMS, ABBREVIATIONS, AND TRADEMARKS

ADS	automatic depressurization system
DBA	design basis accident
DCD	design control document
DECL	double-ended cold-leg
dP	differential pressure
DVI	direct vessel injection
ECCS	emergency core cooling system
FA	fuel assembly
IOZ	inorganic zinc
IRWST	in-containment refueling water storage tank
LOCA	loss of coolant accident
LTCC	long-term core cooling
MRI	metal reflective insulation
NRC	United States Nuclear Regulatory Commission
P/F	particulate to fiber ratio
PWR	pressurized water reactor
PXS	passive core cooling system
QMS	Westinghouse Quality Management System
RAI	request for additional information
RCS	reactor coolant system
SCFM	standard cubic feet per minute
SER	safety evaluation report
STC	Westinghouse Science and Technology Center
TSP	trisodium phosphate
ZOI	zone of influence
AP1000™	is a trademark of the Westinghouse Electric Company LLC
NUKON®	is a registered trademark of Performance Contracting, Incorporated
Plexiglas®	is a registered trademark of Arkema, Incorporated

EXECUTIVE SUMMARY

Westinghouse performed a series of experiments to quantify the effect of fibrous and particulate debris and containment chemical reaction products on the head-loss across the fuel assemblies of an AP1000™¹ pressurized water reactor (PWR) during a postulated loss of coolant accident (LOCA). These experiments were conducted in consideration of Generic Safety Issue 191 (GSI-191), "Assessment of Debris Accumulation on PWR Sump Performance" (Reference 1). This report documents the results of the FA head-loss experiments.

The experiments were performed at the Westinghouse Science and Technology Center (STC) in Churchill, PA. The fuel assembly (FA) design used in testing is consistent with the FA design described in subsection 4.2.2.2 of the AP1000 Design Control Document (DCD) (Reference 2). The flow rates and debris loadings and method of debris addition were varied from test to test. The goal of the testing was to select a combination of debris variables and simulated plant variables that would bound any AP1000 LOCA as defined in Reference 2, and to demonstrate that the AP1000 debris load will not impede long-term core cooling (LTCC). At the onset of the program it was not clear which conditions would produce the highest head-losses and so, a spectrum of different flow rates, debris quantities, debris types, methods of debris addition and other experimental variables were explored to ensure that the most challenging conditions were tested. For the cold-leg break scenario, initial flow rates between [

]^{a,c}

All cold-leg break tests produced FA head-losses that were well within the calculated head-loss limit established for the AP1000 in Reference 3. This was true for all combinations of variables. Maximum AP1000 debris loads per assembly [

]^{a,c} The hot-leg break tests showed that if boiling is present in the core as would be expected, the formation of continuous debris beds will be disrupted and pressure drop increases in the upper core due to debris will be []^{a,c}

These experiments demonstrate that the AP1000 design provides for a considerable margin in the cooling analysis of the AP1000, (Reference 3), and has shown that the core will continue to be cooled with a head-loss of 4.1 psid (at a corresponding flow rate of 65.0 lbm/s) across the core for a cold-leg break. The long-term experimental head-loss values were considerably lower than 4.1 psid when flows were corrected to 65 lbm/s. The long-term cooling analysis of the AP1000 (Reference 3 Case #11) has shown that the core will continue to be cooled with a < 2 psid head-loss at the top of the core with a corresponding flow rate of 214.5 lbm/s. The experimental head-losses for the hot-leg break scenario were considerably lower than []^{a,c}

1. AP1000 is a trademark of the Westinghouse Electric Company LLC.

The debris loads in the test program were considerably below the debris loads used in GSI-191 testing for operating plants because debris load for the AP1000 has been significantly reduced by design. This is true for all three types of debris that must be considered in the evaluation of LTCC: fibrous debris, particulate debris, and solids produced by containment chemical reactions. As presented in Reference 2, the AP1000 design is engineered to reduce the potential for head-loss during long-term cooling operation:

- The AP1000 design eliminates the generation of fibrous debris following a LOCA. The small amount of fibrous debris present in the resident debris is assumed to transport to the screens or to the core;
- Resident (latent) debris is the only source of fibers in an AP1000;
- The AP1000 design reduces the generation of post-accident chemical effects debris;
- The good housekeeping practices required by COL item 6.3.8.1 will limit the amount of resident containment debris;
- The AP1000 design has reduced long-term cooling flow rates compared to active emergency core cooling systems (ECCS) of currently operating PWRs;
- The AP1000 design provides for increased time between the accident and the start of recirculation, which together with the reduced long-term cooling flow rates, enhances the settling of debris;
- The AP1000 requires the use of high density epoxy coatings on walls, floors, and structural surfaces as well as on engineered components. The use of high density epoxy coatings together with the other AP1000 features and characteristics prevent failed high density coatings outside the zone of influence (ZOI) from being transported to the screens or core;
- The AP1000 requires signs and tags used inside containment to be made from high density materials, so that if they are detached they will settle out without being transported to the core; and
- The AP1000 incorporates large advanced screen designs.

1 BACKGROUND

Westinghouse has performed a series of FA head-loss experiments for the AP1000 in response to NRC Generic Safety Issue 191 (Reference 1). The purpose of this test program was to quantify the head-loss across the fuel assemblies during a LOCA considering the debris loadings applicable to the AP1000. The debris loadings considered fibrous and particulate debris and containment chemical effects applicable to the AP1000.

The experiments used a FA design that is consistent with the design described in subsection 4.2.2.2 of the AP1000 DCD (Reference 2). The flow rates and debris loading conditions were selected conservatively so that they bound those expected following a postulated LOCA for the AP1000 as defined in Reference 3. Since the fibrous and particulate debris and chemical loadings bound the conditions calculated for a single AP1000 FA, the data collected from this program is applicable to the whole core.

The evaluation of debris-loading head-loss tests for AP1000 fuel assemblies during a LOCA have been presented in all versions of WCAP-17028-P. Each revision of WCAP-17028-P has increased the knowledge base and understanding of the head-loss across fuel assemblies in the post-LOCA AP1000.

WCAP-17028-P, Revision 0 consisted of four initial head-loss tests that were performed in 2008 to obtain data to support resolution of GSI-191 for the AP1000. The results of these tests included what was first considered to be the bounding resident debris load test, a sensitivity resident debris load test with oscillating flow, a “super sensitivity” resident debris load test, and a repeat sensitivity resident debris load test with constant flow rate. All of these tests included chemical products that bounded the chemical debris load calculated for the AP1000. Only in the super-sensitivity test was there a measurable increase in pressure drop across the assembly with the addition of debris. After discussions with the U.S. Nuclear Regulatory Commission (NRC) on the resolution of GSI-191 issues related to the AP1000, Westinghouse concluded that the debris loads assumed in the first four tests were insufficient to satisfy the debris requirements contained in the safety evaluation report (SER) on NEI 04-07 (Reference 4).

WCAP-17028-P, Revision 1 was written to resolve outstanding issues related to the resolution of GSI-191 resulting from the testing reported in WCAP-17028-P, Revision 0. Resident fiber and particulate debris loads were recalculated to be more in line with the debris loads associated with currently operating plants (Reference 5). Chemical effects were recalculated based on the revised debris load and aluminum content in the AP1000 containment (Reference 5). Twelve tests were conducted utilizing revised debris loads and chemical effects. These tests included a broader range of fibrous debris types, several variations in the flow rates, and variation in the method of chemical debris addition. The results of nine of these twelve FA head-loss tests performed for the AP1000 were summarized in WCAP-17028-P, Revision 1.

During a meeting to discuss WCAP-17028-P, Revision 1, the NRC pointed out that the WCAP contained errors: that the results of the three tests that were excluded from WCAP-17028-P, Revision 1 should be included; that clarification on the licensing basis debris load and limiting case was needed; and that the assurance of AP1000 LTCC success would require additional testing to complement and support the work that had been done to date.

In response to the concerns of the NRC regarding the information in WCAP-17028-P, Revision 1, Westinghouse issued WCAP-17028-P, Revision 2 to correct errors, to provide additional clarification on

the licensing basis debris load and limiting case, and to provide the results of the three tests that were excluded from WCAP-17028-P, Revision 1. Additionally, Westinghouse developed a test matrix to address the NRC concerns related to the debris-loading head-loss tests for AP1000 FAs.

Revision 3 of WCAP-17028-P included data from fourteen additional FA debris tests. WCAP-17028-P, Revision 3 was written to demonstrate and confirm the assurance of LTCC under debris loading conditions for the AP1000. The conditions include a spectrum of plant-specific debris characteristics including chemical effects in order to satisfy GSI-191.

WCAP-17028-P, Revision 4 was written to include nine additional FA tests performed to respond to specific requests for additional information (RAIs) issued by the NRC. The nine tests investigated repeatability, the hot-leg break scenario with debris entry at the top of the core with changing flow patterns, the effect of boiling, the effect of elevated temperature, and the effect of the reactor coolant chemicals (trisodium phosphate and boric acid). WCAP-17028-P, Revision 4 presented the results of all 39 FA debris test assembly head-loss experiments and summarizes the results of experiments performed with [

]^{a,c} All of the experiments were performed to demonstrate the margin available in the AP1000 design. The additional nine FA tests are presented in Section 8 of this report.

WCAP-17028-P, Revision 5 was written to include editorial changes. The technical content did not change from WCAP-17028, Revision 4.

WCAP-17028-P, Revision 6 was written to address an additional 20 lbm of particulate to the AP1000 licensing debris load. Table 9-2 has been updated with the correct dP values. Several typographical errors were acknowledged and addressed in this revision.

These head-loss experiments were performed under the Westinghouse Quality Management System (QMS) requirements.

2 OBJECTIVE

This program was designed to demonstrate assurance of LTCC for the AP1000 in accordance with the NRC guidance provided in GSI-191 and Generic Letter 2004-02. All experiments used in demonstration of assured long term cooling are to comply with the Westinghouse QMS. Experiments should bound or be representative of Design Basis Accident (DBA) conditions as specified in Reference 2 for the AP1000.

3 APPROACH

The test loop, described in detail in test procedures attached in Appendix C of this document, consists of a single []^{a,c} FA inside a Plexiglas^{®1} case, a mixing tank, and the pumps and plumbing required to circulate water and debris. The test loop was configured two different ways, one simulating a cold-leg break and another simulating a hot-leg break.

In order, from top to bottom simulating a cold-leg break, the FA contains [

] ^{a,c} The [

] ^{a,c} just as it would in the actual AP1000 design.

In order, from top to bottom simulating a hot-leg break, the FA contains [

] ^{a,c}

The test loop simulated two additional conditions: [] ^{a,c} These tests required additional equipment on the standard FA set up. The [] ^{a,c} test required an additional heater to heat the coolant in the test loop. The simulated [] ^{a,c} test required an air delivery system and an air flow meter that was added to the test loop.

The test loop flow rates were scaled to a [] ^{a,c} to represent the flow rate at the entrance to the [] ^{a,c} for a cold-leg break scenario and a hot-leg break scenario. The selected flow rates are representative of, or bound, the flows that can be expected through the core during the recirculation phase that follows a LOCA.

The debris loadings that were used in the tests were selected and scaled to bound the amount of debris that could be transported to the AP1000 core. The specified debris loadings were tested in the FA test loop located at the Westinghouse STC. The debris loadings included resident fibrous and particulate debris and chemical effects. The fibrous and particulate debris load and chemical precipitates were prepared outside of the test loop and then added to the mixing tank following the test procedures (Appendix C). All of the experiments included fibrous and particulate debris and chemical reaction products that were added to the mixing tank as water suspensions.

¹ Plexiglas[®] is a registered trademark of Arkema, Incorporated.

In prior industry testing programs the manner in which the debris is added was observed to make a difference in the overall head-loss through the FA. Therefore, the following debris additions schemes were used:

- Sequential additions of particulate, fiber, and chemicals
 - For sequential debris addition tests, an aliquot of the water from the mixing tank was removed and placed in a container for each addition of particulate. The particulate was then well mixed into this water until completely suspended before being added to the mixing tank. The mixing tank volume was allowed to []^{a,c}
 - For sequential debris addition tests, the fiber was added following the test plan using a similar technique to that described above for the particulate. []^{a,c}
 - For sequential debris addition tests, surrogates for chemical reaction products were added to the test loop after all of the fiber and particulate had been added. As defined in the test plan, the chemical precipitate was mixed outside the test loop per the WCAP-16530-NP-A (Reference 11) methodology and then added to the test loop in measured batches.
- Concurrent additions of particulate, fiber and chemicals
 - For concurrent debris addition tests, an aliquot of the water from the mixing tank was removed and placed in a container and the prescribed amounts of particulate and fiber were added to the container. The particulate and fiber were then well mixed in this water until completely suspended before being added to the mixing tank. Concurrent with the addition of particulate and fiber, chemical surrogate was added directly to the mixing tank in the amount prescribed in the test procedure. Concurrent debris additions were made at times specified in the test procedure.

These approaches to introducing the debris into the test loop (sequential or concurrent) are consistent with the NRC guidance on head-loss testing issued on March 31, 2008 (Reference 10, Section 6).

“Sequencing the debris for thin bed testing by adding 100 percent of the plant particulate load to the test flume and subsequently adding fibrous debris in incremental batches of an appropriate size is an acceptable method for performing thin bed testing. Depending on the scaling ratios for the test, this procedure may be overly conservative. As an alternative, a series of tests using homogeneous debris addition is also acceptable provided that a sufficient number of tests is performed to provide confidence that the limiting thin bed head-loss has been achieved”.

The tests could be terminated based on either of the following criteria:

- Exceeding the maximum pressure safety limit established for the test facility or
- By meeting the equilibrium criterion determined by calculating the slope in dP across the full FA [

] ^{a,c}

4 DESCRIPTION OF EXPERIMENTAL APPARATUS

A complete description of the test loop used in the conduct of the AP1000 debris loading head-loss testing is included in Section 5 of the test plan provided in Appendix A of this document and will not be repeated in detail here. Summarized in this section are those items considered important to facilitate an overall understanding of the testing process.

4.1 COMPONENTS USED IN HEAD-LOSS TESTING

Physical Components

Figure 4-1 presents the loop layout of the AP1000 debris loading head-loss test facility for a cold-leg break. Figure 4-2 presents the loop layout of the AP1000 debris loading head-loss test facility for a hot-leg break. Figure 4-3 presents the loop layout of the AP1000 debris loading head-loss test facility []^{a,c} Figure 4-4 presents the loop layout of the AP1000 debris loading head-loss test facility []^{a,c} For additional information on the physical arrangement of the test loop, refer to Section 5 of the test plan provided in Appendix A of this document.

The following components were used in the construction of the test loop at the Westinghouse STC:

- Mixing tank system
 - []^{a,c}
- Recirculation system
 - []
 - []
 - []
 - []^{a,c}
- Test column
 - []
 - []
 - []
 - []^{a,c}
- Computer monitoring system

Mixing Tank System

The mixing tank system includes []^{a,c} The mixing tank is where debris is added during a test. The []^{a,c} helps preclude the settling and loss of debris on the bottom of the tank. The recirculating water in the loop flows out of the []^{a,c} of the tank and into the top of the tank. The tank water temperature []^{a,c} The water temperature can be controlled from a low temperature []^{a,c} to a high temperature of []^{a,c}

[]^{a,c} and the temperature of the water is measured continuously in the tank []^{a,c} Mixing of the tank is achieved by the use of a Performance Pro Cascade
pump []^{a,c} at the top
of the tank. []^{a,c}

a.c

Figure 4-1 Schematic of the Test Loop (Cold-leg Break)



Figure 4-2 Schematic of the Test Loop (Hot-Leg Break)

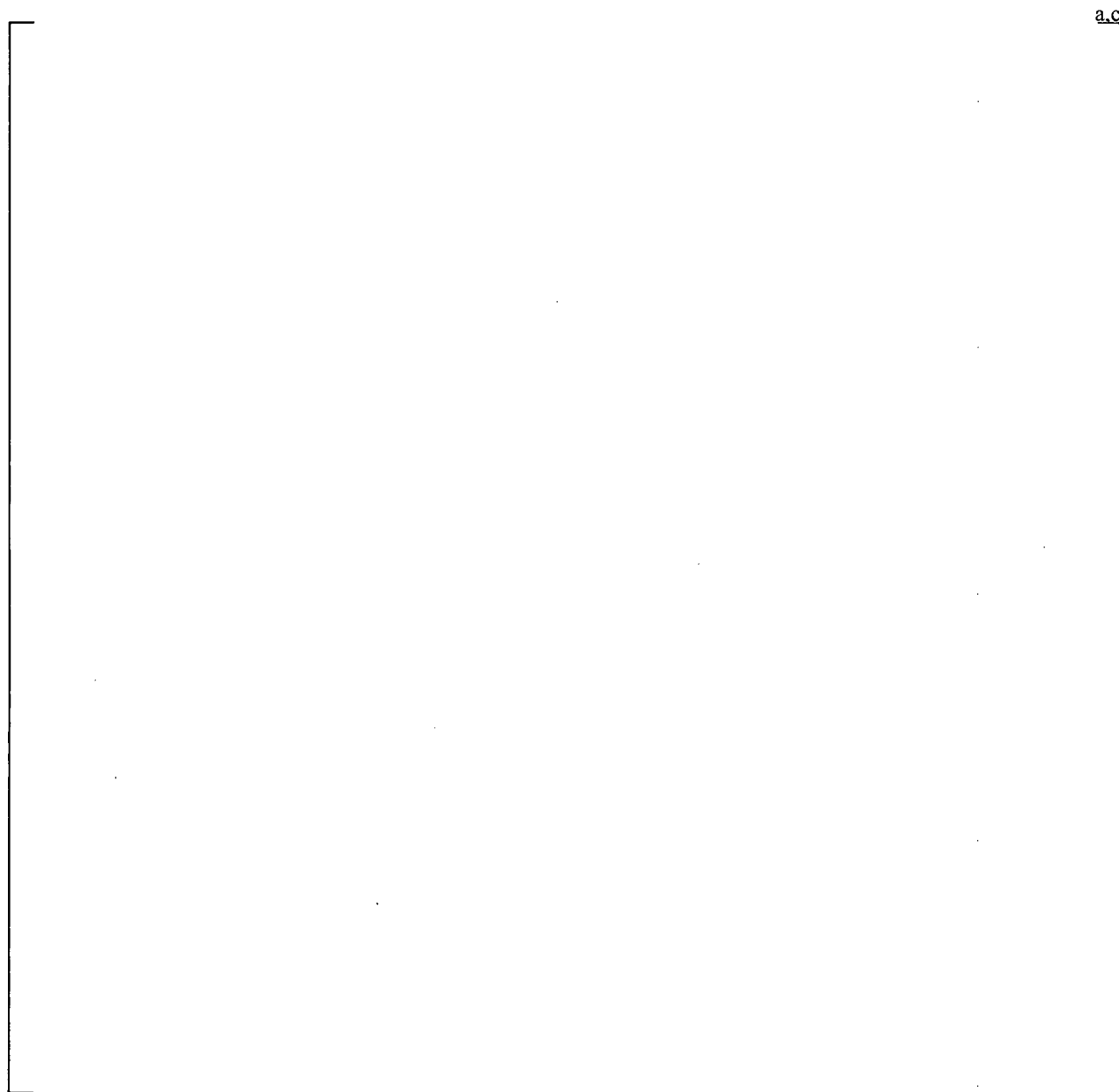


Figure 4-3 Schematic of Test Loop (Heated Test)

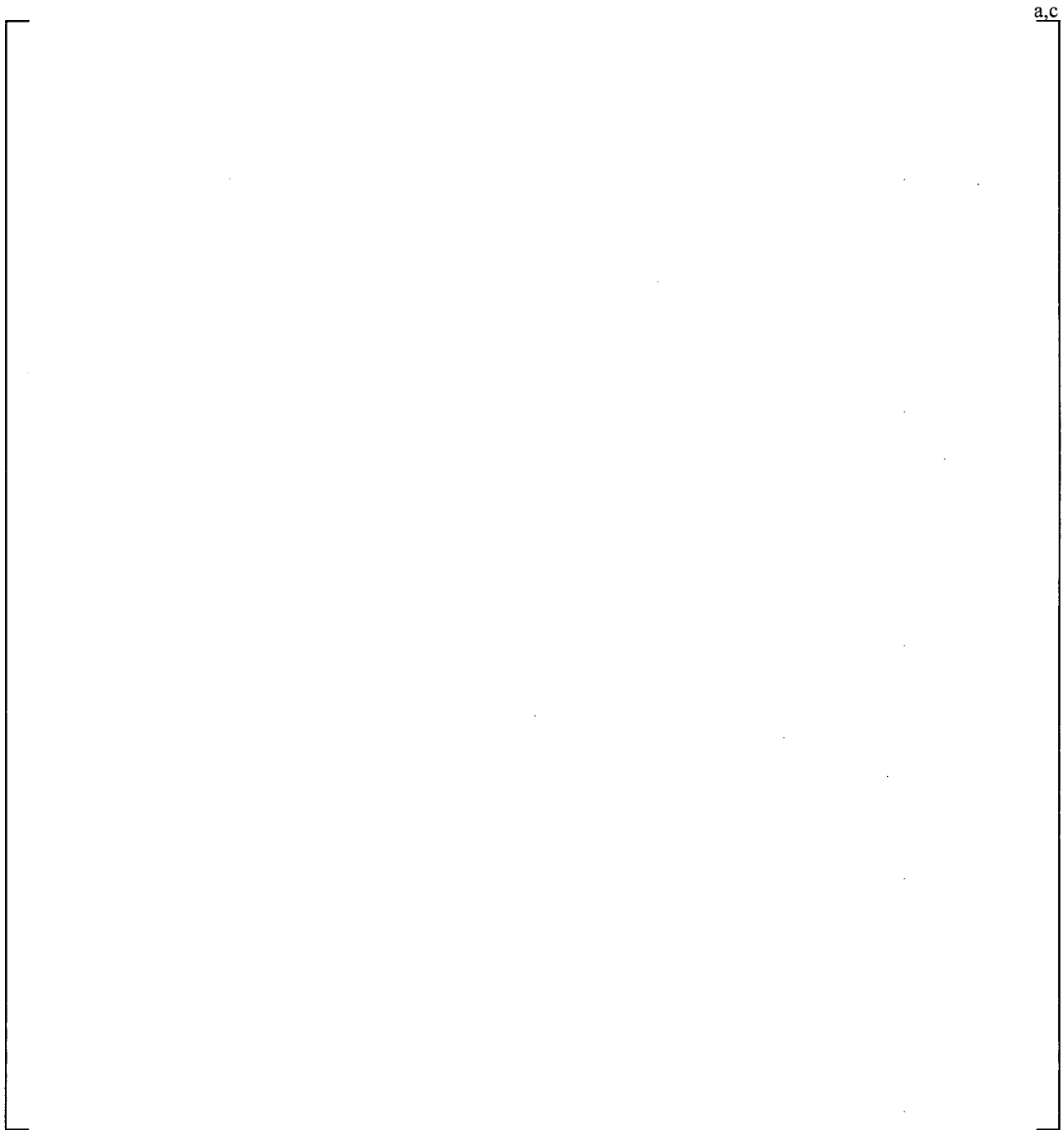


Figure 4-4 Schematic of Test Loop (Boiling Simulation)

Recirculation System

The recirculation system pumps the water from the tank through the test column and back into the tank. A Performance Pro Cascade 3/4 HP pump draws the water out of the bottom of the mixing tank. The flow rate is controlled [

] ^{a,c} regulates the flow rate to maintain that value. For tests that simulate [^{a,c} The recirculation system is in continuous duty to accommodate longer tests.

Test Column

The test column contains the FA and [^{a,c} inside the reactor vessel. Most of the column is made from [^{a,c} to allow easy viewing of what occurs during testing. The test column is made up of two boxes, [^{a,c} These two boxes [

] ^{a,c}
As debris catches on the FA, the dP is measured constantly [

] ^{a,c} At the beginning of the test, the FA is [

] ^{a,c} The FA is held down by [^{a,c} The temperature of the water in the column is measured continuously [^{a,c}

The height of the [

] ^{a,c} of the FA.

Computer Monitoring System

The computer monitoring system continuously records the following data:

- Temperature of the water in the mixing tank
- Temperature of the water in the test column
- Flow rate
- DP (dP) measurements [] ^{a,c}

This data can be recorded at a time interval chosen by the operator. The computer is also used to [

] ^{a,c}

Instrumentation

Table 4-1 gives a listing of instrumentation that was used for the experiments. The following parameters were monitored and recorded during the head-loss experiments:

- Debris sample mass
- Volumetric flow rate
- Loop water temperature
- Loop pressure drop across the bundle

Table 4-1 Instrumentation for Debris Loading Head-loss Testing

a.c.

Note that the test facility ensures that [

] ^{a,c} This conservatively bounds the actual plant conditions because in the event of a LOCA, debris that passes through the FA will be recirculated through sump screens.

An overview of the test facility complete with pictures of debris preparation and test operation is provided in Appendix E. Prior to the start of each experiment, all of the debris planned for introduction into the test loop was prepared according to procedure. The fiber and particulate were weighed out and the chemical precipitate was prepared per WCAP-16530-NP-A procedure (Reference 11). A sample of the chemical

surrogate was tested to assure that the chemical mix met the settling requirements provided in the preparation procedure.

Debris Loads

The AP1000 design minimizes the potential for a LOCA to generate debris that might challenge the core flow path as discussed in References 2 and 5:

- Metal reflective insulation (MRI) is used on components that might be subjected to direct jet impingement loads; MRI is not transported to the AP1000 Containment Recirculation or in-containment refueling water storage tank (IRWST) screens due to the relatively low AP1000 flow rates during recirculation. The AP1000 design prohibits the use of fiberglass within the ZOI and as a result no fibrous debris is generated by the LOCA blowdown. All fiberglass insulation in containment is located outside the ZOI. In addition, any fiberglass insulation used outside the ZOI is jacketed. As a result, AP1000 does not have any LOCA generated fiber debris.
- The AP1000 containment floods up to a higher level. The deeper flood levels significantly reduce the velocities that would occur during recirculation operation, thereby minimizing the potential for debris transport.
- The AP1000 requires the use of high density coatings on walls, floors, and structural surfaces as well as on engineered components. Note that the use of inorganic zinc (IOZ) coatings inside the containment is restricted to the inside surface of the containment shell and to components whose surface temperature exceeds the applicable limit for epoxy coatings. Zinc coatings used inside containment are required to be safety Service Level I to prevent their failure outside the ZOI. All coatings located inside the ZOI are assumed to fail as fines and to transport to the screens or the core.
- The AP1000 requires that signs and tags used inside containment be made from high density materials so that, if they detach, they will settle out without being transported to the screens.
- Protective overhangs prevent heavier debris, including the high density coatings used in the AP1000, from falling onto or just in front of the containment recirculation screens and from being transported to them.
- The containment recirculation screens are large with a complex geometry in order to accommodate collected debris without impacting core flow.
- The AP1000 has several features that significantly reduce the amount of materials that could contribute to the formation of chemical precipitates. The excore detectors are enclosed in stainless steel or titanium preventing circulation of post-accident water past the aluminum detectors. The containment uses a structural steel modular construction which reduces the amount of concrete that can come in contact with post-accident water. This design minimizes the production of calcium phosphate by chemical reactions between the buffer agent, trisodium phosphate (TSP) and concrete post-accident. All concrete surfaces are coated with epoxy.

The AP1000 licensing basis fibrous, particulate, and chemical debris loads that could be transported into the reactor vessel and possibly reach the fuel assemblies, are presented in Table 4-2. These debris loads are based on a total debris load of 200 pounds and a chemical debris load of 57 pounds (Reference 5). Of the 200 pounds of debris, no more than 6.6 pounds may be fiber. The chemical debris load is based on the type and quantity of chemical precipitates which may form in the post-LOCA recirculation fluid for the AP1000 design as reported in Reference 5. It is conservatively assumed that 90% of the fiber, 100% of the particulate, and 100% of the chemical debris is transported to the core in the licensing basis scenario for a cold-leg break case.

Totals in Containment, Particulate	193.4 lb (78.65 kg)
Fiber	6.6 lb (2.99 kg)
Chemical	57.0 lb (25.85 kg)
Transported to Core, Particulate (100%)	193.4 lb (78.65 kg)
Fiber (90%)	5.94 lb (2.69 kg)
Chemical (100%)	57.0 lb (25.85 kg)

Scaling Considerations

A scaling rationale was used to determine the parameters for [

The test fixture []^{a,c} simulated FA with the []^{a,c}

The cross-section of the FA has an []^{a,c} The AP1000 has []^{a,c} The scale factor is

the ratio of the []^{a,c}

- For determining the mass concentration of debris in the plant, the test facility water mass and the AP1000 recirculation mass were used.

$$\left[\begin{array}{c} \vdots \\ \vdots \\ \vdots \end{array} \right]_{a,c}$$

Section 4.2 of Reference 9 (attached in Appendix A of this document) presents additional discussion of scaling considerations used in the FA debris head-loss experiments.

5 ACCEPTANCE CRITERION

The AP1000 safety related systems are designed to indefinitely provide cooling to the reactor core following a LOCA. After the initial injection of water from the core makeup tanks and the accumulators, the reactor coolant system (RCS) is almost depressurized, and water is injected by gravity drain from the IRWST. After the IRWST level drops below a specified setpoint, containment recirculation valves are opened to provide a supply of water for the RCS (Reference 5).

In this recirculation phase, natural circulation provides the driving force; water flowing through the core cooling the fuel bundles is discharged from the stage 4 of the automatic depressurization system (ADS) in the containment as a two phase mixture of steam and water. The steam released from the ADS valves is condensed on the steel surface of the containment vessel, which is cooled on the outside by the passive containment cooling system. The condensed water drains by gravity into a gutter and is then returned to the IRWST for injection into the RCS through the direct vessel injection (DVI) lines. The liquid water flooding the containment is returned to the RCS by the passive safety systems (PXS) containment recirculation screen and piping. However, due to the high flood-up level of the AP1000 design, water could bypass the recirculation screens and enter directly into the reactor vessel as in the case located below the flood level (Reference 5).

With maximum bypass flow, the debris present in the containment may be transported directly into the RCS and eventually into the core. If a debris bed forms across the core, the resulting additional resistance may reduce the core flow rate. In order to assess the impact of additional resistance to flow at the core inlet, a LTCC analysis was performed to determine the minimum flow/maximum dP (dP^1) across the core (Reference 3).

Because of the large volume of water that floods the containment and the relatively slow recirculation flow rate, it will take many hours for the debris to be transported into the RCS. Reference 5 provides an evaluation of the test results from this report that demonstrates that the maximum dP occurs well after [

]^{a,c} This analysis (Reference 3, Case 10) found that for a cold-leg-break, the limiting dP through the core is 4.1 psid with a corresponding minimum flow rate of 65.0 lbm/s (480.7 gpm core flow rate).

Using the scale factor discussed in Section 4.1 and the minimum flow rate of 480.7 gpm for a cold-leg break, the corresponding minimum flow rate for the tests is []^{a,c} The acceptance criterion for the FA tests is that the dP across the FA test article must not exceed 4.1 psid at a flow rate of []^{a,c} This acceptance criterion of 4.1 psid at a flow rate of []^{a,c} will be applied to each of the cold-leg break FA tests.

In the event of a hot-leg break LOCA in an AP1000 the flow in the upper part of the core is expected to oscillate. When the down-flow in a low-power assembly becomes low, steam generation rises. The production of steam, together with other thermal hydraulic forces acting on the system, would result in a change in flow direction from the downward to the upward direction.

1. Note that DP, dP, and ΔP may be used to express the dP in this document.

A second acceptance criterion was developed for the concurrent debris addition tests were performed. The second criterion was based on sensitivity Case 3 in the LTCC analysis (Reference 3). The maximum dP allowed in the core at the beginning of the recirculation phase was 3.5 psid with a flow rate of []^{a,c}

For a hot-leg break, the long-term analysis (Reference 3, Case 11), found that the limiting dP through the core is 2 psid with a corresponding minimum flow rate of 214.5 lbm/s (1602 gpm core flow rate). This is the minimum flow rate that can maintain LTCC. Using the scale factor discussed in Section 4.1 and the minimum flow rate of 1602 gpm for a hot-leg break, the corresponding minimum flow rate for the tests is []^{a,c}. The quality of the flow discharged through the ADS-4 flow paths is approximately 0.10. This was taken into consideration for the corresponding minimum liquid flow rate value. The acceptance criterion for the hot-leg break FA tests is that the dP across the FA test article must not exceed 2 psid at a flow rate of []^{a,c}. This acceptance criterion of 2 psid at a flow rate of []^{a,c} will be applied to each of the hot-leg break FA tests.

5.1 ACCEPTANCE CRITERIA FOR SEQUENTIAL AND CONCURRENT DEBRIS ADDITIONS FOR COLD-LEG TESTS

As seen in Table 8-1, many cold-leg tests were performed with a constant flow rate higher than []^{a,c}

To adjust the experimental results to a lower flow rate, the following correlation was adopted:

$$\left[\frac{\text{dP}_{\text{core}}}{\text{dP}_{\text{core}}^{\text{a,c}}} \right] = \left(\frac{\text{Flow Rate}}{\text{Flow Rate}^{\text{a,c}}} \right)^n \quad \text{Equation (5.1.1)}$$

where:

$$\left[\frac{\text{dP}_{\text{core}}}{\text{dP}_{\text{core}}^{\text{a,c}}} \right] = \left(\frac{\text{Flow Rate}}{\text{Flow Rate}^{\text{a,c}}} \right)^n$$

Herein the following the correlation is adopted for the two acceptance criteria. Its applicability is separately discussed and justified in Section 8.39.3.

5.1.1 Sequential and Concurrent Debris Additions Acceptance Criteria (First Acceptance Criterion)

As previously shown, many cold-leg tests were performed with a constant flow rate higher than [

]^{a,c} by means of equation (5.1.1). The equation becomes:

$$\left[\frac{\Delta P}{\rho \cdot V^2} \right]^{a,c} = \frac{K}{V^b} \quad (\text{Eq. 5.1.2})$$

Where:

$$\left[\frac{\Delta P}{\rho \cdot V^2} \right]^{a,c} = \frac{K}{V^b}$$

Eq. (5.1.2) makes use of the experimental exponents deduced by the flow sweep at the end of the tests. Moreover, the stability of the debris bed was assumed. In order to compare the results against the first acceptance criteria []^{a,c} the results obtained by the AP1000 FA tests are adjusted by eq. (5.1.2) to determine the DP at the acceptance criterion flow rate.

The peak dP measured during the test did not occur in all the tests when the debris bed was at the maximum resistance. This relationship is discussed in Section 5.2 and the basis for this correlation is provided in Section 8.39. This relationship is applied to both sequential debris addition and concurrent debris additions, since this pressure drop represents the largest core head-loss modeled.

Table 5-1 below shows the values of exponent 'b' which applies to both sequential debris addition and concurrent debris additions. CIBAP35, CIBAP38 and CIBAP39 are exempt since they are hot-leg tests.

Table 5-1 Values of the Exponent 'b' to be used in Equation (5.1.1)					

Table 5-1 Values of the Exponent 'b' to be used in Equation (5.1.1) (cont.)						a,c

For example, test CIBAP23 used sequential debris addition and was performed between [

[]^{a,c}]^{a,c}

Therefore, []^{a,c}

5.1.2 Concurrent Debris Additions Acceptance Criteria (Second Acceptance Criterion)

As previously described, a second acceptance criterion was established for tests where concurrent additions of debris were performed. The second criterion was based on sensitivity Case 3 in the LTCC analysis (Reference 3). In this case the max dP allowed in the core at the beginning of the recirculation phase was 3.5 psi with a flow rate of []^{a,c}. The concurrent debris addition FA tests were set up to model the plant timing of debris addition after the start of recirculation. In contrast, the sequential debris addition tests were set up to determine the maximum dP value that would be achieved under the test condition; therefore this acceptance criteria was not applicable for sequential debris addition tests. The second criterion applied to time less than 9 hours (plant time). As summarized in Table 9-2, for all concurrent addition tests the flow prior to 9 hours was higher than []^{a,c}. In order to compare the test results against the second criterion, the experimental results were adjusted to []^{a,c} by means of eq. (5.1.1), that became:

[]^{a,c}

(Eq. 5.1.3)

where:

a,c

$$\left[\right]$$

The exponent used in the correlation was reduced by the factor []^{a,c}. The basis for this reduction factor is given in Section 8.39.3. An example of the application of this process is provided below.

Test CIBAP22 had the highest resistance in the debris bed [

]^{a,c} Using the data from CIBAP22, the dP at 5.3 gpm is

then:

a,c

$$\left[\right]$$

In this case, [

]^{a,c}

5.2 DP/FLOW DEPENDENCE RELATIONSHIP

This section presents the method used to relate the change in dP across the fuel bundle to the change in flow for the AP1000 FA head-loss test program. All AP1000 cold-leg break fuel tests performed to date were considered. The results obtained from these tests provided an experimental basis to investigate the dependence of the loss of pressure through the FA from the flow rate once the debris bed was formed. Tests CIBAP08 through CIBAP11 were performed with oscillating flow rates in order to simulate the LTCC behavior of the AP1000 (Reference 3). Tests CIBAP18 through CIBAP34, plus CIBAP36 and CIBAP37 were performed with flow sweeps after all the termination criteria were met.

The data collected by the tests demonstrates that as the head-loss and the flow rate are related by the following equation, which is based on the Darcy formula, except that the exponent is determined by test results:

$$\left[\right]^{\text{a,c}} \quad (\text{Eq. 5.2.1})$$

where:

$$\left[\frac{\Delta P}{L} \right]^{a,c}$$

When the debris bed is formed and stable, the pressure drop behavior of the debris bed will vary consistently with flow rate. Therefore, $\left[\frac{\Delta P}{L} \right]^{a,c}$ Once the value of $\left[\frac{\Delta P}{L} \right]^{a,c}$ it is possible to evaluate the value of the loss of pressure at any flow rate.

$$\left[\frac{\Delta P}{L} \right]^{a,c} \quad (Eq 5.2.2)$$

And then

$$\left[\frac{\Delta P}{L} \right]^{a,c} \quad (Eq5.2.3)$$

where:

$$\left[\frac{\Delta P}{L} \right]^{a,c}$$

Eq. 5.1.1 above has been used to verify that the AP1000 FA head-loss tests meet the acceptance criteria established above. The applicability of the former correlation is justified in Section 8.39.3 for the two acceptance criterion.

The exponent b has been evaluated for each test by best fit of the experimental data and the results are summarized in the following tables:

Table 5-2 Exponent 'b' Obtained by Best Fit of the Experimental Data from the Tests Performed with Oscillating Flow Rates and Sequential Additions of Particulate, Fiber and Chemical (P/F/C)	

a,c

Table 5-3 Exponent 'b' Obtained by Best Fit of the Experimental Data from the Tests Performed with Sequential Debris Additions (P/F/C) from Section 5.1.1	

a,c

Table 5-4 Exponent 'b' Obtained by Best Fit of the Experimental Data from the Tests Performed with Concurrent Debris Additions from Section 5.1.2	

a,c

Table 5-4 (cont.)	Exponent 'b' Obtained by Best Fit of the Experimental Data from the Tests Performed with Coincident Debris Additions from Section 5.1.2

a,c

Several tests in the AP 1000 FA test program were performed with a []^{a,c} and therefore, no data is available to determine the []^{a,c}. These tests used an []^{a,c}.

Figure 5-1 shows the exponents for a fully formed debris bed estimated in the tests where the flow sweeps were performed. The values are divided into three series representing the exponents obtained for []

] ^{a,c}

Several test parameters were different among those tests (e.g., []^{a,c} etc.) The exponent values were in the range []^{a,c}. The range of variability was []^{a,c} for the three series, and in spite of the sample, the values seem to be consistent with []^{a,c} (Figure 5-2). The exponent relevant to the fully formed bed was []^{a,c}. The exponent was []^{a,c}. The coefficient R (as well as its variability) is related to []^{a,c} and how the []^{a,c} (Figure 5-3). The distribution of the resistance coefficient for the same sample was []^{a,c} (see Figure 5-4).

The []^{a,c} was acceptable for the tests performed with constant flow rate for which no data is available to determine []^{a,c}. Therefore, []^{a,c}.



Figure 5-1 Values of the Exponent 'b' for the Fully Formed Debris Bed, Estimated in Test CIBAP 08 through CIBAP 11 and CIBAP 18 through CIBAP 34 by a Best Fit of the Experimental Data



Figure 5-2 Distribution of the Exponent for the Fully Formed Debris Bed Estimated in Test CIBAP 08 through CIBAP 11 and CIBAP 18 through CIBAP 34



Figure 5-3 Coefficient “R” Values for the Fully Formed Debris Bed Estimated in Test CIBAP 08 through CIBAP 11 and CIBAP 18 through CIBAP 34 by a Best Fit of the Experimental Data



Figure 5-4 Distribution of the Resistance Coefficient for the Fully Formed Debris Bed Estimated in Test CIBAP 08 through CIBAP 11 and CIBAP 18 through CIBAP 34

6 DEBRIS PREPARATION

Debris preparation is an important factor in the justification of the applicability of these FA tests to the AP1000. The following subsections describe the preparation of the debris used in the AP1000 FA head-loss experiments. In-depth information on the debris used in the AP1000 FA head-loss experiments is available in Appendix D.

6.1 PARTICULATE

Silicon carbide (SiC) with a 9.5-micron median particle size was used to simulate the particulate component of the containment debris. The NRC Safety Evaluation for NEI 04-07 identified several features for the particulate component of containment debris: the recommended specific gravity is 1.5 and "... the major contributors to the head-loss are the increasing smaller particles (less than 75 μm) . . ." (Reference 4). Silicon carbide has a specific gravity of about 3.2; although these particles have a relatively high specific gravity, the test loop design prevents them from settling out. Because these silicon carbide particles are about 9.5-microns in size, they act as a fine particulate debris that collects within a fiber bed and results in a maximum head-loss across the recirculation screen (see Reference 4). All particulate material is well mixed into an aliquot of loop water until completely suspended before being introduced in the test. Based on the above, the particulate used in the experiments is applicable to AP1000.

6.2 FIBERS

NUREG/CR-6877, Reference 12, indicates that fiberglass can be used as surrogate for latent fibers. It goes on to say that for latent debris, "the fibrous surrogate fraction should be prepared such that the length-to-diameter ratio is large and that it is conservative to assume that the latent fiber component has similar hydraulic properties to those of fiberglass."

As presented in Appendix D, [

]^{a,c} Based on the above, the fibers used in the experiments are applicable to AP1000.

Fiber types that were used in the AP1000 FA head-loss test program include:

Fiber A: [

]^{a,c}

1. NUKON[®] is a registered trademark of Performance Contracting, Incorporated.

Fiber B: [

] ^{a,c}

Fiber C: [

] ^{a,c}

Fiber D: [

] ^{a,c}

Fiber E: [

] ^{a,c}

Fiber F: [

] ^{a,c}

6.3 CHEMICAL PRECIPITATES

For the AP1000 FA test program, all chemical surrogate was made outside of the loop according to the approved procedure at the maximum allowable concentration of eleven grams per liter. Each batch was tested for settling properties according to the approved procedure in WCAP-16530-NP-A (Reference 11) prior to introduction into the test loop. The batches of chemical debris were added to the test loop at various rates, depending on the requirements of the particular test.

By following the approved method (Reference 6) of producing chemical surrogate and by following the guidance of Reference 10, the chemical surrogate used in the AP1000 FA head-loss tests is applicable to the AP1000 plant.

6.4 DEBRIS LOADS

Table 6-1 provides an overview of the AP1000 post-LOCA design basis debris loads and the debris loads assumed in the AP1000 FA head-loss test program (Reference 5) and ZOI coatings debris per TR26.

Table 6-1 Original vs. Current AP1000 Post-LOCA Debris Load Design Basis			

a,c

7 TEST MATRIX AND INITIAL CONDITIONS

The test matrix was designed to improve the knowledge base of the behavior of the AP1000 design when debris is transported to the core. Sensitivity tests were performed to better understand the influence of several parameters such as the [

] ^{a,c} Tests were performed at constant, oscillating, and variable flow rates. For instance, tests CIBAP01, and CIBAP03 through CIBAP07, CIBAP13 through CIBAP16 and CIBAP39 were performed at a constant flow rate. CIBAP02 and CIBAP08 through CIBAP12 were performed with oscillating flow rates. Tests CIBAP17 through CIBAP34, CIBAP36 and CIBAP 37 were performed with variable (decreasing) flow rates. Tests CIBAP35 and CIBAP38 were performed with a variable flow rate then switched to a constant flow rate.

Tests CIBAP01 through CIBAP21 and test CIBAP23 were performed using sequential additions of particles, then fibers, then chemical surrogate. Tests CIBAP22, and tests CIBAP24 through CIBAP39 were performed with concurrent additions of particles, fibers, and chemical surrogate.

The initial conditions and test parameters of the AP1000 FA head-loss experiments CIBAP01 through CIBAP39 are thoroughly covered in the test procedures presented in Appendix C of this document and are summarized in, Table 7-1 through Table 7-4 below.

For constant flow rate tests, the flow rate used was [

] ^{a,c}

For test CIBAP01 through CIBAP15, the flow rate was based on the DCD base case; in this case the plant flow rate was [

] ^{a,c}

was a conservative round-up of this value.

For test CIBAP16, the flow rate was based on the core flow rate of an LTCC sensitivity analysis, Case 3 of Reference 3, having a total [

] ^{a,c} This case assumes debris dP on the core and screens which reduces the flow rates. The flow rate for test CIBAP16 was [] ^{a,c} This minimum flow rate was also applied to tests CIBAP17 through CIBAP28. In these cases the flow started at higher rates and was reduced as the dP increased.

Sensitivity Case 10 of Reference 3 reports a total injection flow of about 65 lb/s. This Case is the one on which the acceptance criterion was based for a cold-leg break condition, as reported in Section 5.0. This flow rate, scaled to the test, is [

] ^{a,c}

According to the AP1000 Long-term Cooling analysis, Reference 3, in the case of a DVI break located at the reactor vessel, the maximum flow rate [] ^{a,c} Note that

this analysis assumed no dP, so this flow represents a high initial flow. Scaling this flow rate to []^{a,c}

Additionally, the analysis on the double-ended cold-leg guillotine break indicates a maximum core inlet flow rate of about []^{a,c}. In terms of gallons per minute, the flow is []^{a,c}. Scaling this flow rate to one FA results in []^{a,c}.

The maximum flow rate for the cold-leg break tests was selected at []^{a,c}. It should be noted that for the previously discussed cases, the maximum flow rate refers to a clean condition in the FA (no debris). This value was used as starting flow rate during some of the variable flow rate tests. In these tests the flow was reduced as the dP caused by the buildup of debris increased, which simulates the behavior of the plant.

Note that Reference 3 has been updated to include additional sensitivity analysis cases with even higher core flow resistances for a hot-leg break condition. Sensitivity Case 11 reports a total injection flow of 214 lbm/s. This is the case on which the acceptance criterion is based on for a hot-leg break condition, as reported in Section 5.0. This flow rate, scaled to the test, is []^{a,c}.

The maximum flow rate that the loop can handle for the hot-leg break tests was selected at []^{a,c}. According to the AP1000 LTCC analysis, Reference 3, in the case of a double-ended cold-leg (DECL) LOCA located at the reactor vessel, the maximum flow rate through 36 FA (all the outer edge FA) in the core is about 214 lb/s, (1598 gpm). Note that this analysis assumed no dP, so this flow represents a maximum initial flow during a hot-leg case flowing through the downcomer. Scaling this flow rate to []^{a,c}. This flow rate refers to a clean condition in the FA. This value was used as starting downward flow rate for hot-leg break tests CIBAP35 and CIBAP38.

[

] ^{a,c}

The initial loop temperature is set to []^{a,c} for all tests except []^{a,c}.

Table 7-1 Initial Conditions of AP1000 Fuel Assembly Head-Loss Tests CIBAP01 through CIBAP10

[illegible]

a,c

Table 7-2 Initial Conditions of AP1000 Fuel Assembly Head-Loss Tests CIBAP11 through CIBAP20

[illegible]

a,c

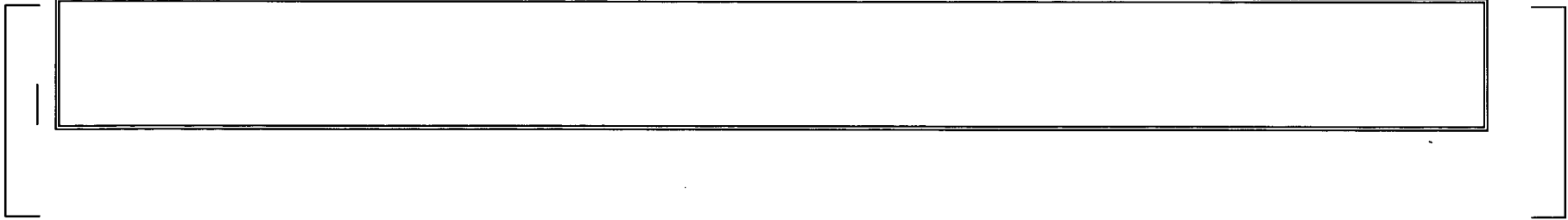
a,c

[illegible]

Table 7-4 Initial conditions of AP1000 Fuel Assembly Head-Loss Tests CIBAP31 through CIBAP39

[illegible]

a,c



a,c

8 TEST RESULTS

8.1 SUMMARY OF AP1000 FUEL ASSEMBLY TESTING

All of the AP1000 FA head-loss tests performed to date are presented in this section. Each of the tests performed in this program considered a debris load of particulate, fiber, and chemicals in various quantities that were intended to be representative of the AP1000 debris load. Each test had specific acceptance and termination criteria based on dP and steady state conditions. Each test was allowed to run to its termination so that the relationship between debris load and FA dP could be presented. As each test was performed, the body of information related to the accumulation of debris on an AP1000 FA was increased.

The following thirty-nine experiments were performed to investigate a spectrum of resident debris loads and chemical effects. The data from all of the experiments, [

] ^{a,c} showed acceptable head-loss across the AP1000 FA.

The results from this test program demonstrate the ability of the AP1000 design to provide assurance of LTCC debris loading conditions expected for the AP1000 following a postulated LOCA. These experiments demonstrate that with the expected AP1000 debris loading conditions, LTCC is assured. Head-losses due to the collection of debris within the fuel assemblies will not challenge either LTCC or the maintaining of a coolable core geometry.

Data from the results of these experiments demonstrate that the design basis debris load that could exist in an AP1000 containment resulted in an FA head-loss that was well within the calculated head-loss limit established for the AP1000 in Reference 3 as defined in Section 5 of this document.

Test runs CIBAP01 through CIBAP04 were initially presented in WCAP-17028-P, Revision 0 and detailed in the Reference 7 test report. Test runs CIBAP05 through CIBAP16 were initially presented in WCAP-17028-P, Revision 1 and detailed in the Reference 8 and 14 test reports. Tests CIBAP07, CIBAP12, and CIBAP15, excluded from WCAP-17028-P, Revision 1, were presented and discussed in WCAP-17028-P, Revision 2. Test runs CIBAP17 through CIBAP30 were included along with the aforementioned tests in WCAP-17029-P, Revision 3 and detailed in the Reference 14 test report. Test runs CIBAP31 through CIBAP39 were included along with the aforementioned tests in this revision and detailed in the Reference 15 test report. Reference 21 documents the data collected during the fuel assembly tests which provided analysis in Section 5 and Section 8.39.

The test reports, References 7, 8, 13, 14 and 15, provide a detailed record of test runs, debris loadings, flow rates, and procedures used to perform these tests. Table 8-1 provides a summary of the debris loads and test results for the 'Evaluation of Debris Loading Head-loss Tests for AP1000 Fuel Assemblies During Loss of Coolant Accidents.'

As described in Appendix E, the same facility and test apparatus configuration was used for each of the AP1000 FA head-loss tests (one noted exception is Test CIBAP17, see Section 8.16). Detailed photographic coverage is provided for tests CIBAP16 (sequential additions), CIBAP24 (concurrent

additions), CIBAP27 (concurrent additions), CIBAP30 (concurrent additions), CIBAP34 (concurrent additions exploring flow patterns), CIBAP36 (concurrent additions simulating hot temperature and reactor coolants), CIBAP38 (concurrent and sequential additions simulating downward flow switched over to upward flow simulating boiling for a hot-leg break) and CIBAP39 (concurrent and sequential additions simulating the upward flow and boiling for a hot-leg break) that follows the progression of debris accumulation on the FA.

Tests CIBAP07, CIBAP12, CIBAP17, and CIBAP 35 are discussed in Section 8.40.

Table 8-1 Summary of AP1000 Fuel Assemblies Head-Loss Tests

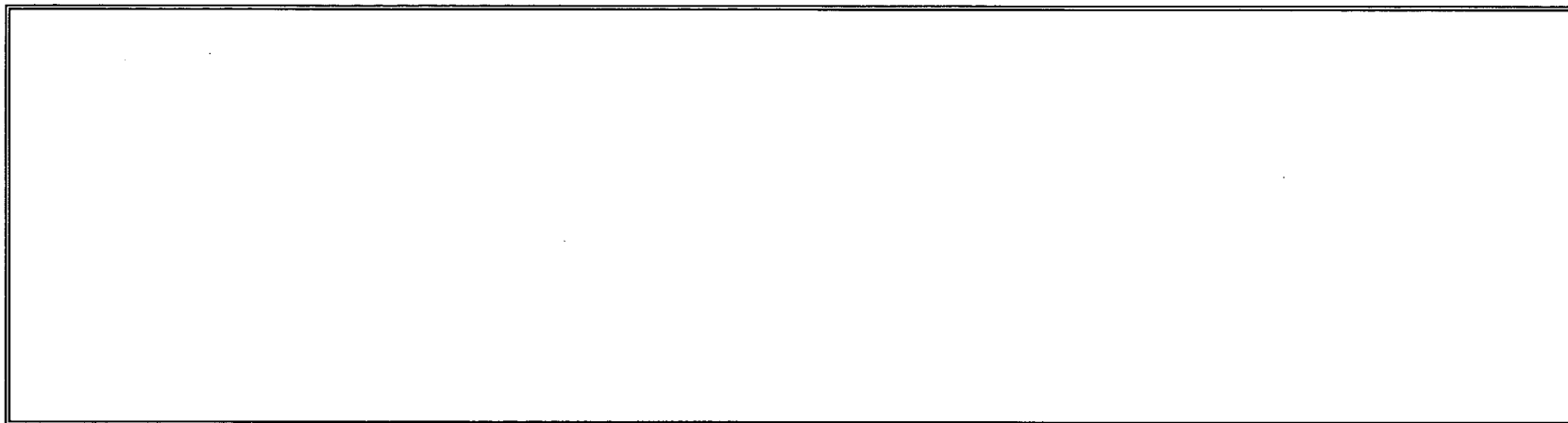
[illegible]

a,c

Table 8-1 Summary of AP1000 Fuel Assemblies Head-Loss Tests (cont.)

[illegible]

a,c



a,c

8.2 TEST #1 (CIBAP01)

This was the first of the AP1000 FA debris loading head-loss experiments performed in the STC test facility for the AP1000. [

] ^{a,c} This experiment was performed according to the test plan STD-MCE-08-79 presented in Appendix C of this document.

As described in test procedure STD-MCE-08-79, [

] ^{a,c}

Figure 8-1 provides the head-loss and flow rate history for test CIBAP01.

a.c

Figure 8-1 Head-Loss and Flow Rate History for Test CIBAP01

8.3 TEST #2 (CIBAP02)

This was the second of the AP1000 FA debris loading head-loss experiments performed in the STC test facility for the AP1000. [

] ^{a,c} This experiment was performed according to the test plan STD-MCE-08-80 presented in Appendix C of this document.

Test #2 was a sensitivity experiment with an increased debris loading as compared to Test #1. [

] ^{a,c}

Following test procedure STD-MCE-08-80, [

] ^{a,c}

Similar to the results of Test #1, the amount of debris that was introduced into the test loop [

] ^{a,c}

a,c

Figure 8-2 Head-Loss and Flow Rate History for Test CIBAP02

8.4 TEST #3 (CIBAP03)

This was the third of the AP1000 FA debris loading head-loss experiments performed in the STC test facility for the AP1000. [

] ^{a,c} This experiment was performed according to the test plan STD-MCE-08-81 presented in Appendix C of this document.

Test #3 was a sensitivity experiment with an increased debris loading as compared to Tests #1 and #2. The purpose of this experiment was to explore the limits of AP1000 resident debris loadings without compromising the reasonable assurance of LTCC. The debris mass loading was significantly increased over the debris loads used in Tests #1 and #2. The amount of fiber was increased by approximately 14 times the amount of fiber used in the bounding case test (CIBAP01).

The goal for this experiment was to reach approximately three feet of head-loss. This value was chosen because it would define a debris load that was high for the AP1000 given the fact that the AP1000 design minimizes the potential to generate LOCA debris. The value of three feet of head-loss also allows a significant margin to the acceptable head-loss value, ensuring a reasonable assurance of LTCC.

Following test procedure STD-MCE-08-81 (Appendix C), the experiment was performed with a constant flow rate of [

] ^{a,c}

NOTE: There was a data acquisition error at the beginning of this experiment which caused a loss of recorded data from the beginning of the test until shortly after the second addition of fibrous debris. The first recorded data shown in Figure 8-3 was taken approximately one-half of a loop turnover after the second introduction of [] ^{a,c} of resident fiber.

The amount of debris that was introduced into the test loop was sufficient to cause head-loss of approximately [

] ^{a,c}



Figure 8-3 Head-Loss and Flow Rate History for Test CIBAP03

8.5 TEST #4 (CIBAP04)

This was the fourth of the AP1000 FA debris loading head-loss experiments performed in the STC test facility for the AP1000. [

] ^{a,c} This experiment was performed according to the test plan STD-MCE-08-82 presented in Appendix C of this document.

Test #4 was a repeat of Test #2 [

] ^{a,c} Observations noted throughout the experiment and the recorded data showed that the head-loss recorded was inconsequential when considering the impact of resident and chemical debris on the assurance of LTCC (Figure 8-4).

Following test procedure STD-MCE-08-82, the debris was introduced into the test loop in the same manner as in Test #2. After loop stabilization was reached, [

] ^{a,c}

Similar to the results of Test #2, there was no reportable head-loss recorded for Test #4. The amount of debris that was introduced into the test loop was not sufficient to cause head-loss that would compromise the reasonable assurance of LTCC.



Figure 8-4 Head-Loss and Flow Rate History for Test CIBAP04

8.6 TEST #5 (CIBAP05)

This was the fifth of the AP1000 FA debris loading head-loss experiments performed in the STC test facility for the AP1000. [

] ^{a,c} This experiment was performed according to the test plan STD-MCE-08-85 presented in Appendix C of this document.

In this case, the debris loadings were the values used in test CIBAP03 (test plan STD-MCE-08-81). The goal was to use the debris loading that was used in Test #3, but with [

] ^{a,c} Test CIBAP05 was different from the first four core inlet blockage tests conducted for the AP1000 primarily because of the difference in the [^{a,c} The amounts of debris were intended to be the same as those used in test CIBAP03. NUKON[®] fiber was still used in the case of test CIBAP05, but the distribution of the [

] ^{a,c} The rest of the conditions, including flow rate, temperature, and debris additions, were the same as those used in test CIBAP03.

The results of test CIBAP05 are summarized in Figure 8-5. After the particulate and fiber was added, [

] ^{a,c} Since the fiber used in this test was non-typical of the latent fiber (individual fibers) expected in the AP1000 containment, the rapid rise in head-loss associated with the large addition of chemicals cannot be readily attributed to only the large quantity of chemicals added. Since the test was very similar to CIBAP03, the results indicate that the interaction of the non-typical fiber and the chemicals together, and not the length of the fiber, played a larger role in the head-loss attained in this test.

The average temperature in the test column for the test was [

] ^{a,c} The plot of flow rate versus time in Figure 8-5 shows that there were a number of jumps in the flow rate. Many of these corresponded to the additions made to the loop and were probably the result of rapid changes in conductivity in the magnetic flow meter rather than real changes in the flow rate. The flow rate went outside of the allowable range of [^{a,c} at some points, but only for brief periods.

a.c

Figure 8-5 Head-Loss and Flow Rate History for Test CIBAP05

8.7 TEST #6 (CIBAP06)

This was the sixth of the AP1000 FA debris loading head-loss experiments performed in the STC test facility for the AP1000. [

] ^{a,c} This experiment was performed according to the test plan STD-MCE-09-18 presented in Appendix C of this document.

In this experiment, the debris loadings were based on a total AP1000 containment resident debris load of [] ^{a,c} bypasses the screen to reach the core.

The amounts of fiber, particulate, and chemical debris [] ^{a,c} This change in fiber type [

] ^{a,c}

Fiber B was used in this particular test to obtain a greater fraction of [] ^{a,c}

Figure 8-6 summarizes the data obtained during the test along with the timing of the debris additions. The maximum head-loss [

] ^{a,c} There were occasional spikes in the head-loss as it was dropping off. These were generally associated with further additions of chemical debris.

The average flow rate during the test was [

] ^{a,c} There were a few large spikes in the flow rate during the test. The spikes in most cases corresponded to the addition of the chemical debris. At the time of the first addition, it appeared that the addition of the chemical produced a rapid increase in the conductivity of the solution producing a few seconds of erroneously high flow values at the magnetic flow meter.

The temperature in the test column was an average of [

] ^{a,c} The pressure drop decreased continuously after addition of all chemical debris, so the test was terminated after 7.7 hours, even though the equilibrium termination criterion was not met.

a.c

Figure 8-6 Head-Loss and Flow Rate History for Test CIBAP06

8.8 TEST #8 (CIBAP08)

This was the eighth of the AP1000 FA debris loading head-loss experiments performed in the STC test facility for the AP1000. [

] ^{a,c} This experiment was performed according to the test plan STD-MCE-09-28 presented in Appendix C of this document.

In this experiment, the debris loadings were based on a total AP1000 containment resident debris load of [

] ^{a,c}

In addition, at any point in time, the flow also oscillates with a period of several minutes and with a minimum flow rate of about [] ^{a,c} This oscillation is seen in the LTCC analysis and simulated in select AP1000 fuel assembly head-loss tests.

Test CIBAP08 used the same total fibrous and particulate debris loading as was used in test CIBAP06. The same fiber as used in test CIBAP06, [] ^{a,c} CIBAP08 had [

] ^{a,c} The primary differences between CIBAP08 and CIBAP06 were the use of [] ^{a,c} in CIBAP08.

The flow rate and pressure drop results, as well as the timing of the debris additions, are summarized in Figure 8-7. Neither the SiC particulate nor the fibrous debris additions caused an increase in the head-loss across the FA. The first chemical debris addition [

] ^{a,c}

The average temperature in the test column and mixing tank during test CIBAP08 was [] ^{a,c} For both of these flow rates, the value stayed within the allowed flow range throughout the test, though it was obvious that there was some variation at different points in the test as the flow rates were manually adjusted. The upper flow rate was closer to [] ^{a,c} during the test, which was still within the allowed range.

For termination, the test was allowed to run for 75 minutes after the final addition of chemical debris. The termination criteria were checked, but since the oscillating flow had an effect on the measured head-loss, the termination criterion was not precisely met. The test was ended because the oscillating flow precluded the possibility of reaching an exact equilibrium condition.

Test CIBAP08 was allowed to run overnight to determine what would happen with pressure, settling, and debris movement after running for an extended period. Neither the dP nor the location of debris capture changed during this extended operation. However, [] ^{a,c}

a,c

Figure 8-7 Head-Loss and Flow Rate History for Test CIBAP08

8.9 TEST #9 (CIBAP09)

This was the ninth of the AP1000 FA debris loading head-loss experiments performed in the STC test facility for the AP1000. [

] ^{a,c} This experiment was performed according to the test plan STD-MCE-09-34 presented in Appendix C of this document.

In this experiment, the parameters were the same as those used for CIBAP08. The debris loadings were based on a total AP1000 containment resident debris load [

] ^{a,c}

In addition, at any point in time, the flow also oscillates with a period of several minutes and with a minimum flow rate of about [] ^{a,c} This oscillation is seen in the LTCC analysis (Reference 3) and simulated in select AP1000 fuel assembly head-loss tests, therefore it was assumed [] ^{a,c} of the fiber would reach the core.

The only difference between this test and test CIBAP08 was that the fiber used for this experiment was obtained from PCI in the [

] ^{a,c}

Test CIBAP09 was conducted to determine the pressure drop characteristics of a debris mix with a [

] ^{a,c} were not significantly different from one another. Therefore, the results of test CIBAP09 and test CIBAP08 should be compared to one another as if they were run under the same conditions.

The results of CIBAP09 were generally similar to those obtained in test CIBAP08. The pressure and flow rate data and the timing of the debris additions for CIBAP09 are given in Figure 8-8. Addition of the SiC particulate had no effect on the head-loss and addition of the fiber [

] ^{a,c}

The temperature in the test column and the mixing tank during the test [] ^{a,c} For both the upper and the lower flow rates, the measured values were within the allowed ranges.

The termination criterion was checked at the end of the test despite this being an oscillating flow test. The slope of the dP versus time curve was below the termination criterion.

a,c

Figure 8-8 Head-Loss and Flow Rate History for Test CIBAP09

8.10 TEST #10 (CIBAP10)

This was the tenth of the AP1000 FA debris loading head-loss experiments performed in the STC test facility for the AP1000. [

] ^{a,c} This experiment was performed according to the test plan STD-MCE-09-35 presented in Appendix C of this document.

In this experiment, the debris loadings were based on a total AP1000 containment resident debris load of [

] ^{a,c} These are the same values that were used in tests CIBAP08 and CIBAP09. This test also employed a [] ^{a,c} in the AP1000.

In addition, at any point in time, the flow also oscillates with a period of several minutes and with a minimum flow rate of about [] ^{a,c} This oscillation is seen in the LTCC analysis (Reference 3) and simulated in select AP1000 fuel assemble head-loss tests therefore it was assumed 60% of the fiber would reach the core.

The fiber used for this experiment was [

] ^{a,c}

Test CIBAP10 had similar conditions to tests CIBAP08 and CIBAP09. The only difference between test CIBAP10 and tests CIBAP08 and CIBAP09 was [

] ^{a,c}

The pressure and flow rate results as well as the timing of the debris additions for CIBAP10 are summarized in Figure 8-9. Some difficulties with the data acquisition system were encountered during this particular test. The flow control program caused the flow rate to hold at [] ^{a,c} for approximately 20 minutes just after four hours had passed in the test. At just over six hours into the test, the data collection program froze and stopped collecting data. It took 45 minutes to correct this problem, so the pressure and flow data between these points were lost. The flow control program continued to operate during this time, and therefore the test itself was not disturbed. These problems, corrected after the test by rebooting the computer, were not experienced in subsequent tests.

Despite these difficulties, the test was successful in showing that the debris loading used was acceptable. The addition of SiC particulate had no effect on the head-loss and the addition of the fiber [

] ^{a,c} The first chemical debris addition [

] ^{a,c}

The average temperature in the test column [

] ^{a,c} The flow rate was within

the acceptable range for the high and low flow rates throughout the test except at three points which are seen on the plot in Figure 8-9. The first was a number of low spikes in the flow rate during the first hour of the test. These low spikes had no effect on the test because they occurred before any debris was added. The second was when the flow control program caused the flow rate to hold at the high value for much longer than it was programmed to. During this time period, the flow rate did not go outside of the allowable range for the higher flow rate. The final excursion was at about 6 hours into the test when the upper flow rate spiked to a value of approximately []^{a,c} This spike at six hours was brief and did not cause a change in pressure drop or a visible rearrangement of the debris bed.

a,c

Figure 8-9 Head-Loss and Flow Rate History for Test CIBAP10

8.11 TEST #11 (CIBAP11)

This was the eleventh of the AP1000 FA debris loading head-loss experiments performed in the STC test facility for the AP1000. [

] ^{a,c} This experiment was performed according to the test plan STD-MCE-09-39 presented in Appendix C of this document.

In this experiment, the debris loadings were based on a total AP1000 containment resident debris load of [^{a,c} It was assumed that all of this resident debris [

] ^{a,c} Test CIBAP11 was conducted with the same debris amounts as Tests 8, 9, and 10, but [^{a,c}

In addition, at any point in time, the flow also oscillates with a period of several minutes and with a minimum flow rate of about [^{a,c} This oscillation is seen in the LTCC analysis (Reference 3) and simulated in select AP1000 fuel assemble head-loss tests, therefore it was assumed 60% of the fiber would reach the core.

The fiber used for this experiment [^{a,c} Table 8-2 specifies the quantities for each of the types of fibrous debris used to create this particular fibrous representation of the latent debris (Reference 8).

Table 8-2 Fibrous Debris Mix Used in Test CIBAP11			a,c

The head-loss and flow rate results as well as the timing of the additions are summarized in Figure 8-10. Neither the addition of SiC particulate nor the addition of the fiber caused an increase in the head-loss. [

] ^{a,c}

In the earlier tests the debris bed [

] ^{a,c}

The average temperature in the test column during the test [

] ^{a,c} Both of these spikes in the flow rate coincided with debris additions and were probably side effects of the variations in the local conductivity of the fluid passing through the magnetic flow meter.

a,c

Figure 8-10 Head-Loss and Flow Rate History for Test CIBAP11

8.12 TEST #13 (CIBAP13)

This was the thirteenth of the AP1000 FA debris loading head-loss experiments performed in the STC test facility for the AP1000. [

] ^{a,c} This experiment was performed according to the test plan STD-MCE-09-42 presented in Appendix C of this document.

In this case, the fibrous debris loadings were set at [] ^{a,c} was used in test CIBAP13 (see Section 6.2, Fiber). The fiber load was based on [

] ^{a,c} It was assumed that all of this resident debris [] ^{a,c} The chemical surrogate was generated outside of the loop using the standard WCAP-16530-NP-A (Reference 11) procedure.

Test CIBAP13 was similar to test CIBAP08 in terms of the type of debris used. [

] ^{a,c}
[] ^{a,c} into the mixing tank at a specified rate. Per test procedure STD-MCE-09-42 presented in Appendix C, the chemicals were [

] ^{a,c} Figure 8-12 summarizes the ALOOH concentration during the test and compares it to twice the calculated amount of chemical concentration in the AP1000 during a LOCA. The use of the factor of two conservatism is in accordance with NRC recommendations. These plots demonstrate that the amount of ALOOH added to test CIBAP13 [

] ^{a,c} The production rate was chosen based on guidance provided in References 10 and 11.

The pressure and flow rate results, as well as the timing of the additions for test CIBAP13, are summarized in Figure 8-11. After the addition of the SiC particulate, [] ^{a,c}
The addition of the fiber caused only a [

] ^{a,c}
The average temperature in the mixing tank during test CIBAP13 was [] ^{a,c} The temperature in the test column was slightly outside of the specified temperature range in the test plan, but this deviation should have had no effect on the test results.

The average flow rate during the test was []^{a,c} The flow had some small spikes during the test, but none of these went outside of the allowable range in the test plan.

a.c

Figure 8-11 Head-Loss and Flow Rate History for Test CIBAP13



Figure 8-12 Concentration of Chemical Debris with Time

8.13 TEST #14 (CIBAP14)

This was the fourteenth of the AP1000 FA debris loading head-loss experiments performed in the STC test facility for the AP1000. [

] ^{a,c} This experiment was performed according to the test plan STD-MCE-09-45 presented in Appendix C of this document.

In this experiment, the particulate, fiber, and chemical debris loadings were set to the same values used in Test CIBAP13. However, the type of fiber used was Fiber [

] ^{a,c} The production rate was chosen based on guidance provided in References 10 and 11.

The pressure and flow rate results, as well as the timing of the debris additions for test CIBAP14, are summarized in Figure 8-13. The gradual additions of chemical debris are noted on the plot. The addition of the SiC particulate [

] ^{a,c} The first continuous addition of ALOOH chemical debris[
addition of ALOOH, the test plan [] ^{a,c} After this first

] ^{a,c} The test was then allowed to stabilize for 8.5 hours until the equilibrium criterion was met. At this point, additional chemical debris was added by pouring the liquid rather than pumping it into the mixing tank. The head-loss reached [] ^{a,c}

Approximately two hours after the second continuous addition of the chemical debris, the water in the loop was cloudy white from the ALOOH in suspension. Five hours later the water had become noticeably clearer. The chemical debris was gradually filtered out of the water causing the clarity and at the same time increasing the head-loss.

The overall appearance of the debris bed was similar to that observed seven hours after the second continuous ALOOH addition. One difference at the end of the test was the accumulation of what was most likely a layer of ALOOH and SiC particulate on the bottom face of the debris bed. Another difference was the amount of chemical debris and SiC particulate that had settled out on top of the FA and also on top of some areas of the support grids. This settling was also seen in other tests and it is reasonable that some settling of debris would take place in low-flow locations of an AP1000 reactor or in containment after a LOCA. However, the turbulence caused by boiling would likely minimize settling at the top of the assembly. Boiling was evaluated in CIBAP38 and CIBAP39 and is discussed in Section 8.37, Section 8.38, and Section 9.17.

The average temperature in the test column during test CIBAP14 was [

] ^{a,c}

There were small spikes in the flow rate throughout the test, but only one of these went outside of the allowable range given in the test plan. At just over four hours into the test, [

] ^{a,c} This appeared to have no effect on

the results of the test.

^{a,c}

Figure 8-13 Head-Loss and Flow Rate History for Test CIBAP14

8.14 TEST #15 (CIBAP15)

This was the fifteenth of the AP1000 FA debris loading head-loss experiments performed in the STC test facility for the AP1000. [

] ^{a,c} This experiment was performed according to the test plan STD-MCE-09-61 presented in Appendix C of this document.

In this case, the fibrous debris loadings were set at [] ^{a,c} was used in test CIBAP15 (see Section 6.2, Fiber). The debris load was based on [

] ^{a,c} It was assumed that all of this fibrous and particulate debris [

] ^{a,c}

Test CIBAP15 included more [

] ^{a,c}

[

] ^{a,c} into the mixing tank at a specified rate. For conservatism, the concentration of chemical debris in the test loop was targeted to be above twice the calculated concentration in the AP1000 during a LOCA event. The use of the factor of two conservatism is in accordance with NRC recommendations. The production rate was chosen based on guidance provided in Reference 10 and Reference 11.

The pressure and flow rate results, as well as the timing of the debris additions for test CIBAP15, are summarized in Figure 8-14. After the addition of the SiC particulate, [

] ^{a,c}

The pressure drop increase occurred [] ^{a,c} This is demonstrated by comparing the trace labeled “dP Upper” to the trace labeled “dP Lower” in Figure 8-14. The pressure drop increase across [

] ^{a,c}

No visible debris beds or blockages formed when the particulate debris was added. [

] ^{a,c}

The average temperature for both the test column and the mixing tank during the test was []^{a,c} which was well within the allowable flow rate. The flow rate did not spike outside of the control band except for a brief excursion when the fiber added. Since this excursion occurred before the bed formed, it had no effect on the test results. The maximum pH during the test was []^{a,c}. This was within the allowable range for the test (5 to 9), so any dissolution of the chemical product surrogate was insignificant.

a,c

Figure 8-14 Head-Loss and Flow Rate History for Test CIBAP15

8.15 TEST #16 (CIBAP16)

This was the sixteenth of the AP1000 FA debris loading head-loss experiments performed in the STC test facility for the AP1000. [

] ^{a,c} This experiment was performed according to the test plan STD-MCE-09-71 presented in Appendix C of this document.

In this case, the fibrous debris loadings were set at [

] ^{a,c} (Figure 8-16). It was assumed that all of this fibrous and particulate debris was transported to the recirculation screen area and that [

] ^{a,c}

The rate of chemical surrogate addition was the same as used for test CIBAP14. The reduced rate of chemical addition [

] ^{a,c}

[

] ^{a,c} into the mixing tank at a specified rate. As in test CIBAP14, [

] ^{a,c} For conservatism, the concentration of chemical debris in the test loop was targeted to be more than twice the calculated concentration in the AP1000 during a LOCA event. The use of the factor of two times the concentration is in accordance with NRC recommendations. The production rate was chosen based on guidance provided in Reference 10 and Reference 11.

The pressure drop increase occurred [] ^{a,c} This is demonstrated by comparing the trace labeled “dP Upper” to the trace labeled “dP Lower” in Figure 8-15. The pressure drop increase across [

] ^{a,c}

The average temperature for both the test column and the mixing tank during the test was [] ^{a,c} The average flow rate during the test was [] ^{a,c} The flow had some small spikes during the test and a brief excursion when the fiber added. This excursion occurred before the bed formed, so it had no effect on the test results. The maximum pH during the test was [] ^{a,c} This was within the allowable range for the test (5 to 9), so any dissolution of the chemical product surrogate was insignificant.

The pressure and flow rate results, as well as the timing of the additions for test CIBAP16, are summarized in Figure 8-15. Starting with a clean assembly (Figure 8-17), the addition of the SiC particulate (Figure 8-18), [] ^{a,c} The addition of the fiber caused only a [] ^{a,c} (Figure 8-19). At this time, the additions of particulate and fiber result in a uniform build-up of debris along the edge of the bottom nozzle and the bottom of the p-grid (Figure 8-20) that increases with the addition of the chemicals. With the more gradual addition of chemicals, the head-loss did not increase as suddenly, however, the first two additions of the chemical

surrogate did result in the head-loss increasing gradually to []^{a,c} Note that between the first and second chemical additions (Figure 8-20 and Figure 8-21), the debris bed on both the lower left and right shows significant break through and reduced accumulation along the bottom of the p-grid. By the third chemical addition, the debris has taken on a smoother appearance and essentially no debris remains at the bottom of the p-grid (Figure 8-22). After the third chemical addition, the dP increase []^{a,c} The pressure drop vs. time curve was fairly level after the fourth chemical addition. The seventh and last chemical addition shows a smooth and well defined debris bed with visible layers of chemicals and very little debris on the bottom nozzle or p-grid (Figure 8-23). The final addition resulted in no additional head-loss increases. Thereafter, the pressure drop began a slow decline and then leveled at a final value of []^{a,c}

a.c

Figure 8-15 Head-Loss and Flow Rate History for Test CIBAP16



Figure 8-16 Debris Load For Test CIBAP16



Figure 8-17 Clean Assembly For Test CIBAP16



Figure 8-18 Addition of Particulates for Test CIBAP16



Figure 8-19 Accumulation of Fiber at Bottom Nozzle and P-Grid for Test CIBAP16

a,c



Figure 8-20 Debris Bed After Chemical Introduction For Test CIBAP16

a,c



Figure 8-21 Debris Bed After the Second Chemical Introduction For Test CIBAP16

a,c



Figure 8-22 Debris Bed After The Third Chemical Introduction For Test CIBAP16

a,c



Figure 8-23 Debris Bed After Final Chemical Introduction For Test CIBAP16

8.16 TEST #17 (CIBAP17)

This was the seventeenth of the FA debris loading head-loss experiments performed in the STC test facility for the AP1000. [

] ^{a,c} This experiment was performed according to test plan STD-MCE-09-101 presented in Appendix C of this document. All debris was added sequentially with particulate followed by fiber followed by chemical surrogate.

In this experiment, the debris loadings were based on a total AP1000 post-LOCA containment debris load [

] ^{a,c} The results of test CIBAP17 are plotted in Figure 8-24.

On the day test CIBAP17 was to be performed, there were delays in starting the test. After the test was started and the particulate debris was introduced into the test loop, it was decided that it was too late in the day to complete the test. The flow through the loop was inadvertently stopped overnight and this was a deviation from the test procedure. The test was completed the next day. Also note that the test loop piping associated with this test was configured differently (see loop diagram Figure 8-25) than that used in previous AP1000 FA head-loss tests. Because of these issues with how this test was run and the different loop configuration used, the test was considered invalid. A root cause analysis was initiated on this test.

The particulate debris that had been in the loop for approximately 24 hours had no effect on the head-loss across the assembly. [

] ^{a,c}

At the onset of chemical addition, [

] ^{a,c}

The pressure drop increase occurred almost exclusively at the bottom nozzle/p-grid location. This can be deduced by comparing the trace labeled “dP Upper” to the trace labeled “dP Lower” in Figure 8-24. The pressure drop increase across the bottom nozzle (dP Lower) was the same as total pressure drop increase

across the entire assembly. The pressure drop between the top of the p-grid and the top of the assembly (dP Upper) was recorded at a maximum of []^{a,c} at the time of test termination.

The average temperature for both the test column and the mixing tank during the test was []^{a,c} The flow rate was []^{a,c}

The pH was measured throughout the test reaching a maximum pH of []^{a,c} This was within the allowable range for the test (5 to 9), so any dissolution of the chemical product surrogate was insignificant.

a.c

Figure 8-24 Head-Loss and Flow Rate History for Test CIBAP17

a,c

Figure 8-25 Schematic of The Test Loop Configuration For CIBAP17

8.17 TEST #18 (CIBAP18)

This was the eighteenth of the FA debris loading head-loss experiments performed in the STC test facility for the AP1000. [

] ^{a,c} This experiment was performed according to test plan STD-MCE-09-102 presented in Appendix C of this document. All debris was added sequentially with particulate followed by fiber followed by chemical surrogate.

In this experiment, the debris loadings were based on a total AP1000 post-LOCA containment debris load [

] ^{a,c} The results of test CIBAP18 are plotted in Figure 8-26.

The addition of particulate and fiber had little effect on the head-loss across the full assembly. The particulate caused zero pressure drop increase and the combination of fiber and particulate resulted in an increase of [] ^{a,c}

At the onset of chemical addition, [

] ^{a,c}

In this test, [

] ^{a,c} per the test procedure and held until the acceptance criterion was met again.

At this point in the test a series of flow sweeps were performed at higher and lower flows than the flow recorded at test termination. The flow sweeps were performed to determine the pressure drop dependence on flow rate.

In test CIBAP18, the pressure drop increase occurred almost exclusively at the bottom nozzle/p-grid location. This is demonstrated by comparing the trace labeled “dP Upper” to the trace labeled “dP Lower” in Figure 8-26. The pressure drop increase across the bottom nozzle (dP Lower) was slightly less than the total pressure drop increase across the entire assembly indicating that some debris was accumulating in the upper portion of the bundle. The pressure drop between the top of the p-grid and the top of the assembly (dP Upper) was recorded at approximately [] ^{a,c} for the portion of the test prior to the flow sweeps.

No visible debris beds or blockages formed when the particulate debris was added. After the fiber addition, a fiber bed developed at the bottom nozzle/p-grid. The dP at this time suggested that the debris bed had significant porosity. When the chemical surrogate was first added, there was not a great deal of

visible change in the bed and bits of fiber were observed above the p-grid. By the time the last chemical addition was in, only a small amount of fiber was observed to remain above the p-grid.

The average temperature for both the test column and the mixing tank during the test was []^{a,c} The flow rate was []

^{a,c} The pH was measured throughout the test reaching a maximum pH of []^{a,c} This was within the allowable range for the test (5 to 9), so any dissolution of the chemical product surrogate was insignificant.

a,c

Figure 8-26 Head-Loss and Flow Rate History for Test CIBAP18

8.18 TEST #19 (CIBAP19)

This was the nineteenth of the FA debris loading head-loss experiments performed in the STC test facility for the AP1000. [

] ^{a,c} This experiment was performed according to test plan STD-MCE-09-103 presented in Appendix C of this document. [^{a,c}

In this experiment, the debris loadings were based on a total AP1000 post-LOCA containment debris load [

] ^{a,c} The results of test CIBAP19 are plotted in Figure 8-27.

The additions of particulate had very little impact on the recorded dP. After the introduction of the fiber, the fiber and particulate together resulted in a dP [^{a,c} Following the recommended loop turnovers, chemical debris was introduced into the loop.

In conjunction with the introduction of chemicals, a flow reduction scheme was initiated to reduce the flow rate commensurate with the increase in dP across the bundle. The addition of chemical debris had a significant effect. The first two chemical additions increased the pressure drop from a value of [

] ^{a,c} At this point, the data was checked to see if it met the termination criteria. After successfully meeting the termination criteria, the flow rate was reduced to [^{a,c} and the dP was allowed to equilibrate. After meeting the termination criteria flow sweeps were started to assess the impact of pressure drop dependence on flow rate.

In test CIBAP19, the pressure drop increase occurred almost exclusively at the [^{a,c}. This is demonstrated by comparing the trace labeled “dP Upper” to the trace labeled “dP Lower” in Figure 8-27. The pressure drop increase across the bottom nozzle (dP Lower) was essentially the same as total pressure drop increase across the entire assembly. The pressure drop between the top of the p-grid and the top of the assembly (dP Upper) changed insignificantly during the test.

No visible debris beds or blockages formed when the particulate debris was added. After the first fiber addition, a fiber bed developed at the bottom nozzle/p-grid. The dP at this time suggested that the debris bed had significant porosity. When the chemical surrogate was first added, there was not a great deal of visible change in the bed. As more chemical was added, a dense white layer formed within the bed at the bottom of the bottom nozzle. Only small amounts of fiber were observed above the p-grid. By the end of the test, the debris bed loaded with chemical precipitates is easily seen.

The average temperature for both the test column and the mixing tank during the test was []^{a,c} The maximum pH during the test was []^{a,c} This was within the allowable range for the test (5 to 9), so any dissolution of the chemical product surrogate was insignificant.

a,c

Figure 8-27 Head-Loss and Flow Rate History for Test CIBAP19

8.19 TEST #20 (CIBAP20)

This was the twentieth of the FA debris loading head-loss experiments performed in the STC test facility for the AP1000. With the debris load and chemical precipitate tested (Table 8-1), the peak head-loss recorded for this test was []^{a,c} This experiment was performed according to test plan STD-MCE-09-107 presented in Appendix C of this document. All debris was added sequentially with particulate followed by fiber followed by chemical surrogate.

In this experiment, the debris loadings were based on a total AP1000 post-LOCA containment debris load []

[]^{a,c} The results of test CIBAP20 are plotted in Figure 8-28.

The additions of particulate and fiber had little effect on the head-loss across the full assembly. The particulate caused zero pressure drop increase and the addition of fiber caused an increase []^{a,c}

In conjunction with the introduction of chemicals, []

[]^{a,c} Flow sweeps were initiated after all termination criteria were met.

The pressure drop increase occurred almost exclusively at the bottom nozzle/p-grid location. This is demonstrated by comparing the trace labeled “dP Upper” to the trace labeled “dP Lower” in Figure 8-28. The pressure drop increase across the bottom nozzle (dP Lower) was the same as total pressure drop increase across the entire assembly. The pressure drop between the top of the p-grid and the top of the assembly (dP Upper), did not change during the test.

No visible debris beds or blockages formed when the particulate debris was added. After the first fiber addition, a fiber bed developed at the bottom nozzle/p-grid. When the chemical surrogate was first added, there was not a great deal of visible change in the bed. As more chemical was added, a white layer formed within the bed at the bottom of the bottom nozzle and the fiber seemed to migrate up the p-grid away from the nozzle. After meeting all termination criteria at []^{a,c} significant amounts of fiber were observed above the p-grid and the debris bed under the bottom nozzle appeared to be settling on the core support plate.

The average temperature for both the test column and the mixing tank during the test was []^{a,c} The flow rate was initially at []^{a,c} over the course of the experiment. The pH was measured throughout the test reaching a maximum pH of []^{a,c} This was within the allowable range for the test (5 to 9), so any dissolution of the chemical product surrogate was insignificant.

a.c

Figure 8-28 Head-Loss and Flow Rate History for Test CIBAP20

8.20 TEST #21 (CIBAP21)

This was the twenty-first of the FA debris loading head-loss experiments performed in the STC test facility for the AP1000. [

] ^{a,c} This experiment was performed according to test plan STD-MCE-09-108 presented in Appendix C of this document. All debris was added sequentially with particulate followed by fiber followed by chemical surrogate.

In this experiment, the debris loadings were based on a total AP1000 post-LOCA containment debris load [

] ^{a,c} The results of test CIBAP21 are plotted in Figure 8-29.

The additions of particulate and fiber had little effect on the head-loss across the full assembly. The particulate caused zero pressure drop increase and the fiber with particulate resulted in an increase [

] ^{a,c} At the onset of chemical addition, a flow reduction scheme was used to reduce the flow rate commensurate with the increase in dP associated with the chemicals. The test flow and dP initially tracked well with the performed flow reduction. [

] ^{a,c} Per the test procedure, the flow rate [] ^{a,c} held until the termination criterion was met. At this point in the test flow sweeps were performed to determine the pressure drop dependence on flow rate.

As in the other tests, the pressure drop increase occurred almost exclusively at [] ^{a,c} This can be seen by comparing the trace labeled “dP Upper” to the trace labeled “dP Lower” in Figure 8-29. The pressure drop increase across the bottom nozzle (dP Lower) was the same as total pressure drop increase across the entire assembly. The pressure drop between the top of the p-grid and the top of the assembly (dP Upper) measured [] ^{a,c} during the pre-flow sweep portion of the test.

When the particulate material was added, no blockages were observed at any location and the particulate was well distributed about the test article. After the fiber addition, a fiber bed developed between the bottom nozzle and the p-grid. The fiber bed appeared to have significant porosity as the dP due to fiber and particulate was about [] ^{a,c} When the chemical product surrogate was added, the bed porosity appeared to go down as indicated by the rise in dP. After the second chemical addition, the fiber bed showed signs of instability such that the dP dropped,

recovered and dropped again prior to the third chemical addition. Further chemical additions resulted in small increases with []^{a,c} Late in the test, the chemicals were readily seen in the debris bed with only small amounts of fiber observed above the p-grid. Even though the bed looked very thick, the makeup of the bed must have been such that fluid could pass through it with relative ease because no further increase in dP was observed.

The average temperature for both the test column and the mixing tank during the test was []^{a,c} The flow rate was initially at []^{a,c} The pH was measured throughout the test reaching a maximum pH of []^{a,c} This was within the allowable range for the test (5 to 9), so any dissolution of the chemical product surrogate was insignificant.

a,c

Figure 8-29 Head-Loss and Flow Rate History for Test CIBAP21

8.21 TEST #22 (CIBAP22)

This was the twenty-second FA debris loading head-loss experiments performed in the STC test facility for the AP1000. [

] ^{a,c} This experiment was performed according to test plan STD-MCE-09-109 presented in Appendix C of this document. [^{a,c}

In this experiment, the debris loadings were based on a total AP1000 post-LOCA containment debris load [

] ^{a,c} The results of test CIBAP22 are plotted in Figure 8-30.

The first concurrent addition of particulate, fiber, and chemical precipitates had little effect on the head-loss across the full assembly resulting in [

] ^{a,c}
As in the previous tests, a flow reduction scheme was used to reduce the flow rate commensurate with the increase in dP across the FA bundle. In previous tests, the reduction scheme was only applied at the introduction of the chemical precipitates. For this test, the reduction scheme was applied from the beginning of the test as the dP attributed to debris accumulation increased.

[

] ^{a,c}

An interesting observation from this test is that the fiber appeared to accumulate around the bottom of the p-grid prior to accumulating around the bottom nozzle. This accumulation begins to appear just prior to the second addition and continues through the fourth addition when a debris bed begins to form around the edges of the bottom nozzle. Also seen in this concurrent debris addition test is the accumulation of fibers in the middle of the first grid above the p-grid and along the bottom of the second grid above the p-grid.

The pressure drop increase occurred almost exclusively at the bottom nozzle/p-grid location as in the other tests. This can be seen by comparing the trace labeled “dP Upper” to the trace labeled “dP Lower” in Figure 8-30. The pressure drop increase across the bottom nozzle (dP Lower) was approximately the same as total pressure drop increase across the entire assembly. [

] ^{a,c}

[]^{a,c} held until termination criteria were met, and flow sweeps were to be initiated. As seen in Figure 8-30 the flow sweep program did not run.

The average temperature for both the test column and the mixing tank during the test was []^{a,c}. The flow rate was initially at []^{a,c}. The pH was measured throughout the test reaching a maximum pH of []^{a,c}. This was within the allowable range for the test (5 to 9), so any dissolution of the chemical product surrogate was insignificant.

a.c

Figure 8-30 Head-Loss and Flow Rate History for Test CIBAP22

8.22 TEST #23 (CIBAP23)

This was the twenty-third FA debris loading head-loss experiments performed in the STC test facility for the AP1000. [

] ^{a,c} This experiment was performed according to test plan STD-MCE-09-113 presented in Appendix C of this document. All debris was added sequentially.

In this experiment, the debris loadings were based on a total AP1000 post-LOCA containment debris load [

] ^{a,c} The results of test CIBAP23 are plotted in Figure 8-31.

This is a repeat of test CIBAP17. For this test, there were no delays in starting the test as discussed in Section 8.16. This test uses the same loop plumbing as described in Section 4.1.

The addition of the particulate had no effect on the loop dP. The particulate caused zero pressure drop increase and the addition of fiber resulted in an [

] ^{a,c}
The third chemical addition resulted in the [

] ^{a,c} At this point, the steady state termination criterion was met and flow sweeps were initiated.

As in the other AP1000 FA debris tests, the pressure drop increase occurred almost exclusively at the bottom nozzle/p-grid location. This is demonstrated by comparing the trace labeled “dP Upper” to the trace labeled “dP Lower” in Figure 8-31. The pressure drop increase across the bottom nozzle (dP Lower) was the same as total pressure drop increase across the entire assembly. The pressure drop between the top of the p-grid and the top of the assembly (dP Upper), did not change during the test.

As in the previous sequential addition tests, a flow reduction scheme were used at the onset of chemical addition to reduce the flow rate commensurate with the increase in dP associated with the chemical additions. The test flow and dP initially tracked well with the performed flow reduction as seen in Figure 8-31. At approximately 4.19 hours into the test, the slope of the flow reduction was set to 0.0 at a flow rate of [] ^{a,c} During this steady state condition the fourth through seventh chemical additions were prepared and introduced into the loop.

When the particulate material was added, no blockages were observed at any location and the particulate was well distributed about the test article. After the fiber addition, a fiber bed developed at the bottom nozzle and between the bottom nozzle and the p-grid. Due to the small increase in dP, it is assumed that the fiber bed must have had significant porosity. After the chemical surrogate was added, the bed

porosity decreased as indicated by the rise in dP. At this point in the test, with all of the fiber, particulate, and first chemical addition in the loop, the debris looked rough and uneven. After the second chemical addition, the debris began to look smoother and the amount of debris located on the p-grid had been greatly reduced. By the seventh and final chemical addition, the debris was very smooth with visible layers of chemicals and only a small amount of fiber above the p-grid.

The average for both the test column and the mixing tank during the test was []^{a,c} The flow rate was initially at []^{a,c} The pH was measured throughout the test reaching a maximum pH of []^{a,c} This was within the allowable range for the test (5 to 9), so any dissolution of the chemical product surrogate was insignificant.

a.c

Figure 8-31 Head-Loss and Flow Rate History for Test CIBAP23

8.23 TEST #24 (CIBAP24)

This was the twenty-fourth FA debris loading head-loss experiments performed in the STC test facility for the AP1000. [

] ^{a,c} This experiment was performed according to test plan STD-MCE-09-115 presented in Appendix C. [

] ^{a,c}

In this experiment, the debris loadings were based on a total AP1000 post-LOCA containment debris load [

] ^{a,c} The results of test CIBAP24 are plotted in Figure 8-32.

The first concurrent addition of particulate, fiber, and chemical precipitates had little effect on the head-loss across the full assembly resulting in [

] ^{a,c} and held until termination criteria were again met, then flow sweeps were performed to provide insight on the pressure drop dependence on flow rate.

As in the previous tests in this series, a flow reduction scheme was used to reduce the flow rate commensurate with the increase in dP across the FA bundle (Figure 8-33). For this test the reduction scheme was applied from the beginning of the test as the dP attributed to debris accumulation increased during the concurrent additions. The test flow and dP tracked well with the performed flow reduction as seen in Figure 8-32. [

] ^{a,c}

As witnessed in test CIBAP22, the fiber accumulated around the bottom of the p-grid (Figure 8-35, Figure 8-35, Figure 8-36) prior to accumulating around the bottom nozzle (Figure 8-37). This accumulation began to appear just prior to the second addition and continued through the fourth addition when a debris bed began to form around the edges of the bottom nozzle. Also witnessed in this concurrent debris addition test was the accumulation of fibers in the middle of the first grid above the p-grid (Figure 8-38) and along the bottom of the second grid above the p-grid (Figure 8-39). The accumulation of debris in these areas is atypical when considering the other AP1000 FA tests. It suggests that individual fibers arriving at the FA bottom nozzle in lesser amounts may have a greater chance of migrating through the fuel bundle. By the end of the test, the debris bed had taken on a smooth, rounded appearance (Figure 8-40) and was not continuous around the edges of the bottom nozzle thus leaving many break-through areas where flow is not impeded.

Even with a noticeable accumulation of fiber away from the bottom nozzle, the pressure drop increase occurred almost exclusively at the bottom nozzle/p-grid location as in the other tests. This can be seen by

comparing the trace labeled “dP Upper” to the trace labeled “dP Lower” in Figure 8-32. The pressure drop contribution from the upper assembly []^{a,c}

The average temperature for both the test column and the mixing tank during the test was []^{a,c} The pH was measured throughout the test reaching a maximum pH of []^{a,c} This was within the allowable range for the test (5 to 9), so any dissolution of the chemical product surrogate was insignificant. The flow rate reached a steady state condition at []^{a,c} held until termination criteria were met and flow sweeps were initiated.

8.23.1 Varying Initial Flow Rates

It has not been concluded whether varying the flow increases or decreases the head-loss. All of the subsequent AP1000 FA tests have been conducted with varying flows because that is how the plant will operate. The initial flow has been set at []^{a,c} since that flow seems to result in higher head-losses than other initial flows. The flow rate of []^{a,c} (comparing tests CIBAP20 and CIBAP23) for sequence debris addition. However, for concurrent debris addition (comparing tests CIBAP22 and CIBAP24), []^{a,c} but the initial head-loss trend was more severe. Based on this sensitivity study the initial flow rate of []^{a,c} will be used as most conservative for the remaining tests, either sequence or concurrent debris additions. The dPs for tests CIBAP20, CIBAP22 through CIBAP24 can be found in Table 8-1 for comparison.



Figure 8-32 Head-Loss and Flow Rate History for Test CIBAP24



Figure 8-33 Flow Versus dP During Test CIBAP24



Figure 8-34 Accumulation of Debris at the Bottom of the P-Grid After Second Concurrent Debris Addition in Test CIBAP24



Figure 8-35 Accumulation of Debris at the Bottom of the P-Grid After Third Concurrent Debris Addition in Test CIBAP24



Figure 8-36 Accumulation of Debris at the Bottom of the P-Grid After Fourth Concurrent Debris Addition in Test CIBAP24



Figure 8-37 Accumulation of Debris Around the Edge of the Bottom Nozzle After Seventh Concurrent Debris Addition in Test CIBAP24



Figure 8-38 Accumulation of Debris in the Middle of the First Grid Above the P-Grid After the Ninth Addition in Test CIBAP24



Figure 8-39 Accumulation of Debris Around the Bottom of the Second Spacer Grid After the Ninth Addition in Test CIBAP24



Figure 8-40 Accumulation of Debris Around the Bottom Nozzle and P-Grid at the End of Test CIBAP24 Prior to Flow Sweeps

8.24 TEST #25 (CIBAP25)

This was the twenty-fifth FA debris loading head-loss experiments performed in the STC test facility for the AP1000. [

] ^{a,c} This experiment was performed according to test plan STD-MCE-09-116 presented in Appendix C. [

] ^{a,c}

In this experiment, the debris loadings were based on a total AP1000 post-LOCA containment debris load [

] ^{a,c} The results of test CIBAP25 are plotted in Figure 8-41. This test is similar to test CIBAP24 except that the chemicals are [^{a,c}

The first concurrent addition of particulate, fiber, and chemical precipitates had little effect on the head-loss across the full assembly resulting in [

] ^{a,c}

During this time, the test procedure was being followed to reduce the flow rate commensurate with the increase in dP attributed to debris accumulation within the FA.

Approximately 17 minutes following the eleventh chemical addition, a flow anomaly occurred that caused a flow excursion in the loop. The upper flow meter which was controlling the flow in the loop, registered a minimum flow of zero gpm which caused the flow to increase significantly. The increase in flow was monitored by the lower flow meter; it registered a peak flow of [

] ^{a,c} Then the dP reacted to the flow anomaly by falling to [^{a,c}
(Figure 8-41). Observations at the time of the flow anomaly indicated that large 'chunks' of the debris formations around the bottom nozzle and p-grid broke off and were swept away. [

] ^{a,c}

Even though the test experienced a significant anomaly, it was continued as planned. The flow rate was [^{a,c} All subsequent chemical additions were made. After the final chemical addition, the prerequisite number of loop turnovers was performed; the data was checked and found to meet the termination criteria. Flow sweeps were performed as written in the test plan.

As seen in CIBAP24, the fiber accumulated around the bottom of the p-grid prior to accumulating around the bottom nozzle. This accumulation began to appear just after the second addition and continued through the fourth addition when a debris bed began to form around the edges of the bottom nozzle.

Even with a noticeable accumulation of debris away from the bottom nozzle, the pressure drop increase occurred almost exclusively at the bottom nozzle/p-grid location as in the other tests. This can be seen by comparing the trace labeled “dP Upper” to the trace labeled “dP Lower” in Figure 8-41. The pressure drop contribution from the upper assembly was []^{a,c}

The average temperature for both the test column and the mixing tank during the test was []^{a,c}. The pH was measured throughout the test reaching a maximum pH of []^{a,c}. This was within the allowable range for the test (5 to 9), so any dissolution of the chemical product surrogate was insignificant.



Figure 8-41 Head-Loss and Flow Rate History for Test CIBAP25

8.25 TEST #26 (CIBAP26)

This was the twenty-sixth FA debris loading head-loss experiments performed in the STC test facility for the AP1000. [

] ^{a,c} This experiment was performed according to test plan STD-MCE-09-123 presented in Appendix C. [

] ^{a,c}

In this experiment, the debris loadings were based on a total AP1000 post-LOCA containment debris load [

] ^{a,c} The results of test CIBAP26 are plotted in Figure 8-42. This test is similar to test CIBAP25 except that the [

] ^{a,c}

The [] ^{a,c} of concurrent debris additions of particulate, fiber, and chemical precipitates resulted in a pressure differential across the full assembly of about [

] ^{a,c} The remaining five ‘chemical-only’ additions resulted in no further increases in the recorded dP.

During this time, the test procedure was being followed to reduce the flow rate commensurate with the increase in dP. By the fourteenth addition, the flow rate had been reduced from [

] ^{a,c} Over the next hour and 15 minutes the steady state test criterion was again met and the automated flow sweeps were initiated.

In this test, with the debris being added concurrently over 18 hours, the fiber barely began to accumulate around the bottom of the p-grid after the third addition. After the fifth addition, with [

] ^{a,c}

Even with a noticeable accumulation of debris away from the bottom nozzle upper bundle dP, the pressure drop increase occurred almost exclusively at the bottom nozzle/p-grid location as in the other tests. This can be seen by comparing the trace labeled “dP Upper” to the trace labeled “dP Lower” in Figure 8-42. The pressure drop contribution from the upper assembly [

] ^{a,c}

The average temperature for both the test column and the mixing tank during the test was []^{a,c} The pH was measured throughout the test reaching a maximum pH of []^{a,c} This was within the allowable range for the test (5 to 9), so any dissolution of the chemical product surrogate was insignificant.

a.c

Figure 8-42 Head-Loss and Flow Rate History for Test CIBAP26

8.26 TEST #27 (CIBAP27)

This was the twenty-seventh of the FA debris loading head-loss experiments performed in the STC test facility for the AP1000. [

] ^{a,c} This experiment was performed according to test plan STD-MCE-09-125 presented in Appendix C. This test was a repeat of test CIBAP25, except that [

In this experiment, the debris loadings were based on a reduced AP1000 post-LOCA containment debris [

] ^{a,c} The results of test CIBAP27 are plotted in (Figure 8-43). All debris was added concurrently.

The first concurrent addition of particulate, fiber, and chemical precipitates had little effect on the head-loss across the full assembly resulting in [

] ^{a,c}

During this time, the test procedure was being followed to reduce the flow rate commensurate with the increase in dP (Figure 8-44).

Similar to test CIBAP25, the fiber accumulated around the bottom of the p-grid (Figure 8-45) prior to accumulating around the bottom nozzle (Figure 8-46). This accumulation begins to appear just after the second addition and continues through the fourth addition when a debris bed begins to form around the edges of the bottom nozzle (Figure 8-47). By the time of the sixth addition, the debris buildup along the edges of the bottom nozzle and bottom of the p-grid are significant. Unlike test CIBAP25, there is no visible accumulation of debris at the first spacer grid. After the seventh concurrent addition, the accumulation of chemicals in the debris bed is easily seen (Figure 8-48) the debris bed still had rough edges (Figure 8-49). Between the ninth (Figure 8-50) and twelfth (Figure 8-51) additions, the debris bed took on a smoother appearance and there was a visible breakthrough of the debris bed along the lower left and upper right edge of the bottom nozzle. Once these breakthrough areas were established, they remained clear for the remainder of the test as seen in Figure 8-53. The dP peaked at [

] ^{a,c} By the time of the fourteenth addition, the edges of the debris bed (Figure 8-52) were smooth, well-defined, and continued to thicken as the test progressed without a corresponding increase in dP. After the seventeenth addition, the dP was monitored until the steady state dP condition was met. With all acceptance criteria met, flow sweeps were initiated to determine the pressure drop dependence on flow rate. As seen in Figure 8-53 the debris was very thick and very smooth, yet did not cause an increase in the steady state dP.

The pressure drop increase occurred almost exclusively at the bottom nozzle/p-grid location as in the other tests. This can be seen by comparing the trace labeled “dP Upper” to the trace labeled “dP Lower” in Figure 8-43. The pressure drop contribution from the upper assembly was approximately []^{a,c}

The average temperature for both the test column and the mixing tank during the test was []^{a,c}. The pH was measured throughout the test reaching a maximum pH of []^{a,c}. This was within the allowable range for the test (5 to 9), so any dissolution of the chemical product surrogate was insignificant^{a,c}

Figure 8-43 Head-Loss and Flow Rate History for Test CIBAP27



Figure 8-44 Flow Versus dP during Test CIBAP27



Figure 8-45 Accumulation of Debris Around the Bottom Nozzle and P-Grid after the Third Concurrent Addition in Test CIBAP27



Figure 8-46 Accumulation of Debris Around the Bottom Nozzle and P-Grid at the Fourth Concurrent Addition in Test CIBAP27



Figure 8-47 Accumulation of Debris Around the Bottom Nozzle and P-Grid at the Fifth Concurrent Addition in Test CIBAP27



Figure 8-48 Accumulation of Debris Around the Bottom Nozzle and P-Grid 30 Minutes into the Fifth Concurrent Addition in Test CIBAP27

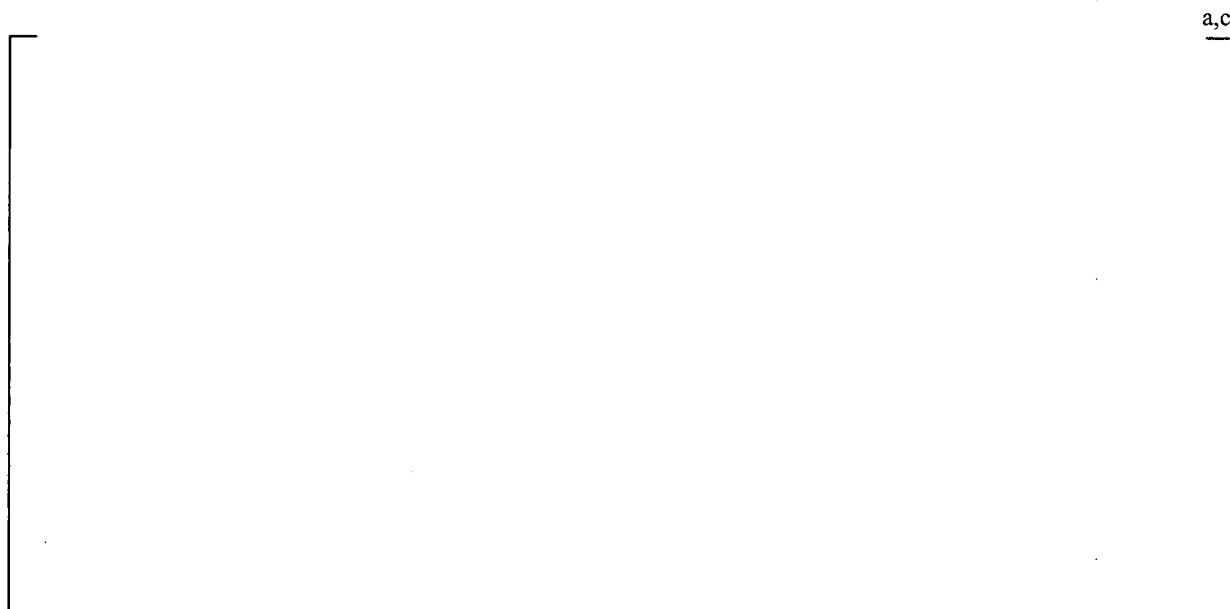


Figure 8-49 Accumulation of Debris Around the Bottom Nozzle and P-Grid 30 Minutes into the Ninth Chemical Addition in Test CIBAP27



Figure 8-50 Accumulation of Debris Around the Bottom Nozzle and P-Grid at the Time of the Tenth Chemical Addition in Test CIBAP27



Figure 8-51 Accumulation of Debris Around the Bottom Nozzle and P-Grid 30 Minutes into the Twelfth Chemical Addition in Test CIBAP27



Figure 8-52 Accumulation of Debris Around the Bottom Nozzle and P-Grid 15 Minutes After the Fourteenth Chemical Addition in Test CIBAP27



Figure 8-53 Accumulation of Debris Around the Bottom Nozzle and P-Grid Prior to Flow Sweeps in CIBAP27

8.27 TEST #28 (CIBAP28)

This was the twenty-eighth of the FA debris loading head-loss experiments performed in the STC test facility for the AP1000. [

] ^{a,c} This experiment was performed according to test plan STD-MCE-09-132. This test was a repeat of test CIBAP27 [

] ^{a,c}

In this sensitivity experiment, the debris loadings were based on a reduced AP1000 post-LOCA containment debris load of [

] ^{a,c} The results of test CIBAP28 are plotted in Figure 8-54. All debris was added concurrently.

The first concurrent addition of silicon carbide particulate, fiber, and chemical precipitates had little effect on the head-loss across the full assembly resulting in a [

] ^{a,c}

During this time, the test procedure was followed using the procedure information to reduce the flow rate commensurate with the increase in dP.

Similar to test CIBAP25, the fiber accumulated around the bottom of the p-grid prior to accumulating around the bottom nozzle. This accumulation began to appear after the second addition and continued through the fourth addition when a debris bed began to form around the edges of the bottom nozzle. By the time of the sixth addition, the debris buildup along the edges of the bottom nozzle and bottom of the p-grid were significant. Unlike test CIBAP25, there was no visible accumulation of debris at the first spacer grid. After the seventh and last concurrent addition, the accumulation of chemicals in the debris bed still had rough edges. Between the ninth and twelfth additions, the debris bed took on a smoother appearance. The dP peaked at [

] ^{a,c} By the time of the fourteenth addition, the edges of the debris bed were smooth, well-defined, and continued to thicken as the test progressed without a corresponding increase in dP. After the seventeenth addition, the dP was monitored until the steady state dP condition was met. With all acceptance criteria met, flow sweeps were initiated to determine the pressure drop dependence on flow rate.

The pressure drop increase occurred almost exclusively at the bottom nozzle/p-grid location as in the other tests. This can be seen by comparing the trace labeled "dP Upper" to the trace labeled "dP Lower" in Figure 8-54. The pressure drop contribution from the upper assembly was approximately [

] ^{a,c}

The average temperature for both the test column and the mixing tank during the test was []^{a,c}. The pH was measured throughout the test and reached a maximum pH of []^{a,c}. This was within the allowable range for the test (5 to 9), and therefore any dissolution of the chemical product surrogate was insignificant.

a.c

Figure 8-54 Head-Loss and Flow Rate History for Test CIBAP28

8.28 TEST #29 (CIBAP29)

This was the twenty-ninth FA debris loading head-loss experiments performed in the STC test facility for the AP1000. [

] ^{a,c} This experiment was performed according to test plan STD-MCE-09-133. This test was a repeat of test CIBAP27, except the [

] ^{a,c}

In this experiment, the debris loadings were based on a reduced AP1000 post-LOCA containment debris load of [

] ^{a,c} The results of test CIBAP29 are plotted in Figure 8-55. All debris was added concurrently.

The first concurrent addition of particulate, fiber, and chemical precipitates had little effect on the head-loss across the full assembly resulting in a [

] ^{a,c}

During this time, the test procedure was followed using the procedure information to reduce the flow rate commensurate with the increase in dP.

Similar to previous concurrent debris addition tests, the fiber accumulated around the bottom of the p-grid prior to accumulating around the bottom nozzle. This accumulation begins to appear just after the second addition and continued through the fourth addition when a debris bed began to form around the edges of the bottom nozzle. Similar to test CIBAP22, there was visible accumulation of debris at the second spacer grid, but in this test there was very little on the first spacer grid. By the time of the sixth addition, the debris buildup along the edges of the bottom nozzle and bottom of the p-grid were significant. After the seventh concurrent addition, the accumulation of chemicals in the debris bed was easily seen and the debris bed still had rough edges. The dP peaked at [] ^{a,c} By the time of the fifteenth addition, the edges of the debris bed were smooth, well-defined, and continued to thicken as the test progressed without a corresponding increase in dP. After the seventeenth and final addition, the dP was monitored until the steady state dP condition was met. With all acceptance criteria met, flow sweeps were initiated to determine the pressure drop dependence on flow rate. The debris was thick and smooth at the time of the flow sweeps, yet did not cause an increase in the steady state dP.

The pressure drop increase occurred almost exclusively at the bottom nozzle/p-grid location as in the other tests. The accumulation of debris in the second spacer grid showed a [

] ^{a,c}

The average temperature for both the test column and the mixing tank during the test was []^{a,c} The pH as measured throughout the test reaching a maximum pH of []^{a,c} This was within the allowable range for the test (5 to 9), so any dissolution of the chemical product surrogate was insignificant.

a,c

Figure 8-55 Head-Loss and Flow Rate History for Test CIBAP29

8.29 TEST #30 (CIBAP30)

This was the thirtieth FA debris loading head-loss experiments performed in the STC test facility for the AP1000. [

] ^{a,c} This experiment was performed according to test plan STD-MCE-09-135 presented in Appendix C. [

] ^{a,c}

In this experiment, the debris loadings were based on a reduced AP1000 post-LOCA containment debris load of [

] ^{a,c} The results of test CIBAP30 are plotted in Figure 8-56.

The first concurrent addition of silicon carbide particulate, fiber, and chemical precipitates had little effect on the head-loss across the full assembly resulting in a [

] ^{a,c}

During this time, the test procedure was being followed using the procedure information to reduce the flow rate commensurate with the increase in dP.

Similar to previous tests, the fiber accumulated around the bottom of the p-grid prior to accumulating around the bottom nozzle (Figure 8-57). This accumulation began to appear just after the second addition and continued through the fourth addition, when a debris bed began to form around the edges of the bottom nozzle Figure 8-58. By the time of the fifth addition (Figure 8-59), the debris buildup along the edges of the bottom nozzle and bottom of the p-grid were apparent. Unlike test CIBAP29, there was minimal accumulation of debris at the first and second spacer grids early in the test. After the seventh concurrent addition, the accumulation of chemicals in the debris bed was observed and the debris bed still had rough edges. Between the ninth and twelfth additions, the debris bed took on a smoother appearance (Figure 8-60 and Figure 8-61) as the chemical coated the debris bed. The dP peaked at [

] ^{a,c} Between the fifteenth and sixteenth additions, the dP dropped again due to a break through within the debris bed. After the seventeenth addition (Figure 8-62), the dP was monitored until the steady state dP condition was met. With all acceptance criteria met, flow sweeps were initiated to determine the pressure drop dependence on flow rate. Near the end of the flow sweeps, the debris was thick and smooth (Figure 8-63), yet did not cause an increase in the steady state dP.

Of note in this test is the initial accumulation of debris along the edge of the upper left of the bottom nozzle opening as seen in Figure 8-58. By the time of the fifth addition (Figure 8-59), an opening began to appear along the upper left edge. By the ninth addition, a clean path was established (Figure 8-60) and it remained open until test termination (Figure 8-63).

The pressure drop increase occurred almost exclusively at the bottom nozzle/p-grid location as in the other tests. This can be seen by comparing the trace labeled “dP Upper” to the trace labeled “dP Lower” in Figure 8-56. [

] ^{a,c}

^{a,c}

Figure 8-56 Head-Loss and Flow Rate History for Test CIBAP30



Figure 8-57 Accumulation of Debris at the Bottom Nozzle and P-Grid 30 Minutes After the Third Concurrent Addition in Test CIBAP30



Figure 8-58 Accumulation of Debris at the Bottom Nozzle and P-Grid 30 Minutes After the Fourth Concurrent Addition in Test CIBAP30



Figure 8-59 Accumulation of Debris at the Bottom Nozzle and P-Grid 30 Minutes After the Fifth Concurrent Addition in Test CIBAP30



Figure 8-60 Accumulation of Debris at the Bottom Nozzle and P-Grid 30 Minutes After the Ninth Chemical Addition in Test CIBAP30



a,c

Figure 8-61 Accumulation of Debris at the Bottom Nozzle and P-Grid 30 Minutes After the Twelfth Chemical Addition in Test CIBAP30



a,c

Figure 8-62 Accumulation of Debris at the Bottom Nozzle and P-Grid 30 Minutes After the Seventeenth Chemical Addition in Test CIBAP30



Figure 8-63 Accumulation of Debris at the Bottom Nozzle and P-Grid Near the End of the Flow Sweeps in Test CIBAP30

8.30 TEST #31 (CIBAP31)

This was the thirty-first of the FA debris loading head-loss experiments performed in the STC test facility for the AP1000. With the debris load and chemical precipitate tested, the peak head-loss recorded for this test was [

] ^{a,c} The results of test CIBAP31 are plotted in Figure 8-64.

[

] ^{a,c}

During this time, the test procedure was being followed to reduce the flow rate commensurate with the increase in dP.

Similar to previous tests, the fiber accumulated around the bottom of the p-grid prior to accumulating around the bottom nozzle. This accumulation began to appear just after the second addition and continued through the fourth addition when a debris bed began to form around the edges of the bottom nozzle. By the time of the fifth addition, the debris buildup along the edges of the bottom nozzle and bottom of the p-grid were apparent. There was little accumulation of debris at the first and second spacer grids early in the test. After the seventh concurrent addition, the accumulation of chemicals in the debris bed was observed and the debris bed still had rough edges. Between the ninth and twelfth additions, the debris bed took on a smoother appearance as the chemical coated the debris bed on the bottom nozzle only. The debris bed on the bottom of the p-grid was not as smooth and the accumulation was more sporadic along the grid. By the time of the ninth addition, the edges of the debris bed were smooth, well-defined and the dP continued to increase. It continued to thicken as the test progressed with only a small increase in dP. Between the eleventh and thirteenth additions the dP dropped due to a breakthrough within the debris bed, but the dP eventually climbed back up. After the seventeenth addition, the dP became steadier and was monitored until the steady state dP condition was met. [

] ^{a,c} With all acceptance criteria met, flow sweeps were initiated to determine the pressure drop dependence on flow rate. Near the end of the flow sweeps, the debris bed was thick and smooth, yet it did not cause an increase in the steady state dP.

The pressure drop increase occurred almost exclusively at the bottom nozzle/p-grid location as in the other tests. This can be seen by comparing the trace labeled “dP Upper” to the trace labeled “dP Lower” in Figure 8-64. [

] ^{a,c}

The average temperature for both the test column and the mixing tank during the test was []^{a,c}
The pH was measured throughout the test reaching a maximum pH of []^{a,c}. This was within the allowable range for the test (5 to 9), so any dissolution of the chemical product surrogate was insignificant.



Figure 8-64 Head-loss and Flow Rate History for Test CIBAP31

8.31 TEST #32 (CIBAP32)

This was the thirty-second of the FA debris loading head-loss experiments performed in the STC test facility for the AP1000. [

] ^{a,c} This experiment was performed according to test plan STD-MCE-10-03. This test was an exact repeat of test CIBAP30. [

] ^{a,c} The results of test CIBAP32 are plotted in Figure 8-65. [

[

] ^{a,c}

During this time, the test procedure was being followed to reduce the flow rate commensurate with the increase in dP.

Similar to previous tests, the fiber accumulated around the bottom of the p-grid prior to accumulating around the bottom nozzle. This accumulation began to appear just after the second addition and continued through the fourth addition when a debris bed began to form around the edges of the bottom nozzle. By the time of the fifth addition, the debris buildup along the edges of the bottom nozzle and bottom of the p-grid were apparent. Unlike test CIBAP31, the debris collected evenly across the bottom nozzle and bottom of the p-grid. There was very little accumulation of debris at the first and second spacer grids early in the test. After the seventh and last concurrent addition, the accumulation of chemicals in the debris bed was observed and the debris bed still had rough edges. Between the ninth and twelfth additions, the debris bed took on a smoother appearance as the chemical coated the debris bed. By the time of the fourteenth addition, the edges of the debris bed were smooth and well-defined. It continued to thicken as the test progressed with only a small increase in dP, showing more of an increase than CIBAP31. Between the fourteenth and sixteenth additions, the dP dropped again due to a breakthrough within the debris bed. [

] ^{a,c} The dP was monitored and continued to rise steadily until the last addition. At that point, the dP finally became steady. With all acceptance criteria met, flow sweeps were initiated to determine the pressure drop dependence on flow rate. Near the end of the flow sweeps, the debris bed was thick and smooth, yet it did not cause an increase in the steady state dP.

The pressure drop increase occurred almost exclusively at the bottom nozzle/p-grid location as in the other tests. The accumulation of debris in the second spacer grid shows [

] ^{a,c}

The average temperature for both the test column and the mixing tank during the test was [] ^{a,c}
The pH was measured throughout the test reaching a maximum pH of [] ^{a,c} This was within the allowable range for the test (5 to 9), so any dissolution of the chemical product surrogate was insignificant.

] ^{a,c}

Figure 8-65 Head-loss and Flow Rate History for Test CIBAP32

8.32 TEST #33 (CIBAP33)

This was the thirty-third of the FA debris loading head-loss experiments performed in the STC test facility for the AP1000. [

] ^{a,c} This experiment was performed according to test plan STD-MCE-10-04. This test was an exact repeat of test CIBAP30. [

] ^{a,c} All debris was added concurrently.

[

] ^{a,c}

Throughout the test, the test procedure was followed using the procedure information to reduce the flow rate commensurate with the increase in dP.

Similar to previous tests, the fiber accumulated around the bottom of the p-grid prior to accumulating around the bottom nozzle. This accumulation began to appear just after the second addition and continued through the fourth addition when a debris bed began to form around the edges of the bottom nozzle. By the time of the fifth addition the debris buildup along the edges of the bottom nozzle and bottom of the p-grid were apparent. There was very little accumulation of debris at the first and second spacer grids early in the test. After the seventh concurrent addition, the accumulation of chemicals in the debris bed was observed and the debris bed still had rough edges. Between the ninth and twelfth additions, the debris bed took on a smoother appearance as the chemical coated the debris bed. It continued to thicken as the test progressed with only a [] ^{a,c} Between the fifteenth and sixteenth additions, the dP dropped again due to a breakthrough within the debris bed. By the time of the seventeenth addition, the edges of the debris bed were smooth and well-defined. After the seventeenth addition, the dP was monitored until the steady state dP condition was met. With all acceptance criteria met, flow sweeps were initiated to determine the pressure drop dependence on flow rate. Near the end of the flow sweeps, the debris bed was thick and smooth, yet it did not cause an increase in the steady state dP.

The pressure drop increase occurred almost exclusively at the bottom nozzle/p-grid location as in the other tests. [

] ^{a,c}

The average temperature for both the test column and the mixing tank during the test was []^{a,c}
The pH was measured throughout the test reaching a maximum pH of []^{a,c} This was within the allowable range for the test (5 to 9), so any dissolution of the chemical product surrogate was insignificant.



Figure 8-66 Head-loss and Flow Rate History for Test CIBAP33

8.33 TEST #34 (CIBAP34)

This was the thirty-fourth of the FA debris loading head-loss experiments performed in the STC test facility for the AP1000. With the debris load and chemical precipitate tested the peak head-loss recorded for this test was []^{a,c} This experiment was performed according to test plan STD-MCE-10-05. This test was a repeat of CIBAP30, but with a modified flow profiling scheme. In CIBAP30 and other recent tests, [

] ^{a,c} At the end of the test, the flow was varied more quickly to determine the pressure drop dependence on flow rate. Thus, this experiment included flow profiling both at the end of the test and also at earlier times when peak pressure drops were often experienced.

The peak pressure of []^{a,c} In this experiment the debris loadings were based on a reduced AP1000 post-LOCA containment debris load of 180 pounds, consisting of 6.6 pounds of fiber, 173.4 pounds of particulates and 57 pounds of chemical precipitates (Reference 5). [

] ^{a,c} The results of test CIBAP34 are plotted in Figure 8-67. All debris was added concurrently.

[

] ^{a,c}

Throughout the remainder of the test, after the first addition, the test procedure was followed using the information in the test plan to reduce the flow rate commensurate with the increase in dP. This procedure was utilized for [

] ^{a,c}

Similar to previous tests, the fiber accumulated around the bottom of the p-grid prior to accumulating around the bottom nozzle. This accumulation began to appear just after the second addition and continued through the fourth addition (Figure 8-68 and Figure 8-69) when a debris bed began to form around the edges of the bottom nozzle. By the time of the fifth addition, the debris buildup along the edges of the bottom nozzle and bottom of the p-grid were apparent. After the seventh concurrent addition, the accumulation of chemicals in the debris bed was observed and the debris bed still had rough edges. Between the ninth and twelfth additions (Figure 8-70 and Figure 8-71), the debris bed took on a smoother appearance as the chemical coated the debris bed. It continued to thicken as the test progressed. Between the thirteenth and fourteenth additions, the dP dropped slightly but recovered after the fourteenth addition. []^{a,c} In tests CIBAP27, CIBAP29, CIBAP30, CIBAP31, CIBAP32 and CIBAP33 the dP peaked after the twelfth addition (between the

twelfth and seventeenth additions). By the time of the seventeenth addition, the edges of the debris bed were smooth and well-defined. After the seventeenth addition, the dP was monitored until the steady state dP condition was met. With all acceptance criteria met, flow sweeps were initiated to determine the pressure drop dependence on flow rate. Near the end of the flow sweeps, the debris bed was thick and smooth, yet it did not cause an increase in the steady state dP (Figure 8-72).

The pressure drop increase occurred almost exclusively at the bottom nozzle/p-grid location as in the other tests. [

] ^{a,c}

The average temperature for both the test column and the mixing tank during the test was [] ^{a,c}
The pH was measured throughout the test reaching a maximum pH of [] ^{a,c} This was within the allowable range for the test (5 to 9), so any dissolution of the chemical product surrogate was insignificant.



Figure 8-67 Head-loss and Flow Rate History for Test CIBAP34



Figure 8-68 Accumulation of Debris at the Bottom Nozzle and P-Grid Right before the Fourth Addition in Test CIBAP34

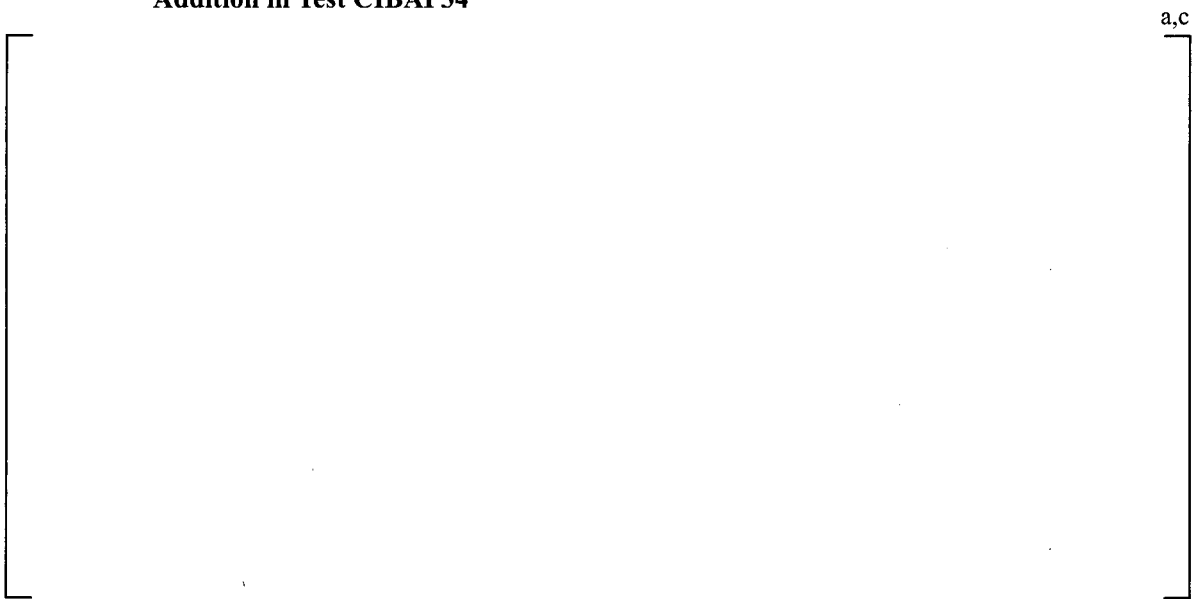


Figure 8-69 Accumulation of Debris at the Bottom Nozzle and P-Grid 30 Minutes after the Fourth Concurrent Addition in Test CIBAP34



Figure 8-70 Accumulation of Debris at the Bottom Nozzle and P-Grid 30 Minutes after the Ninth Chemical Addition in Test CIBAP34



Figure 8-71 Accumulation of Debris at the Bottom Nozzle and P-Grid 30 Minutes after the Twelfth Chemical Addition in Test CIBAP34



Figure 8-72 Accumulation of Debris at the Bottom Nozzle and P-Grid 30 Minutes after the Last Chemical Addition in Test CIBAP34

8.34 TEST #35 (CIBAP35)

This was the thirty-fifth of the FA debris loading head-loss experiments performed in the STC test facility for the AP1000. The goal of this test was to observe the effects of adding debris to a model FA under reverse flow conditions that might exist in an AP1000 reactor after a hot-leg break. The test evaluated the distribution of debris blockages within the top portion of the assembly, and the relationship between pressure and flow. To model AP1000 behavior on a hot-leg break, further testing of debris blockage with reverse flow was needed. With the debris load and chemical precipitate tested, the peak head-loss recorded for this test was []^{a,c}

This experiment was performed according to test plan STD-MCE-10-07. Debris was introduced slowly with reverse flow. The flow rate started out at the maximum pump flow of approximately []^{a,c}. The maximum flow was maintained until the pressure drop due to debris reached a value of []^{a,c}. At that point, the flow was automatically controlled to maintain a pressure drop of 0.85 psi across the assembly.

In this sensitivity experiment, the debris loadings were based on a reduced AP1000 post-LOCA containment debris load of 180 pounds, consisting of 6.6 pounds of fiber, 173.4 pounds of particulates and 57 pounds of chemical precipitates (Reference 5). []^{a,c}

The results of test CIBAP35 are plotted in Figure 8-73. All debris was added concurrently.

The first concurrent addition of silicon carbide particulate, fiber, and chemical precipitates affected the head-loss across the full assembly more than the first addition affected the dP of CIBAP31-34 up-flow tests. Immediately after the first addition, the dP resulted in []^{a,c}

The subsequent concurrent additions of the combined three debris types over next five hours resulted in increases of []^{a,c}

However, this test was a scoping test for the upcoming down-flow tests.

Unlike the previous tests, the fiber accumulated around top nozzle because of reverse flow. The water flowed entered through a 1.5" nozzle at the top of the test column and flowed downward and exited through a port at the bottom of the column. The flow at the top of the column passed through an acrylic structure which simulated the upper internals.

This accumulation began to appear on the top of the top grid after the first addition. After the second concurrent addition the dP peaked at []^{a,c}. After the third concurrent addition, the bed on the top grid became thicker and showed a smoother appearance. Also, after the third addition it became apparent that debris was settling on the bottom of the top nozzle and was forming a bed. The dP at this time became steady but the flow began to decrease quickly. By the sixth addition there was a noticeable bed on an intermediate grid. The bed on the top grid thickened, causing flow resistance.

The average temperature for both the test column and the mixing tank during the test was []^{a,c}
The pH was measured throughout the test, reaching a maximum pH of []^{a,c}. This was within the allowable range for the test (5 to 9), so any dissolution of the chemical product surrogate was insignificant.



Figure 8-73 Head-loss and Flow Rate History from Test CIBAP35

8.35 TEST #36 (CIBAP36)

This was the thirty-sixth of the FA debris loading head-loss experiments performed in the STC test facility for the AP1000. With the debris load and chemical precipitate tested, the peak head-loss recorded for this test was []^{a,c} This experiment was performed according to test plan STD-MCE-10-10. This test was a repeat of CIBAP30, with the difference being that chemicals were added to the loop to simulate reactor coolant and the loop was heated. []

[]^{a,c} The results of test CIBAP36 are plotted in (Figure 8-74.) All debris was added concurrently. The schematic of the test loop for CIBAP36 can be found in Figure 4-3.

The first concurrent addition of silicon carbide particulate, fiber, and chemical precipitates had little effect on the head-loss across the full assembly []^{a,c} One hour later the second concurrent addition increased the pressure drop to []^{a,c} The subsequent concurrent additions of the combined three debris types over next five hours resulted in increases of []

[]^{a,c}

Throughout the test, the test procedure was followed using the procedure information to reduce the flow rate commensurate with the increase in dP.

Similar to previous tests, the fiber accumulated around the bottom of the p-grid prior to accumulating around the bottom nozzle. This accumulation began to appear just after the second addition and continued through the third addition when a debris bed began to form around the edges of the bottom nozzle Figure 8-75. By the time of the fifth addition, the debris buildup along the edges of the bottom nozzle and bottom of the p-grid were apparent. The accumulation of the debris on the bottom nozzle formed a thin bed, but covered the entire surface at the ninth addition (Figure 8-76). The debris that was collected on the bottom of the p-grid collected mainly to one side and the debris was clumped together. After the eleventh addition, the debris bed on the bottom nozzle took on a smoother appearance as the chemical coated the bed. It continued to thicken as the test progressed with only a small increase in dP (Figure 8-77 and Figure 8-78). Between the fifteenth and sixteenth additions, the dP dropped again due to a breakthrough within the debris bed. After the seventeenth addition, Figure 8-79, the dP was monitored until the steady state dP condition was met. At this time the edges of the debris bed were smooth and well- defined. With all acceptance criteria met, flow sweeps were initiated to determine the pressure drop dependence on flow rate. Near the end of the flow sweeps, the debris bed was thick and smooth, yet it did not cause an increase in the steady state dP.

Overall, adding the chemicals to simulate reactor coolant and increasing the loop temperature to []^{a,c} resulted in a lower dP compared to the previous tests.

The pressure drop increase occurred almost exclusively at the bottom nozzle/p-grid location as in the other tests. The accumulation of debris in the [

] ^{a,c}

[

] ^{a,c}

a,c



Figure 8-74 Head-loss and Flow Rate History for Test CIBAP36



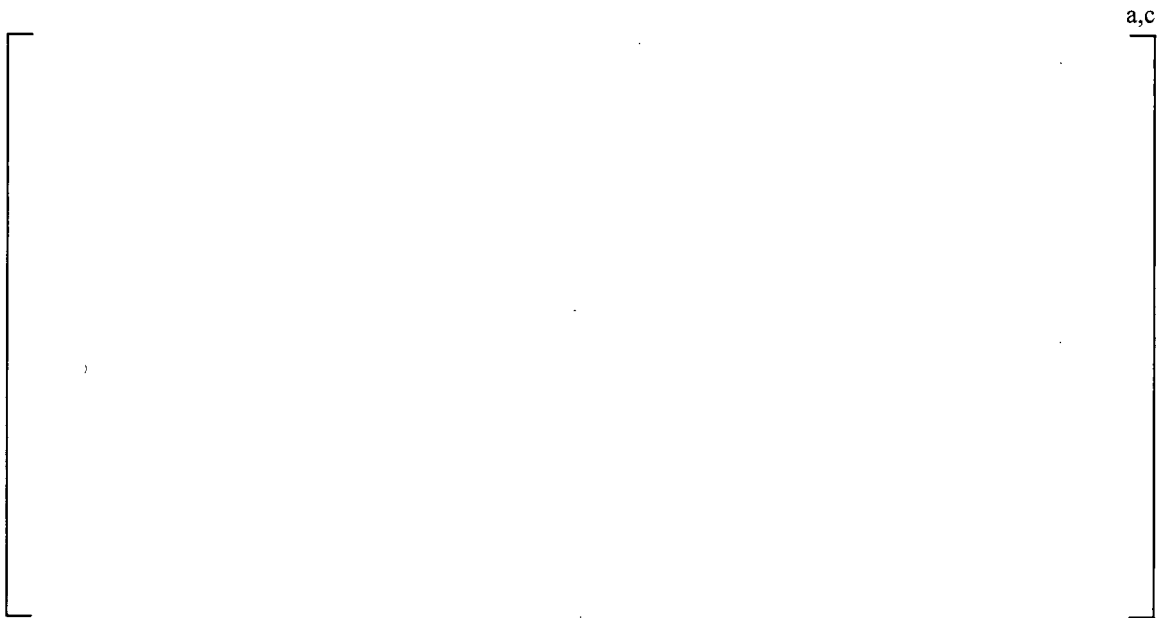
Figure 8-75 Accumulation of Debris at the p-grid 30 Minutes after the Third Concurrent Addition in Test CIBAP36



Figure 8-76 Accumulation of Debris at the p-grid 30 Minutes after the Ninth Chemical Addition in Test CIBAP36



**Figure 8-77 Accumulation of Debris at the p-grid 30 Minutes after the Fifteenth Chemical Addition
in Test CIBAP36**



**Figure 8-78 Accumulation of Debris at the Third Grid 30 Minutes after Fifteenth Chemical in Test
CIBAP36**



Figure 8-79 Accumulation of Debris at the p-grid at the End of the Test CIBAP36

8.36 TEST #37 (CIBAP37)

This was the thirty-seventh of the FA debris loading head-loss experiments performed in the STC test facility for the AP1000. With the debris load and chemical precipitate tested, the peak head-loss recorded for this test was []^{a,c} This experiment was performed according to test plan STD-MCE-10-11. The test was conducted at a temperature of []

[]^{a,c} The results of test CIBAP37 are plotted in (Figure 8-80). All debris was added concurrently. This test is a repeat of CIBAP36. CIBAP37 was conducted to evaluate the effects of TSP, Boric Acid and high temperature experimenting on repeatability. The schematic of the test loop for CIBAP37 is found in Figure 4-3.

[]

[]^{a,c} after the eleventh addition. Throughout the test, the test procedure was followed using the procedure information to reduce the flow rate commensurate with the increase in dP.

Similar to previous tests, the fiber accumulated around the bottom of the p-grid prior to accumulating around the bottom nozzle. This accumulation began to appear just after the first addition and continued through the fourth addition when a debris bed began to form around the edges of the bottom nozzle. By the time of the fifth addition, the debris development along the edges of the bottom nozzle and bottom of the p-grid were apparent. Debris started to collect on the third grid from the bottom nozzle, which was unlike the previous tests. After the ninth addition, the debris bed on the p-grid took on a smoother appearance as the chemical coated the bed. []

[]^{a,c} After the thirteenth addition, the chemical on the bed of the p-grid became more apparent. It continued to thicken as the test progressed with only a small increase in dP. After the seventeenth addition, the dP was monitored until the steady state dP condition was met. At this time the edges of the debris bed were smooth and well-defined. With all acceptance criteria met, flow sweeps were initiated to determine the pressure drop dependence on flow rate. Near the end of the flow sweeps, the debris bed was thick and smooth, yet []^{a,c}

[]

[]^{a,c}

The pressure drop increase occurred almost exclusively at the bottom nozzle/p-grid location as in the other tests. [

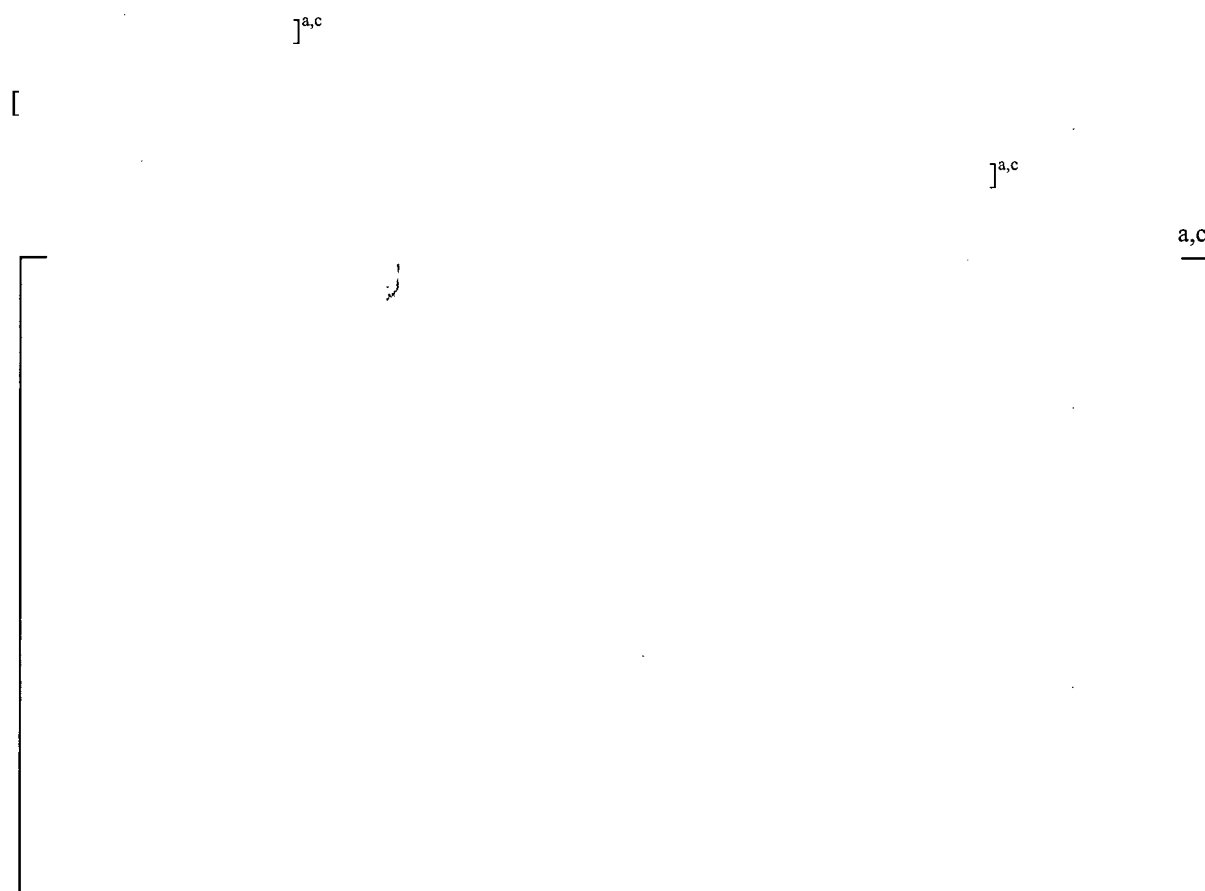


Figure 8-80 Data Plot from Test CIBAP37 Baseline dP Corrected to Zero

8.37 TEST #38 (CIBAP38)

This was the thirty-eighth of the FA debris loading head-loss experiments performed in the STC test facility for the AP1000. This experiment was performed according to test plan STD-MCE-10-13. The goal of this test was to observe the effects of adding debris to a model FA under simulated hot-leg break conditions. With the debris load and chemical precipitate tested, the peak head-loss recorded for this test was []^{a,c} The conditions simulated in this test were reverse flow, followed by upward flow with boiling. The location of the debris within the assembly and its movement were monitored as well as how the debris affected coolant flow within the assembly. [

] ^{a,c} The schematic of the test loop can be found in Figure 4-2 for the down-flow portion of the test and Figure 4-4 for the up-flow with simulating boiling.

In an actual hot-leg LOCA in an AP1000, the flow in the upper part of the core is expected to oscillate over several minutes. When the down-flow in a low-power assembly becomes low, the steam generated rises upwards. The production of steam, together with other thermal hydraulic forces acting on the system, would result in a change in flow direction from a downward to an upward direction. This flow reversal and its effect on a debris bed were explored in test CIBAP38. [

] ^{a,c}

[

] ^{a,c}

[

] ^{a,c} The results of test CIBAP38 are plotted in Figure 8-81.

[

] ^{a,c}

The average temperature for both the test column and the mixing tank during the test was [] ^{a,c}
The pH was measured throughout the test reaching a maximum pH of [] ^{a,c}. This was within the allowable range for the test (5 to 9), so any dissolution of the chemical product surrogate was insignificant.

a,c



Figure 8-81 Data Plot from Test CIBAP38 Baseline dP Corrected to Zero



Figure 8-82 Photograph of the Top-Grid 59 Minutes after the First Concurrent Addition in Test CIBAP38



Figure 8-83 Photograph of the Top-Grid after Stable Air and Water Flow are Achieved in Test CIBAP38



Figure 8-84 Photograph of the Top Grid Seconds before Simulating Boiling Began



Figure 8-85 Photograph of the Top Grid 6 Seconds after Simulated Boiling Began

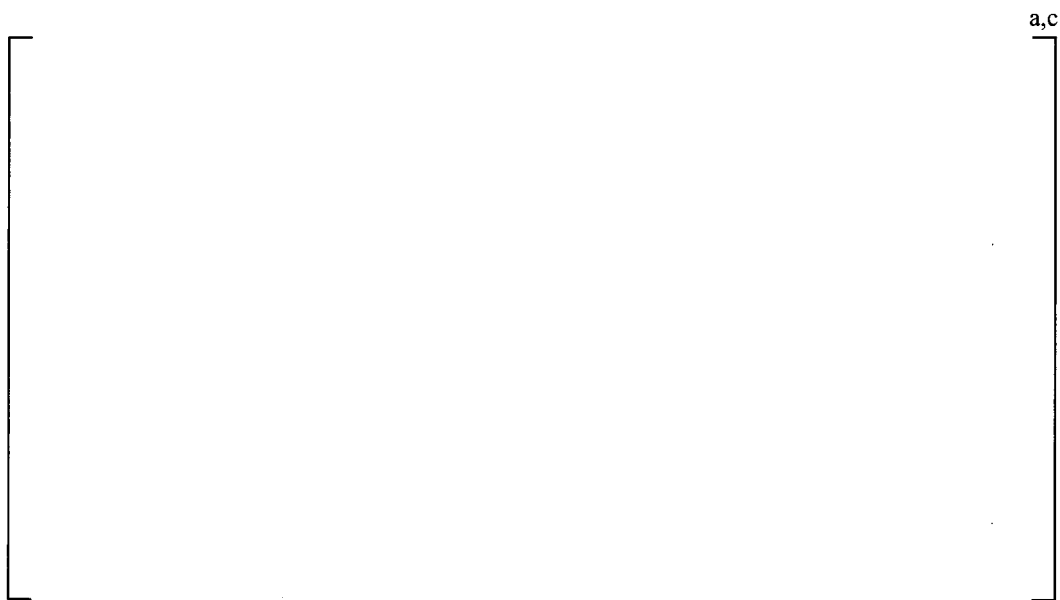


Figure 8-86 Photograph of the Top Grid 12 Seconds after Simulated Boiling Began



Figure 8-87 Photograph of the Top Grid 19 Seconds after Simulated Boiling Began



Figure 8-88 Photograph of the Top Grid 24 Seconds after Simulated Boiling Began



Figure 8-89 Photograph of a Spacer 51 Minutes after First Addition (SiC) During Up-flow in Test CIBAP38



Figure 8-90 Photograph of the Top-Grids 51 Minutes after First Addition (SiC) During Up-flow in Test CIBAP38



Figure 8-91 Photograph of the Top-Grid 51 Minutes after First Addition (SiC) During Up-flow in Test CIBAP38



Figure 8-92 Photograph of the p-grid after Flow Sweeps in Test CIBAP38

8.38 TEST #39 (CIBAP39)

This was the thirty-ninth of the FA debris loading head-loss experiments performed in the STC test facility for the AP1000. With the debris load and chemical precipitate tested, the peak head-loss recorded for this test was roughly [

] ^{a,c} This experiment was performed according to test plan STD-MCE-10-15, which simulated boiling during the whole experiment.

The goal of this test was to observe the effects of adding debris to a model FA under simulated hot-leg break conditions. The conditions simulated in this test were upward flow of coolant with boiling. The location of the debris within the assembly and its movement were monitored as well as how the debris affected coolant flow within the assembly.

After a hot-leg break in the AP1000, debris may be transported into the break and then into the upper plenum of the reactor. From there it may be carried deeper into the core by coolant which flows down through the outer, low-power assemblies and then up through the central, high-power assemblies. The down-flow is expected to penetrate downward about 25 to 30% of the core height (Reference 3). Debris may collect at spacer grids during up-flow causing a pressure drop and reducing flow of coolant. In an actual hot-leg LOCA in an AP1000, the flow in the upper part of the core is expected to oscillate over several minutes. When the down-flow in a low-power assembly becomes low, the steam generation increases. The production of steam, together with other thermal hydraulic forces acting on the system, would result in a change in flow direction from the downward to upward direction. This flow reversal and its effect on a debris bed were explored in test CIBAP38. [

] ^{a,c} The schematic of the test loop can be found in Figure 4-4.

[

] ^{a,c} The results of test CIBAP39 are plotted in (Figure 8-93). All debris was added concurrently and two chemical additions were added at the end.

[

] ^{a,c}

Flow profiling was performed at the beginning of the test before the debris was added (clean loop).

Forty minutes after each debris addition, another flow sweep was performed. [

] ^{a,c} This was done to determine if any debris blockage or flow resistance was present vs. a clean FA. The profiling was done without air flow to increase the sensitivity of the measurement, since pressure readings during the air flow were highly variable. Flow sweeps were done instead of maintaining a constant flow with no air flow, because measurement of the dP variation with flow is not sensitive to zero shifts in the dP sensors. Air can be trapped in the dP tap lines, which if not completely removed, will cause an erroneous dP reading due to the change in static head. The change in pressure during a flow profile, however, will not be affected by trapped air.

There was a significant dP increase between the clean assembly profiling and assembly profiling after debris addition. The maximum dP increase in going from [] ^{a,c} occurred during the first flow profiling after debris addition. [] ^{a,c} However, this change in pressure drop observed during profiling after debris is insignificant in comparison to our available head of [] ^{a,c}

[] ^{a,c}

The average temperature for both the test column and the mixing tank during the test was [] ^{a,c}

The pH was measured throughout the test reaching a maximum pH of [] ^{a,c} This was within the allowable range for the test (5 to 9), so any dissolution of the chemical product surrogate was insignificant.

^{a,c}



Figure 8-93 Data Plot from Test CIBAP39 Baseline dP Corrected to Zero



Figure 8-94 Photograph of the Spacer Grid 34 Minutes after the First Concurrent Addition in Test CIBAP39

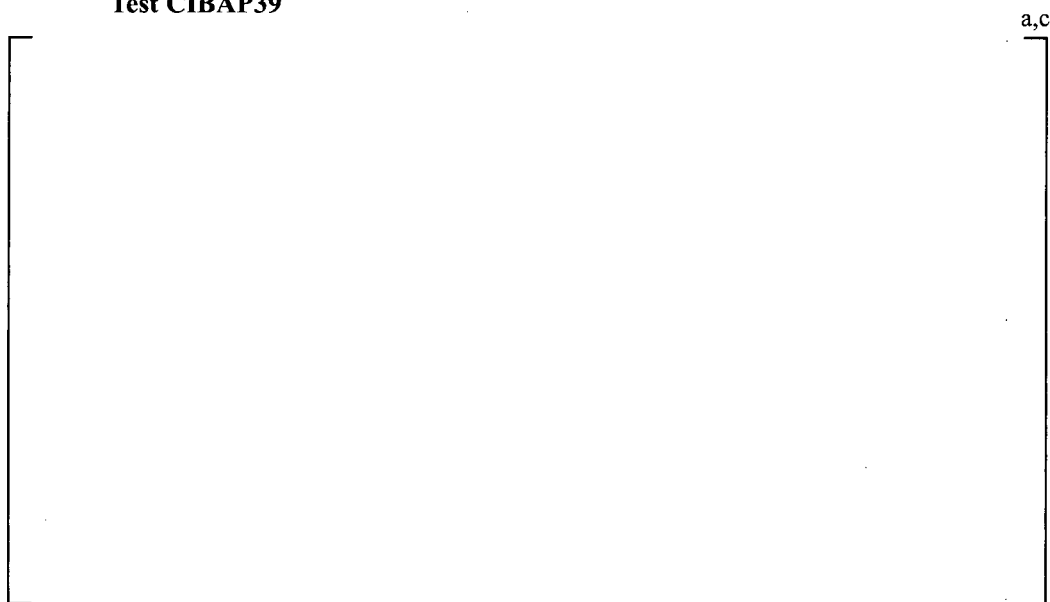


Figure 8-95 Photograph of the Spacer Grid 34 Minutes after the Second Concurrent Addition in Test CIBAP39



Figure 8-96 Photograph of the Spacer Grid 30 Minutes during Water and Air Flow Stabilization for 60 Minutes after the Last Chemical Addition



Figure 8-97 Photograph during Water and Air Flow Stabilization for 60 Minutes after the Last Chemical Addition



Figure 8-98 Photograph of the Top-Grid during Water and Air Flow Stabilization for 60 Minutes after the Last Chemical Addition

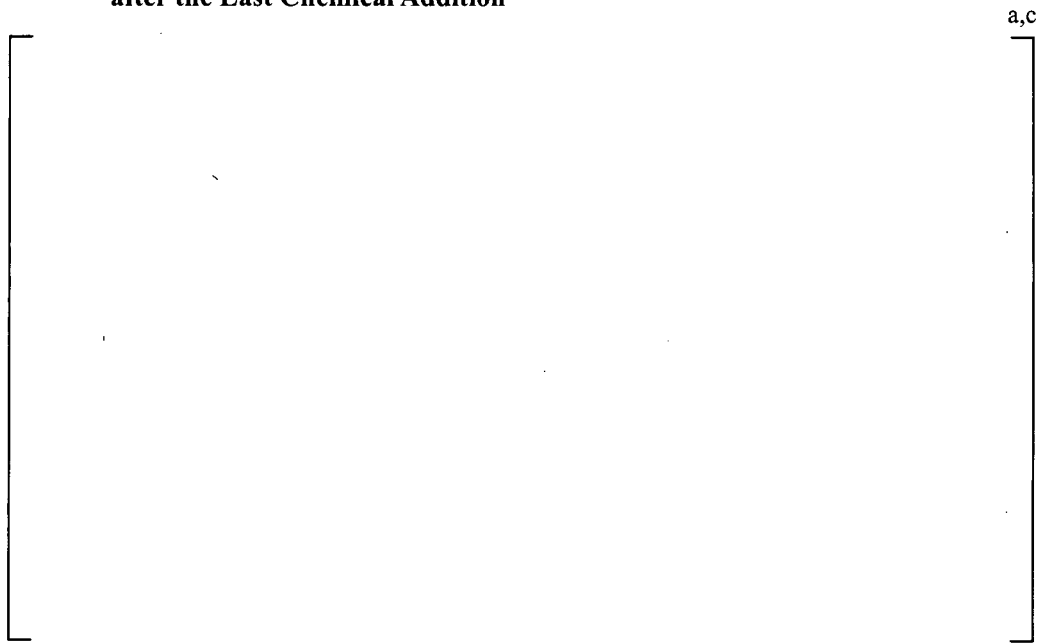


Figure 8-99 Photograph of the Spacer Grid during the Last Flow Profile in Test CIBAP39

8.39 PRESSURE DIFFERENTIAL WITH FLOW

The results obtained from the AP1000 FA tests have been used to provide an experimental basis to determine the dependence of the pressure loss through the FA on the flow rate once a debris bed was formed as described in Section 5.1. The following three subsections describe this evaluation. The first shows the analysis of flow/dP data from the later portions of each test when the bed dP stopped changing. The second subsection evaluates the stability of the bed resistance during these times. The third subsection evaluates the flow/dP at the peak dP condition and compares it with the stable bed behavior.

8.39.1 Variation of dP with Variation of Flow and End-of-Test Data

Tests CIBAP18 through CIBAP34, CIBAP36 and CIBAP37 were performed with flow sweeps at the end of each test to investigate the dependence of the loss of pressure through the FA on the flow rate as discussed in Section 5.0. Tests CIBAP08 through CIBAP11 were performed with oscillating flow rates in order to simulate the long-term behavior of the AP1000 as discussed above in the test results Section 8.0. The oscillatory nature of tests CIBAP08 through CIBAP11 provides another way to investigate the dependence of the loss of pressure through the FA on the flow rate.

The pressure drop (dP) versus flow relationship plots for tests CIBAP08 through CIBAP11 and tests CIBAP18 through CIBAP30 are presented in Reference 14, and test CIBAP31 through CIBAP34, CIBAP36 and CIBAP37 are presented in Reference 15. Examples from each of the test series are provided below.

Tests CIBAP09 and CIBAP11 were sequential addition tests performed with oscillating flow between []^{a,c} (Section 8.9, Figure 8-8 and Section 8.11, Figure 8-10). The resulting dP vs. flow curves are shown in Figure 8-100 and Figure 8-101 along with the power curve fit that provides the exponent used in Eq. 5.1.1 to define the relationship of the test data to the acceptance criterion of 4.1 psid (Section 5.0). For tests CIBAP08 through CIBAP11 the data was taken after all debris had been added and the flow and dP had stabilized.

The “hysteresis” shown in Figure 8-100 and Figure 8-101 is unique to all of the oscillating flow tests. The two dense clouds of points at the bottom and at the top of the loop are the data collected when the flow rate was constant at []^{a,c} respectively (steady state conditions). These data fit the power law relationship well as is shown in Figure 8-100 and Figure 8-101. The data collected during the increasing and decreasing flow rate phase of each cycle are distributed along a loop contour. In particular (see Figure 8-102):

- During the flow increase from []^{a,c} the data follows the upper part of the loop, and,
- when the flow rate returns to []^{a,c} the data follows the lower part of the loop.

This behavior is related to an instrumentation time delay. The output signal of the flow meter is the average of five consecutive samples. This is not a running average; the next output signal is the average of the next five samples. The sample frequency of the flow meter is []^{a,c}
Thus, the flow meter provides an output signal:

[]^{a,c}

Also, the data acquisition computer samples the flow meter [

] ^{a,c} when the changes in flow rate are slow as in the case of the flow sweeps performed in tests CIBAP18 through CIBAP34, CIBAP36 and CIBAP37. Therefore, during the rapid changes such as in test CIBAP08 through test CIBAP11, a hysteresis which is strictly an artifact of the sampling of the instruments, appears in the data.



Figure 8-100 dP Versus Flow For Test CIBAP09



Figure 8-101 dP Versus Flow For Test CIBAP11

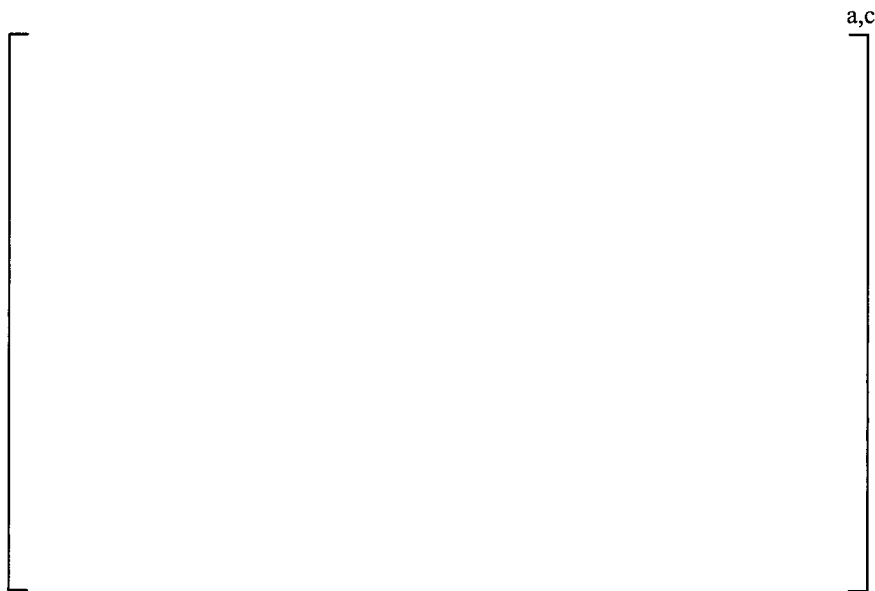


Figure 8-102 dP First and Last Flow Cycle in Test CIBAP 11

Tests CIBAP20 and CIBAP21 were sequential addition tests performed with flow between []^{a,c} (see Section 8.19, Figure 8-28 and Section 8.20, Figure 8-29). The resulting dP vs. flow curves are shown in Figure 8-103 and Figure 8-104 along with the power curve fit that provides the exponent used in Eq. 5.1.1 defining the relationship of the test data to the acceptance criterion as defined in Section 5.0. For tests CIBAP17 through CIBAP21, and CIBAP23, the data was taken from the flow sweeps after all debris had been added and the flow had stabilized. In these cases the data follows the power law relationship between dP and flow rate very well. Moreover, for all of the tests, the debris bed quickly reaches a stable resistance that does not change when the maximum and minimum flow values for the flow sweeps is repeated. This is generally true for all tests in which flow sweeps were performed.



Figure 8-103 dP Versus Flow For Test CIBAP20



Figure 8-104 dP Versus Flow For Test CIBAP21

Test CIBAP25, CIBAP26, CIBAP30 through CIBAP34, CIBAP36 and CIBAP37 were concurrent addition tests performed with flow rates between []^{a,c} (see Section 8.24, Figure 8-41 and Section 8.25 Figure 8-42) and between []^{a,c} (see Section 8.29-Section 8.33, Section 8.35 and Section 8.36, Figure 8-56, Figure 8-64, Figure 8-65, Figure 8-66, Figure 8-67, Figure 8-74, Figure 8-80). The resulting dP vs. flow curve for tests CIBAP 25, CIBAP26 and CIBAP30 are shown in Figure 8-105, Figure 8-106 and Figure 8-107 along with the power curve fit that provide the exponents used in Eq. 5.1.1 defining the relationship of the test data to the acceptance criterion as defined in Section 5.0. For tests CIBAP22, CIBAP24 through CIBAP34, CIBAP36 and CIBAP37, the data was taken from the flow sweeps after all debris had been added and the flow had stabilized. In these cases the data follows the power law relationship between dP and flow rate very well. The debris bed remains

stable once it is formed and pressure drops are repeated when the flow sweeps are repeated. Moreover, the exponent of the power law describing the data for the concurrent debris addition tests is similar to that seen in the sequential debris addition tests.



Figure 8-105 dP Versus Flow For Test CIBAP25



Figure 8-106 dP Versus Flow For Test CIBAP26



Figure 8-107 dP Versus Flow For Test CIBAP30

8.39.2 Bed Stability During Flow Sweeps

As discussed above, the experimental data indicates that during the flow sweep operations the debris bed quickly reaches a stable resistance that remains constant when the maximum and minimum flow sweep value is repeated. For example, in Figure 8-108 the data from test CIBAP20 (Figure 8-103) is displayed. The curve that fits the data collected during the [

]^{a,c} The coefficients for the two curves are nearly the same value, indicating that the debris bed resistance does not change.

a,c



Figure 8-108 dP Versus Flow for Test CIBAP20

There is one test in which a small, but well defined, variation in the debris bed resistance was observed. The dP versus flow rate data from test CIBAP18 is shown in Figure 8-109.

As seen in Figure 8-109, the data collected during the first [

] ^{a,c} For Test CIBAP18, the exponent was then estimated [

] ^{a,c}



Figure 8-109 dP Versus Flow during the First and the Last Part of the Flow Sweeps in Test CIBAP18

From the data discussed above, it is concluded that for the AP1000 debris loads tested, the debris bed collected at the bottom of the FA is stable. Specifically, the hydraulic characteristics of the bed were not observed to change significantly as [

] ^{a,c}

8.39.3 Basis for the Developed Correlation

As discussed in previous sections, many of the AP1000 tests have been conducted with variable flow rates where the flow was changed during the test as the dP increased to simulate the actual behavior of the plant. The acceptability of the AP1000 FA tests is verified by a criterion based on the LTCC sensitivity Case #10 (Reference 3). This first part of the cold-leg acceptance criteria allows a maximum head-loss of [^{a,c}] Moreover, to simulate the expected behavior of the AP1000 in the post LOCA LTCC, the later tests were performed by concurrent additions of [^{a,c}] and an additional cold-leg acceptance criteria was defined. The second part of the cold-leg acceptance criteria applies to time [^{a,c}] The second criterion is based on LTCC sensitivity Case #3 and applies to times [^{a,c}] This second criterion allows a maximum head-loss of [^{a,c}]

The use of both the criteria, as well as the correlation adopted, is discussed here.

As discussed previously, the later of the AP1000 tests were conducted with variable flow rates where the flow was changed during the test. In order to compare the results against both the first and the second criteria, the experimental results needed to be adjusted to a lower flow rate []^{a,c}

The data collected by the tests resulted in the development of the following equation which defines the relationship between head-loss and the flow rate. This equation is based on the Darcy formula and the exponent is determined by test results:

$$\left[\right]^{a,c} \quad \text{Eq 8.39.1}$$

When the debris bed is formed and stable, the pressure drop behavior of the debris bed will vary consistently with flow rate. In other words, []^{a,c} This also means that once the value of []^{a,c} it is possible to evaluate the value of the loss of pressure at any flow rate.

$$\left[\right]^{a,c} \quad \text{(Eq 8.39.2)}$$

And then

$$\left[\right]^{a,c} \quad \text{(Eq 8.39.3)}$$

where:

$$\left[\right]^{a,c}$$

The applicability of the former correlation is separately discussed and justified in the following for the two acceptance criteria.

Applicability to the First Acceptance Criterion

To compare the test results against the first acceptance criterion, the following equation is used, deduced on the basis of Eq. (8.39.3):

$$\left[\frac{\Delta P}{\rho V^2} \right]^{a,c} \quad (Eq.8.39.4)$$

where:

$$\left[\frac{\Delta P}{\rho V^2} \right]^{a,c}$$

Eq. (8.39.4) is deduced by Eq. (8.39.3) and makes use of the experimental exponents deduced by the flow sweep at the end of the tests. Moreover, the stability of the debris bed is assumed. In order to compare the results against the first acceptance criteria $\left[\frac{\Delta P}{\rho V^2} \right]^{a,c}$ the results obtained by the AP1000 FA tests are adjusted by Eq. (8.39.4) to determine the dP at the acceptance criteria flow rate.

Test CIBAP 34 was performed to investigate the nature of the flow/dP relationship throughout the test to allow comparison of the bed behavior for a fully formed and stable debris bed as well as for the initially formed debris bed.

Flow sweeps were performed throughout the duration of test CIBAP 34 and the experimental results confirm that the dP and the flow are related by a power law relationship as shown in Eq 8.39.1 even in the case of a debris bed not yet fully formed. In Figure 8-110 the dP vs. Flow data from test CIBAP 34 are reported. Each series of data is referred to a flow sweep and a best-fit curve for each series is shown also. As can be noted, Eq 8.39.1 provides an adequate fit to the data. However, both the coefficient "R" as well as the exponent "b" will evolve as the debris bed evolves.

Figure 8-111 shows the estimated values for both the $\left[\frac{\Delta P}{\rho V^2} \right]^{a,c}$ during test CIBAP 34. The results show a $\left[\frac{\Delta P}{\rho V^2} \right]^{a,c}$ to the final bed performance. They also indicate that the bed saturates with chemicals and after a point does not change.

The results from test CIBAP 34 indicate that the relationship between the dP and the flow is not affected by the decrease of flow rate during the test. Moreover, the exponent evaluated for the formed debris bed by the flow sweep in test CIBAP 34 is representative of a debris bed at its maximum resistance $\left[\frac{\Delta P}{\rho V^2} \right]^{a,c}$

[

]^{a,c}

Figure 8-112 shows the dP measured during test CIBAP 34 and the dP adjusted at []^{a,c} The peak dP occurred between []^{a,c} The debris bed reached its maximum resistance [

]^{a,c} The reason the adjusted dP is higher at this later time is that the flow rate in the test loop was reduced. Therefore, the adjustment to []^{a,c} did not reduce the flow as much. In test CIBAP 34 it can be noted that the dP adjusted to []^{a,c} remains constant when the flow rate is decreased from []^{a,c} indicating that the debris bed was stable.

This Revision has been updated to consider the dP []^{a,c} of the test, in tests such as CIBAP 34. This results in using the highest adjusted dP to compare against the current acceptance criterion.

For the AP1000 FA test results for which an experimental exponent was evaluated, it is possible to discriminate among two general types of tests. The first type of test shows the adjusted dP reaching a maximum value and then remained constant. This indicates that the bed resistance reached its maximum and did not change during the remainder of the test. Tests CIBAP 20, CIBAP 21, CIBAP 22, CIBAP 23, CIBAP 24, CIBAP 28, CIBAP 29, CIBAP 31, CIBAP 32, CIBAP 34, CIBAP 36 and CIBAP 37 belong to this first type. Test CIBAP 11 can be included in this first type also because the resistance of the bed did not change after the maximum was reached. The second type of tests shows a different behavior after the debris bed reached its maximum resistance. The value of the resistance decreased before the end of the test. Test CIBAP 08, CIBAP 09, CIBAP 10, CIBAP 18, CIBAP 19, CIBAP 25, CIBAP 26, CIBAP 27, CIBAP 30 and CIBAP 33 belong to this second type. This decrease in the bed resistance can be caused by a settlement of the bed (slow limited decrease of the resistance) as in the case of test CIBAP 27, or to a breakthrough in the bed (fast drop in the bed resistance), as in the case of test CIBAP 30 (Figure 8-113).

For tests of the first type, the exponent evaluated at the end of the test by the flow sweep is representative of a fully-formed bed at its maximum resistance. The use of such an exponent in the correlation is suitable to properly adjust the measured dP to []^{a,c} The use of such an exponent to evaluate the results of the tests of the second type could result in an underestimation of the adjusted dP.

Test CIBAP 34 belongs to the first type of test. However, in the end of the sweep interval, a spike in the flow resulted in a change of the bed resistance, suggesting that a breakthrough was caused by the spike. Thus, the last sweeps performed were not considered for the estimation of the exponent for the maximum resistance debris bed. However, the last part of the sweep offered sufficient data to estimate an exponent for the reduced-resistance debris bed. This exponent was []^{a,c} the exponent relevant to the maximum resistance bed. On this basis, a sensitivity study was performed to evaluate the effect of a reduced exponent on the dP []^{a,c} for the tests of the second type. This study considered a reduction of []^{a,c} exponents.

Table 8-3 shows the results of this study. The effect of the assumed reduction of the exponent on the adjusted dP is minimal. [

] ^{a,c} the difference in the results is negligible. Thus, for the tests of the second type, the exponent evaluated by means of the flow sweep is suitable to be used in the correlation to calculate the maximum resistance DP [] ^{a,c}

The impact of a 10% reduction on the exponent for the tests of the second type was also evaluated in the AP1000 FA debris test statistical study (Reference 19). The statistical results indicate that the probability to exceed the acceptance criteria increases less [] ^{a,c} for both the pressure drop and the natural log dP when the exponent is reduced by 10%. The results [] ^{a,c} are summarized in the table below (Table 8-4). The impact of the possible uncertainties related to the exponent is then limited on the overall probability to exceed the limits in the AP1000 core. This confirms the choice to use the exponent evaluated by means of the flow sweep (stable bed exponent) for both first type and second type of tests.

Table 8-3 Sensitivity Analysis on the Exponent for Type 2 Tests

^{a,c}

Table 8-4 Probability to Exceed Acceptance Criteria, 95% UB Standard Deviation		

^{a,c}



Figure 8-110 Evolution of the dp-Flow Relationship during Test CIBAP 34



Figure 8-111 Evolution of the Exponent and Coefficient Characterizing the dp-Flow Relationship during Test CIBAP 34

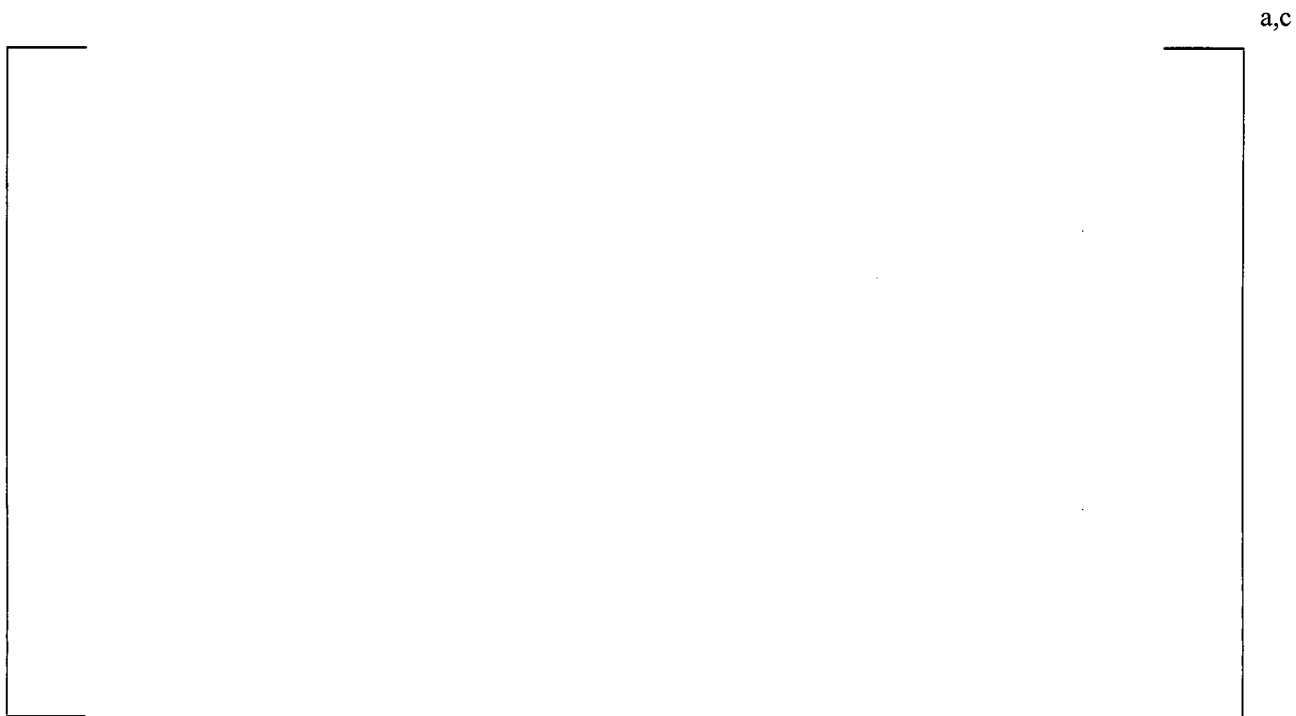


Figure 8-112 Comparison Between the Measured DP and the DP Adjusted at []^{a,c} gpm for Test CIBAP 34



Figure 8-113 Comparison Between the Measured DP And the DP adjusted at []^{a,c} gpm for Test CIBAP 30

Applicability to the Second Acceptance Criterion

The first acceptance criterion is based on the LTCC sensitivity Case 10 (Reference 3) and its limit []^{a,c} is related to the decay heat []^{a,c} after the LOCA. The second criterion is based on the LTCC sensitivity Case #3 (Reference 3), which assumes the maximum blockage condition in the core at the beginning of the recirculation. It is related to a higher level of the decay heat than Case 10.

The second criterion is aimed to verify that during the recirculation, for any level of the decay heat between the start of the recirculation phase (LTCC sensitivity case 3) and []^{a,c} (LTCC sensitivity case 10), the core will be satisfactorily cooled, requiring that the loss of head through the core []^{a,c}. Note that the concurrent debris addition FA tests were set up in order to model the plant timing of debris addition after the start of recirculation. Thus, the test time can be related to the plant time. In contrast, the sequential debris addition tests were set up to determine the maximum DP value that would be achieved under the test condition, with no reference to the time at which it would occur in the plant. For this reason the second acceptance criterion is not applicable to the sequential debris addition tests, but only to the concurrent debris addition tests.

Concerning the applicability of equation (8.39.3) to the second acceptance criterion, the use of the stable bed exponent would result in a greater underestimation of the adjusted DP. Looking at the results of test CIBAP 34, the exponent at []^{a,c} and the bed resistance is still increasing. This suggests that a reduction []^{a,c} should be applied at the stable bed exponent to extrapolate the test results at higher flow rate []^{a,c}. For conservatism, a reduction []^{a,c} on the exponent has been considered in this Revision when the second criterion is applied.

This reduction is based on the difference between the fully formed bed exponent and the lowest exponent estimated in test CIBAP 34. For the second acceptance criterion eq. (8.39.3) then becomes:

$$\left[\frac{\Delta P}{\rho V^2} \right]^{a,c} = \left[\frac{\Delta P}{\rho V^2} \right]^{a,c} \quad (\text{Eq. 8.39.5})$$

where:

$$\left[\frac{\Delta P}{\rho V^2} \right]^{a,c} = \left[\frac{\Delta P}{\rho V^2} \right]^{a,c}$$

Table 8-5 shows the test results and dP adjusted according to the second acceptance criterion.

Table 8-5 Test Results and dP Adjusted at 5.3 gpm for Comparison Against the Second Acceptance Criterion

a,c

Conclusions

The evaluation of the results obtained by the AP1000 FA tests to verify if they meet or not meet the first acceptance criterion []^{a,c} is based on the following correlation:

$$[]^{a,c}$$

The results from test CIBAP 34 indicates that the mathematical structure of the relationship between the dP and the flow is unaffected by the decrease of flow rate during the test.

To adjust the results obtained at higher flow rate []^{a,c} the dP at the maximum debris bed resistance is the proper input to use, instead of the measured peak dP, because it results in a higher adjusted dP for those tests where the peak occurred before the maximum bed resistance was reached.

The exponent used in the correlation can affect the results [

] ^{a,c} However, the analysis performed showed that the proper exponent to be used has to be related to the maximum resistance of the bed. For the Type 1 tests, the resistance does not change after its maximum is reached, and the debris bed remains stable. The exponent evaluated by the sweep at the end of the test is representative of a stable debris bed at its maximum resistance; thus it is the proper exponent to use in the correlation to verify if the results meet the first acceptance criterion.

For Type 2 tests, the resistance of the debris bed when the sweeps were performed was lower than the maximum resistance. The exponent for these tests may be [] ^{a,c} less than the value it would have if the bed resistance remained constant. The effect of this reduced exponent has been evaluated by a sensitivity analysis and the results indicate that it can be neglected. Thus the exponent estimated by the flow sweep at the end of the test will be used to extrapolate the results from higher flow rate [] ^{a,c}

In Section 5.2, the use of an average value of the exponent for those tests where an experimental exponent is not available has been discussed and justified. The experimental results suggest that the exponent relevant to the fully formed bed is independent from the way the debris were added, as well as from the way the flow rate was changed during the debris bed formation. In other words, the exponent is independent from the way the bed was formed and its variability is small. Moreover, from the point of view of the acceptability of the test results, it should be noted that even with an extremely low exponent [

] ^{a,c} This is true even when the second acceptance criterion [] ^{a,c} is applied to the max dP measured [] ^{a,c} plant time in the concurrent debris addition tests.

From a physical point of view, the relationship that relates the dP and the flow must be [

] ^{a,c}. This is consistent with the experimental evidence; even when the debris bed is not fully formed, the lowest value estimated for the exponent [] ^{a,c} In spite of the possible uncertainty related to the use of the stable bed exponent, as well as to the use of an average exponent, the dP limits are never exceeded for either criterion 1 or 2. Finally, it noted that both the acceptance criteria are based on sensitivity cases performed in the LTCC analysis (on Case #10 per the first and Case #3 per the second) and both are extremely conservative. The fact that the test results would meet the acceptance criterion means that these tests are sufficient, in spite of the variability of the test results and the uncertainty associated with the application of the developed correlations. Finally the AP1000 debris test statistical study (Reference 19) calculates a core average dP at [] ^{a,c} assuming a distribution of FA resistances; this dP is only 1.35 psi, which demonstrates a large margin to the current acceptance limit of 4.1 psi.

The second acceptance criterion applies only to the concurrent debris addition tests of [

] ^{a,c} The correlation for the second criterion is then:

$$\left[\begin{array}{c} \text{ } \\ \text{ } \\ \text{ } \end{array} \right] \begin{array}{c} \text{a,c} \\ \text{ } \\ \text{ } \end{array}$$

The reduction of []^{a,c} on the exponent is based on the experimental results obtained by test CIBAP 34.

8.40 INVALIDATED TESTS

CIBAP07 – This test was excluded due to a modification of the test loop that had been implemented prior to CIBAP07. A bypass line was added after the pump to reduce the back pressure on the pump during these relatively low flow rate tests. In this case, the valve in the bypass line was open too wide and when the back pressure increased due to the increased head-loss, too much flow was diverted through the bypass line and reduced the flow to the test column below allowable levels as set in the test plan. With the rapid drop in flow rate below the allowable level set forth in the test plan, the data was deemed to be unusable.

CIBAP12 – This test was excluded due to the addition of the constituent chemicals to the loop. The procedure for testing chemicals in the loop requires that the chemicals be mixed outside the loop per WCAP-16530-NP-A. For this test, the chemical constituents were added to the loop individually to see the effect of in-situ mixing of the chemicals. When the chemical constituents were added to the mixing tank there was a large fluctuation in the measured flow rate. This fluctuation was due to the rapid change in conductivity when the chemicals were added to the loop. The magnetic flow meter can account for changes in conductivity, but not if the changes occur too rapidly. Since the flow control system adjusts the flow rate based on feedback from the flow meter, the flow control system was attempting to compensate for the perceived spikes in the flow rate resulting in large fluctuations in the recorded data. With the rapid fluctuations in the recorded data, the data was deemed to be unusable. Additionally, this test would not have been allowed as part of the licensing basis since the chemicals were not created outside of the loop per the accepted WCAP-16530-NP-A procedure.

CIBAP17 – This test is considered invalid because there were problems with how it was conducted and with the loop configuration being different from the other AP1000 tests. Section 8.16 provides additional discussion of the problems with this test.

CIBAP35 – This test is considered exploratory because it was a pre-test to determine the effects of down-flow (debris loads, test loop schematic, flow rate and pressure limitations) for test CIBAP38.

9 CONCLUSIONS

9.1 TEST PROGRAM SUMMARY

This document presents the results of thirty-nine FA head-loss experiments that were performed to quantify the head-loss across AP1000 fuel assemblies during post-LOCA LTCC. The purpose of these experiments was to demonstrate that there is reasonable assurance that the AP1000 can provide adequate core cooling in the long-term following a LOCA.

The experiments, performed to assess the head-loss across the AP1000 fuel assemblies during LOCAs, considered a variety of parameters that might occur in the AP1000. In order to compare the different tests and to evaluate whether each test was successful, the LTCC analysis (Reference 3) was considered. As discussed in Section 5.0, the LTCC analysis for a cold-leg break allows for a 4.1 psi head-loss at a flow of []^{a,c}. None of the tests, CIBAP01-CIBAP34, CIBAP36 and CIBAP37, performed for the AP1000 had flows that were this low during the debris addition phase. In fact, the more recent AP1000 tests are run with flow rates that are representative of no-debris dP conditions and end with flow rates that are dependent on the magnitude of the core debris dP. [

] ^{a,c}

In order to determine whether a test meets the LTCC criteria, the maximum dP measured in each test is scaled, as described immediately below, based on both the flow that existed when the maximum dP occurred and the minimum acceptance flow []^{a,c} for a cold-leg break. This scaled flow provides a simple way to compare tests and to determine if the test met the acceptance criteria.

This scaling is conducted using the equation and parameters discussed in Section 5.0. [

] ^{a,c} Also note that the flow sweeps reduced the flow rate to the acceptance criteria flow so that this data is directly applicable. Such data is also available for tests CIBAP08 through CIBAP11 due to the use of oscillating flows during the tests. For Tests CIBAP01 through CIBAP06 and CIBAP13 through CIBAP16 an average exponent []^{a,c} was used. These results are shown in Table 9-1 and also in Figure 9-1. The data show considerable margin between the scaled dP and the current LTCC limit. The maximum scaled dP from the tests is []^{a,c}. In contrast, the sequential debris addition tests were set up to determine the maximum dP value that would be achieved under the test conditions. [

] ^{a,c}

For the concurrent debris addition tests that utilized flow reduction schemes, an additional limit was considered based on sensitivity Case 3 in the LTCC analysis (Reference 3). The additional criterion requires that the max dP measured during the test at a scaled flow of [

^{a,c} In all of the concurrent addition tests the flow rate was higher than []^{a,c} into the test. The test results are compared to this additional acceptance criteria are shown in Table 9-2.

The reasoning behind the acceptance criteria of [

criticism can be applied to the concurrent debris addition FA tests.]^{a,c} This acceptance

Table 9-1 AP1000 Fuel Debris Tests Scaled Results

[illegible]

Table 9-1 AP1000 Fuel Debris Tests Scaled Results
(cont.)

[illegible]

a,c

a,c

[illegible]

ac

[

] ^{a,c}

9.1.1 Latent Fiber Length

The AP1000 by design is a low-fiber plant. No fiber is produced by the LOCA. All of the fiber available for transport is latent fiber and the amount of this fiber is carefully controlled. The limiting break locations are cold-leg or (DVI breaks that become flooded by the water in the containment. In such LOCAs all of the fiber that can be transported into the RCS flows through the break. As a result, the fiber that reaches the core will not have passed through a screen and will have characteristics of the original latent fiber.

Several tests were performed to determine the fiber length that produces the maximum head-loss. Six tests were performed to make this determination. [

] ^{a,c}

Two additional tests (CIBAP13 and CIBAP14) were conducted to further evaluate [

] ^{a,c}

Questions arose on effect of the pump of fiber length and on the fibers used in AP1000 testing. [

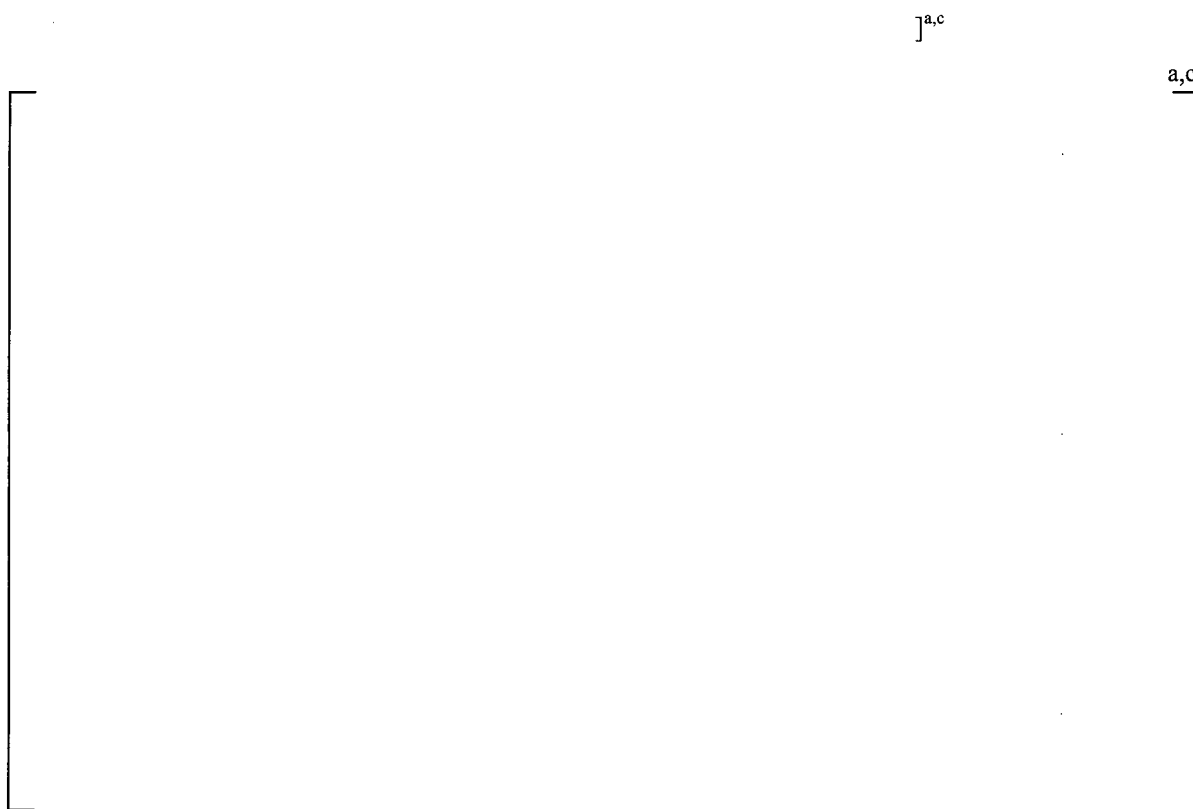


Figure 9-2 Fibers Photographed Near the End of Test CIBAP11

[

]a,c



Figure 9-3 Resident Fibers Collected from Plant B Described in NUREG/CR 6877

[

] ^{a,c}

In these tests, as well as the other AP1000 cold-leg break tests, most of the FA head-loss occurred [^{a,c}

9.1.2 Chemical Addition Rate

The early AP1000 tests showed that there was minimal, if any, head-loss after the addition of all of the particles and fibers. However, when the chemicals were added [

] ^{a,c}

For example, in some of the earlier tests (CIBAP01 through CIBAP05), [

] ^{a,c}

In subsequent tests (for example, tests CIBAP06 through CIBAP11), the initial chemical addition was [

[

] ^{a,c}

The second evolution of the chemical addition method was to make the addition [

] ^{a,c}

The third method of chemical addition was to add the AlOOH chemical solution [

] ^{a,c} This practice was started on test CIBAP21. This method of introduction did not produce clearly different pressure drops, but was retained for tests after CIBAP21 since it was thought to be the most realistic.

In summary, [

] ^{a,c} the addition of chemical surrogates to the AP1000 licensing basis debris loads induced an increase in head-loss across the FA, and this increase was always within acceptance limits.

Another phenomenon that was observed [

] ^{a,c}

9.1.3 Debris Quantities

Most of the AP1000 FA testing used the maximum debris amounts. The maximum amounts of debris in the tests varied slightly since this testing was used to establish some of the debris limits, especially for the amount of fiber.

Ultimately, a plant design limit of [

] ^{a,c}

For a hot-leg break scenario, it was assumed that [

] ^{a,c}

The maximum limits for particles and chemicals were developed from the AP1000 design characteristics and not from the FA tests. It was assumed that [

] ^{a,c}

The plant design limit for particulate is [

] ^{a,c} All of this particulate was assumed to

transport into the RCS. [

] ^{a,c} of particles used in CIBAP22 through CIBAP26 FA tests. [

] ^{a,c} Several lower particulate to fiber loading ratios

were tested to determine the most limiting ratio for AP1000 FA testing. Test CIBAP27 was performed with a basis of [

] ^{a,c} Test CIBAP28 was performed with a basis of [

] ^{a,c} The [] ^{a,c} particulate to fiber ratio proved to be most

limiting and was used through the rest of the tests. Tests CIBAP29 through CIBAP34, CIBAP36, CIBAP37, and CIBAP39 were all performed with this most limiting particulate to fiber ratio, using [

] ^{a,c}

The maximum chemical production calculated for 30 days following a LOCA is [] ^{a,c}

(Reference 5). All of this chemical is assumed to transport into the RCS. When scaled, this results in a maximum of [

] ^{a,c} ALOOH used in the FA tests.

In addition to assuming the maximum amounts of particle, fiber, and chemical debris, consideration was also given to lesser amounts of debris since less than 100% transport could occur in the plant.

Less fiber was not tested because increasing amounts of fiber have always resulted in higher head-losses in AP1000 FA testing. In addition, the [

] ^{a,c}

Less chemical was also not tested because every test run [

] ^{a,c}

9.1.4 Flow Variations

In the AP1000 plant, the flow rates tend not to be constant following a LOCA because the flows are driven by a natural circulation process. As a result, as debris accumulates in the core region and the head-loss increases, the core flow will slow down. The debris accumulation takes many hours because of the large containment water volume and low passive safety system flow rates.

In addition, at any point in time, the flow also oscillates for a period of several minutes and with a minimum flow rate of about []^{a,c}. This oscillation is seen in the LTCC analysis and simulated in select AP1000 FA head-loss tests as discussed below.

Several FA head-loss tests were conducted where the flow rate was oscillated throughout the test. This included tests CIBAP08 through CIBAP11. The best comparison of these tests with non-oscillating tests is between test CIBAP08 and CIBAP06. These tests were identical except that test CIBAP06 used a constant flow rate of []^{a,c} and test CIBAP08 used an oscillating flow rate between []^{a,c}.

Another difference between these tests is that in test CIBAP08 the initial chemical addition was less []^{a,c}. This is not a significant difference since both tests had an initial head-loss peak that later decreased. In addition, test CIBAP08 had a lower peak head-loss []^{a,c}.

The conclusion is that the oscillating flow characteristic of AP1000 seems to reduce the head-losses. It is thought that the oscillating flow benefits the head-losses because the variation in flow and head-loss tends to increase the tendency to form bed breakthroughs or "bore holes." The effect of such breakthroughs is commonly seen as sudden decreases in head-loss during a test. Using oscillating flows during the AP1000 tests was discontinued because of the complexity of running the tests and for concerns about wear on the flow control valve.

Later AP1000 tests have been conducted using varying flow rates where the flow was initially high and then was decreased during the test as the head-loss built up. This process simulates the natural circulation interaction with the debris head-loss. Several different initial flows that represent different break sizes/locations have been tested. The final flow was based on the LTCC analysis with the maximum head-loss. Except for tests CIBAP29 and CIBAP30, this minimum flow was designed to be []^{a,c}. The latest LTCC analysis has shown that the minimum flow can be even []^{a,c} and was used for CIBAP31 through CIBAP34, CIBAP36 and CIBAP37. The actual minimum flow used during these tests was dependent on the actual head-loss seen in the test. For some tests the head-loss was relatively low and as a result the flow was not reduced to the minimum just as would happen in the plant.

Tests CIBAP15 and CIBAP16 provide a baseline for an evaluation of flow conditions since they were conducted at similar debris loads, but at constant flows. Test CIBAP15 was run at a constant []^{a,c}. Test CIBAP18 started at []^{a,c} but since its head-loss was very low, the flow was only reduced to []^{a,c}. The maximum head-loss of CIBAP18 was much less than either of these two constant flow tests. However, some of the other varying flow tests resulted in higher head-losses. It has not been concluded whether varying the flow increases or decreases the head-loss. All of the subsequent AP1000 FA tests have been conducted with varying flows since that is how the plant will operate. The initial flow has been set at []^{a,c} since that flow seems to result in higher head-losses than other initial flows. []^{a,c}

(comparing tests CIBAP20 and CIBAP23) for sequence debris addition. However, for

concurrent debris addition (comparing tests CIBAP22 and CIBAP24), [
] ^{a,c} but the initial head-loss trend was more severe.

Tests CIBAP35, CIBAP38 and CIBAP39 evaluated hot-leg flow conditions. Tests CIBAP35 and CIBAP38 were conducted using varying flow rates where the flow was initially high [
] ^{a,c} Once test CIBAP35 reached [
] ^{a,c} Test CIBAP38 began at [
]

down-flow rates of [
] ^{a,c} Overall, the hot-leg flow tests with
flow tests with upward flow of [
] ^{a,c} (simulating boiling) did not have a impact on head-loss.] ^{a,c} The hot-leg

9.1.5 Debris Addition Sequence

The initial AP1000 FA debris tests (CIBAP01 through CIBAP21) were conducted using sequential debris addition; all the particles were added, then all the fiber, and finally all of the chemicals. It was determined that it could not be shown that the AP1000 would operate this way and it could not be shown that this debris addition sequence would result in bounding head-loss. As a result it was decided to repeat one of the sequential tests using a concurrent debris addition method where the particles, fibers and chemicals were added at the same time in multiple batches.

The rate of debris additions [
]

] ^{a,c} is considered the minimum time since it
assumes all of the particles and fibers are transported into the RCS in the time it takes to pass
one containment water volume through the RCS and the core is assumed to trap 100% of this debris (none
of the particles or fibers leaks/passes through the fuel).

Test CIBAP22 was the first concurrent addition test and was a repeat of test CIBAP20 which was a sequential test. Between these tests, the concurrent test had a head-loss that was [
] ^{a,c} As a result, additional concurrent tests were performed. These tests included:

- Thin bed effect – The particles and fibers were introduced in [
] ^{a,c} more batches. Even with this gradual addition of debris, there was no indication of a thin bed effect.
- Testing different initial flow rates [
] ^{a,c} As discussed in Section 9.1.4, the flow rates in the concurrent debris addition tests were initiated at a higher flow rate and the flow was decreased as the dP increased. The final flow was determined by how much the dP increased. Both [
] ^{a,c} were used as the initial flow rate. [
] ^{a,c} but had a more rapid initial dP increase rate so it was considered bounding (or at least comparable).
- Adding the particles/fibers at a slower rate (CIBAP25). [
] ^{a,c}

- Adding the chemicals at a 67% slower rate (CIBAP26). []^{a,c}
- Adding fewer particles. []^{a,c}
- Repeat tests. The most limiting test observed (CIBAP27) was repeated five times. Test CIBAP27 used []^{a,c}

] ^{a,c} than test CIBAP27. []

] ^{a,c} Therefore, even though there was significant variation between these repeat tests, none of them had a higher dP than the original test and all had considerable margin to the current acceptance limits.

9.1.6 Coolant Chemistry and Temperature

Tests before CIBAP36 were all conducted with a target temperature of []^{a,c} These conditions are not representative of what would be expected for a LOCA in an AP1000. The coolant would contain a mixture of []^{a,c} Pure water and a low test temperature were used in testing because these conditions were thought to be []^{a,c} To confirm this, tests CIBAP36 and CIBAP37 were performed with []^{a,c} CIBAP37 was a repeat of CIBAP36.

The following factors were considered in developing tests CIBAP36 and CIBAP37:

Boric acid in the passive core cooling system water would come from two sources. Some of the boric acid would originate in the RCS coolant, where boric acid is added for a reactivity shim. Additional boric acid is added after the LOCA to ensure that the core remains non-critical using the core make-up tanks, the accumulators, and the IRWST. []

] ^{a,c}

[]

] ^{a,c}

Temperatures in the core will remain near 212°F for many days during the LTCC period. However, the test loop materials of construction could be operated safely only to []^{a,c} so this value was selected as the test temperature.

Tests CIBAP36 and CIBAP37 had []^{a,c} The average maximum pressure drop for the elevated temperature tests was []^{a,c} which compares to an average maximum pressure drop of []^{a,c} for room temperature tests CIBAP27, CIBAP29, CIBAP30, CIBAP31, CIBAP32, CIBAP33 and CIBAP34. The average maximum dP was reduced by a factor of []^{a,c} The maximum pressure drop data is plotted in Figure 9-4.



Figure 9-4 Comparison of Tests at []^{a,c} with Boric Acid and TSP to Room Temperature Water Tests

There were multiple factors for the reduced pressure drop in tests CIBAP36 and CIBAP37. One major factor would be the change in viscosity of the coolant between []^{a,c} For flow through a porous medium, the pressure drop should be proportional to the viscosity of the fluid according to Darcy's Law (Eq. 9-1.)

$$Q = \frac{\kappa \cdot A \cdot \Delta P}{\mu \cdot L} \quad (\text{Eq. 9-1})$$

Where

- Q = volumetric flow rate (ft³/s)
- κ = permeability (ft²)
- A = area (ft²)
- μ = dynamic viscosity (lbf-s/in²)
- L = length of porous bed (ft)
- ΔP = dP drop across bed (psid)

Since the flow was experimentally determined to vary as approximately the velocity to the a,c there was clearly an inertial component to the flow, and the pressure drop would be less influenced by the drop in viscosity with increasing temperature.

The viscosity of water decreases by a factor of a,c Exact data is not available for a boric acid/ TSP solution of the concentration tested here, but data obtained for a 2466 ppm boric acid/ 1% TSP solution showed that the viscosity compared to water increased by 8%. Thus, the a,c

Additional decreases in the head-loss may have been due to specific chemical interactions with the fiber. Trisodium phosphate is a known powerful alkaline cleaning agent, and it may have altered the surface properties of the fiber making it more slippery and less likely to form a blockage. This scenario is supported by the observation that a,c in both CIBAP36 and CIBAP37. a,c

a,c

9.1.7 Effect of Debris Addition with Different Break Scenarios (Hot-Leg vs. Cold-Leg)

In the AP1000, debris can transport into the RCS through the flooded hot-leg and possibly into the upper parts of the core. In an actual hot-leg LOCA in an AP1000, the flow in the upper part of the core is expected to oscillate over several minutes. When the down-flow in a low-power assembly becomes low, the steam generation rises. The tests prior to CIBAP35 were all conducted simulating a cold-leg break scenario and without simulating boiling. However, in response to an NRC RAI, hot-leg break scenarios were conducted to prove that cold-leg break tests are more limiting even if debris entering the top of the core would occur in a hot-leg break. These conditions were to be tested for an expected hot-leg break LOCA in an AP1000.

In the event of a double-ended guillotine hot-leg break, Westinghouse assumes the post-LOCA containment debris load would be equal to 200 pounds, consisting of 6.6 pounds of fiber, 193.4 pounds of particulates and 57 pounds of chemical precipitates. Westinghouse assumes that all the debris is transported into the core through the outer ring. As shown in a,c

The following factors were considered in developing tests CIBAP38 and CIBAP39.

- CIBAP38: The purpose of this test was to investigate the debris behavior in the outer FAs where flow could be downward and transport debris into the upper part of these FAs. The test also investigated the impact of changing the direction of flow from the downward to the upward direction representing steam with boiling present in the upward direction.
- CIBAP39: The purpose of this test was to investigate the debris behavior in central FAs that will be exposed to constant upward flow of water and steam.

CIBAP38 was conducted to represent the down-flow in a low-power assembly that produces steam and results in a change in flow from the downward to upward direction. This flow reversal and its effect on a debris bed were explored in test CIBAP38. [

] ^{a,c}

Test CIBAP39 was conducted solely to represent the hot-leg break condition representing the steam in the upward flow direction and the local boiling phenomenon affecting the behavior of the debris plugging the core. The air was injected at the same rate in test CIBAP38, [

] ^{a,c}

Tests CIBAP38 and CIBAP39 had very low pressure drops, [

] ^{a,c}

[

] ^{a,c}



Figure 9-5 AP1000 FA Schematic

9.2 APPLICABILITY OF TESTING TO AP1000 DESIGN

The experiments performed for the 'Evaluation of Debris Loading Head-loss Tests for AP1000 Fuel Assemblies During Loss of Coolant Accidents' used an FA design that for the purposes of this testing is consistent with the FA design described in subsection 4.2.2.2 of the AP1000 DCD (Reference 2). The specific AP1000 bottom nozzle design was used to ensure that the actual geometry of this component was included in the AP1000 test. The other components, [

] ^{a,c}

The fibrous and particulate debris types and chemical effects used in the AP1000 FA head-loss experiments have been identified as those that would be expected in an operating AP1000. The flow rates (Section 7) and debris loads (Section 6) [

] ^{a,c} as proposed for the AP1000. Based on the discussion provided in the noted sections, the flow rates and scaled debris loads and flow rates used in the experiments are applicable to the AP1000.

The fibrous, particulate, and chemical effects debris used in the experiments were prepared per procedure as discussed in Sections 6.1, 6.2, and 6.3 using the noted preparation procedures. The fibrous, particulate, and chemical effects debris used in the experiments are applicable to the AP1000.

The experiments were performed with representative debris and chemical precipitates at flows that bound the flows expected in the post-LOCA AP1000. As can be observed from the experimental data, including graphs and photographs, the amount of debris that can be transported to the AP1000 fuel assemblies is minimal and is not sufficient to form a debris bed capable of reducing flow into the core to less than the minimum shown to provide adequate core cooling. This was shown to be true for the licensing basis debris and chemical effects load. The resulting head-loss in all experiments is considered to be insufficient to preclude the reasonable assurance of LTCC for the AP1000.

Experiments were performed with prototypical solution chemistry (boric acid and TSP) and at an elevated temperature. Before these experiments were performed, all tests used pure water and a low test temperature because these conditions were thought to be conservative relative to the actual reactor conditions. The experiments performed with the reactor coolant chemicals (boric acid and TSP) at the elevated temperature collected less debris resulting in a lower dP. These sensitivity tests proved that the pure water and low temperature tests that were run throughout the test program are most limiting.

Experiments were performed with down-flow and up-flow with simulated boiling for a flooded hot-leg break. These tests proved that the cold-leg tests are more limiting than the hot-leg tests. The debris entering the core inlet and forming a bed at the bottom nozzle for a cold-leg break without simulated boiling proved to have a greater dP compared to both the up-flow and down-flow simulating the hot-leg break.

Considering the test apparatus, the debris loads, the flow rates, and the preparation of materials, the resulting data from this test program is directly applicable to the AP1000 design.

10 SUMMARY

Thirty-nine FA head-loss experiments were conducted for the AP1000 design as part of the response to GSI-191, "Assessment of Debris Accumulation on PWR Sump Performance." These FA head-loss experiments were performed for the AP1000 to quantify the head-loss across the FAs considering fibrous and particulate debris and containment chemical effects applicable to the AP1000.

The experiments performed used an FA design that, for the purposes of the testing, is consistent with the FA design described in subsection 4.2.2.2 of the AP1000 DCD (Reference 2). The flow rates and fibrous and particulate debris loading conditions were selected conservatively so that they bound those expected following a postulated LOCA for the AP1000. The FA, debris loads, and flow rates are directly applicable to the AP1000 as described in Section 4.0 of this report.

The thirty-nine FA head-loss experiments that were performed for the AP1000 design investigated a spectrum of fibrous and particulate debris loads and chemical effects. The results from thirty-five¹ of these experiments demonstrate the ability of the AP1000 to provide reasonable assurance of LTCC under the fibrous and particulate debris loading and chemical effects conditions expected for the AP1000 following a postulated LOCA.

The AP1000 design [

]^{a,c} and,

requires good house keeping practices. The AP1000 design is engineered to reduce the potential for head-loss during long-term cooling operation. These experiments show that the design basis AP1000 fibrous and particulate debris, and chemical effects, (that is, the maximum amount of debris that could exist) does not induce a head-loss through the FA that would reduce flow into the core to less than the minimum shown to provide adequate LTCC and the maintaining of a coolable core geometry following a LOCA.

1. Tests 7, 12, 17 and 35 were invalidated. See Section 8.40

11 REFERENCES

1. Generic Safety Issue, GSI-191, "Assessment of Debris Accumulation on PWR Sump Performance," 1998.
2. APP-GW-GL-700, Revision 17, "AP1000 Design Control Document," 2008.
3. APP-PXS-GLR-001, Revision 4, "Impact on AP1000 Post-LOCA Long-Term Cooling of Postulated Containment Sump Debris," February 2010.
4. NEI 04-07 PRESSURIZED WATER REACTOR SUMP PERFORMANCE EVALUATION METHODOLOGY Revision 0 December 2004 Volume 2 – Safety Evaluation by the Office of Nuclear Reactor Regulation Related to NRC Generic Letter 2004-02, Revision 0, December 2004.
5. APP-GW-GLR-079, Revision 7, "AP1000 Verification of Water Sources for Long-Term Recirculation Cooling Following a LOCA," February 2010.
6. Letter from H. K. Nieh (NRC) to G. Bischoff (PWROG), "Final Safety Evaluation for Pressurized Water Reactor Owners Group (PWROG) Topical Report (TR) WCAP-16530-NP, 'Evaluation of Post-Accident Chemical Effects in Containment Sump Fluids to Support GSI-191,' (TAC No. MD1119)," December 2007.
7. STD-MCE-09-8, Revision 0, "Summary of the Results from the AP1000 Core Inlet Blockage Tests," February 2009.
8. STD-MCE-09-47, Revision 0, "Summary of the Results from the AP1000 Core Inlet Blockage Tests: CIBAP05 to CIBAP14," June 2009.
9. APP-FA01-T1P-001, Revision 1, "Test Plan For AP1000 Debris Loading Head-loss Across FA," June 2009.
10. Revised Guidance for Review of Final Licensee Responses to Generic Letter 2004-02, "Potential Impact of Debris Blockage on Emergency Recirculation During Design Basis Accidents at Pressurized Water Reactors," March 2008. [ML080230234]
11. WCAP-16530-NP-A, "Evaluation of Post-Accident Chemical Effects in Containment Sump Fluids to Support GSI-191," March 2008.
12. NUREG/CR-6877, "Characterization and Head-Loss Testing of Latent Debris from Pressurized-Water-Reactor Containment Buildings," July 2005.
13. STD-MCE-09-74, Revision 0, "Summary of the Results from the AP1000 Core Inlet Blockage Tests: CIBAP15 and CIBAP16," July 2009.

14. STD-MCE-09-139, Revision 0, "Summary of the Results from the AP1000 Core Inlet Blockage Tests: CIBAP17 Through CIBAP30," November 2009.
15. STD-MCE-10-19, Revision 0, "Summary of the Results from the AP1000 Core Inlet Blockage Tests: CIBAP31 Through CIBAP39," February 2010.
16. XX1 CRC Handbook of Chemistry and Physics, 55th Edition, Robert Weast, Ed. (CRC Press, Cleveland, Ohio) 1974, p F-49.
17. G. Zigler, J. Brideau, D. V. Rao, C. Shaffer, F. Souto, W. Thomas, NUREG/CR-6224, "Parametric Study of the Potential for BWR ECCS Strainer Blockage Due to LOCA Generated Debris" Final Report, October 1995
18. Appendix VII, "Characterization of Pressurized-Water-Reactor Latent Debris", part of GSI-191 SE, Revision 0 "Safety Evaluation of NEI Guidance on PWR Sump Performance", Nuclear Regulatory Commission (<http://www.nrc.gov/reactors/operating/ops-experience/pwr-sump-performance/reg-guidance-files/ml043280017-appvii.pdf>)
19. APP-GW-GLR-092, Rev. 0, "Statistical Evaluation of AP1000 Fuel Assembly Debris-Loading Head-Loss Tests," February 2009.
20. Excel File: Air Flow Rate Calculation. February 2010. (Note: This document is electronically attached to this calculation note as void_fraction_quality.xls_634129099781359963_WCAP-17028-NP)
21. APP-FA01-T2C-001, "Support Documentation for the AP1000 Fuel Assembly Test Analysis," June 2010.

APPENDIX A
APP-FA01-T1P-001 REVISION 0: TEST PLAN FOR AP1000 DEBRIS
LOADING HEAD-LOSS ACROSS FUEL ASSEMBLY

This Appendix is proprietary in its entirety.

a,c

a,c

a,c

a,c

a,c

a,c

a,c

a,c

a,c

a,c

a,c

a,c

a,c

a,c

a,c

a,c

a,c

a,c

a,c

APPENDIX B
APP-FA01-T1P-001 REVISION 1: TEST PLAN FOR AP1000 DEBRIS
LOADING HEAD-LOSS ACROSS FUEL ASSEMBLY

a,c

a,c

a,c

a,c

a,c

a,c

a,c

a,c

a,c

a,c

a,c

a,c

a,c

a,c

a,c

a,c

a,c

Appendix C
TEST PROCEDURES FOR AP1000 DEBRIS
LOADING HEAD LOSS ACROSS FUEL ASSEMBLY

C.1 TEST PLAN FOR LOOP TEST CIBAP01

STD-MCE-08-79

a,c

a,c

a,c

a,c

a,c

a,c

a,c

a,c

a,c

a,c

a,c

a,c

a,c

a,c

a,c

a,c

C.2 TEST PLAN FOR LOOP TEST CIBAP02

STD-MCE-08-80

a,c

a,c

a,c

a,c

a,c

a,c

a,c

a,c

a,c

a,c

a,c

a,c

a,c

a,c

a,c

a,c

a,c

C.3 TEST PLAN FOR LOOP TEST CIBAP03

STD-MCE-08-81

a,c

a,c

a,c

a,c

a,c

a,c

a,c

a,c

a,c

a,c

a,c

a,c

a,c

a,c

a,c

a,c

a,c

a,c

C.4 TEST PLAN FOR LOOP TEST CIBAP04

STD-MCE-08-82

a,c

a,c

a,c

a,c

a,c

a,c

a,c

a,c

a,c

a,c

a,c

a,c

a,c

a,c

a,c

a,c

a,c

C.5 TEST PLAN FOR LOOP TEST CIBAP05

STD-MCE-08-85

a,c

a,c

a,c

a,c

a,c

a,c

a,c

a,c

a,c

a,c

a,c

a,c

a,c

a,c

a,c

C.6 TEST PLAN FOR LOOP TEST CIBAP06

STD-MCE-09-18

a,c

a,c

a,c

a,c

a,c

a,c

a,c

a,c

a,c

a,c

a,c

a,c

a,c

a,c

a,c

a,c

C.7 TEST PLAN FOR LOOP TEST CIBAP08

STD-MCE-09-28

a,c

a,c

a,c

a,c

a,c

a,c

a,c

a,c

a,c

a,c

a,c

a,c

a,c

a,c

a,c

a,c

C.8 TEST PLAN FOR LOOP TEST CIBAP09

STD-MCE-09-34

a,c

a,c

a,c

a,c

a,c

a,c

a,c

a,c

a,c

a,c

a,c

a,c

a,c

a,c

a,c

a,c

C.9 TEST PLAN FOR LOOP TEST CIBAP10

STD-MCE-09-35 Revision 1

a,c

a,c

a,c

a,c

a,c

a,c

a,c

a,c

a,c

a,c

a,c

a,c

a,c

a,c

a,c

a,c

a,c

C.10 TEST PLAN FOR LOOP TEST CIBAP11

STD-MCE-09-39

a,c

a,c

a,c

a,c

a,c

a,c

a,c

a,c

a,c

a,c

a,c

a,c

a,c

a,c

a,c

a,c

C.11 TEST PLAN FOR LOOP TEST CIBAP13

STD-MCE-09-42

a,c

a,c

a,c

a,c

a,c

a,c

a,c

a,c

a,c

a,c

a,c

a,c

a,c

a,c

a,c

a,c

a,c

C.12 TEST PLAN FOR LOOP TEST CIBAP14

STD-MCE-09-45

a,c

a,c

a,c

a,c

a,c

a,c

a,c

a,c

a,c

a,c

a,c

a,c

a,c

a,c

a,c

a,c

C.13 TEST PLAN FOR LOOP TEST CIBAP15

STD-MCE-09-61

a,c

a,c

a,c

a,c

a,c

a,c

a,c

a,c

a,c

a,c

a,c

a,c

a,c

a,c

a,c

a,c

a,c

a,c

C.14 TEST PLAN FOR LOOP TEST CIBAP16

STD-MCE-09-71

a,c

a,c

a,c

a,c

a,c

a,c

a,c

a,c

a,c

a,c

a,c

a,c

a,c

a,c

a,c

a,c

a,c

a,c

C.15 TEST PLAN FOR LOOP TEST CIBAP17

STD-MCE-09-101

a,c

a,c

a,c

a,c

a,c

a,c

a,c

a,c

a,c

a,c

a,c

a,c

a,c

a,c

a,c

a,c

a,c

a,c

a,c

a,c

a,c

a,c

C.16 TEST PLAN FOR LOOP TEST CIBAP18

STD-MCE-09-102

a,c

a,c

a,c

a,c

a,c

a,c

a,c

a,c

a,c

a,c

a,c

a,c

a,c

a,c

a,c

a,c

a,c

a,c

a,c

a,c

a,c

C.17 TEST PLAN FOR LOOP TEST CIBAP19

STD-MCE-09-103

a,c

a,c

a,c

a,c

a,c

a,c

a,c

a,c

a,c

a,c

a,c

a,c

a,c

a,c

a,c

a,c

a,c

a,c

a,c

a,c

a,c

a,c

C.18 TEST PLAN FOR LOOP TEST CIBAP20

STD-MCE-09-107

a,c

a,c

a,c

a,c

a,c

a,c

a,c

a,c

a,c

a,c

a,c

a,c

a,c

a,c

a,c

a,c

a,c

a,c

a,c

a,c

a,c

a,c

C.19 TEST PLAN FOR LOOP TEST CIBAP21

STD-MCE-09-108

a,c

a,c

a,c

a,c

a,c

a,c

a,c

a,c

a,c

a,c

a,c

a,c

a,c

a,c

a,c

a,c

a,c

a,c

a,c

a,c

a,c

a,c

C.20 TEST PLAN FOR LOOP TEST CIBAP22

STD-MCE-09-109

a,c

a,c

a,c

a,c

a,c

a,c

a,c

a,c

a,c

a,c

a,c

a,c

a,c

a,c

a,c

a,c

a,c

a,c

a,c

a,c

a,c

a,c

a,c

C.21 TEST PLAN FOR LOOP TEST CIBAP23

STD-MCE-09-113

a,c

a,c

a,c

a,c

a,c

a,c

a,c

a,c

a,c

a,c

a,c

a,c

a,c

a,c

a,c

a,c

a,c

a,c

a,c

a,c

C.22 TEST PLAN FOR LOOP TEST CIBAP24

STD-MCE-09-115

a,c

a,c

a,c

a,c

a,c

a,c

a,c

a,c

a,c

a,c

a,c

a,c

a,c

a,c

a,c

a,c

a,c

a,c

a,c

a,c

a,c

C.23 TEST PLAN FOR LOOP TEST CIBAP25

STD-MCE-09-116 Revision 1

a,c

a,c

a,c

a,c

a,c

a,c

a,c

a,c

a,c

a,c

a,c

a,c

a,c

a,c

a,c

a,c

a,c

a,c

a,c

a,c

a,c

a,c

C.24 TEST PLAN FOR LOOP TEST CIBAP26

STD-MCE-09-123

a,c

a,c

a,c

a,c

a,c

a,c

a,c

a,c

a,c

a,c

a,c

a,c

a,c

a,c

a,c

a,c

a,c

a,c

a,c

a,c

a,c

a,c

a,c

C.25 TEST PLAN FOR LOOP TEST CIBAP27

STD-MCE-09-125

a,c

a,c

a,c

a,c

a,c

a,c

a,c

a,c

a,c

a,c

a,c

a,c

a,c

a,c

a,c

a,c

a,c

a,c

a,c

a,c

a,c

a,c

a,c

C.26 TEST PLAN FOR LOOP TEST CIBAP28

STD-MCE-09-132

a,c

a,c

a,c

a,c

a,c

a,c

a,c

a,c

a,c

a,c

a,c

a,c

a,c

a,c

a,c

a,c

a,c

a,c

a,c

a,c

a,c

a,c

a,c

a,c

C.27 TEST PLAN FOR LOOP TEST CIBAP29

STD-MCE-09-133 Revision

a,c

a,c

a,c

a,c

a,c

a,c

a,c

a,c

a,c

a,c

a,c

a,c

a,c

a,c

a,c

a,c

a,c

a,c

a₂c

a,c

a,c

a,c

C.28 TEST PLAN FOR LOOP TEST CIBAP30

STD-MCE-09-135

a,c

a,c

a,c

a,c

a,c

a,c

a,c

a,c

a,c

a,c

a,c

a,c

a,c

a,c

a,c

a,c

a,c

a,c

a,c

a,c

a,c

a,c

C.29 TEST PLAN FOR LOOP TEST CIBAP31

STD-MCE-10-02

a,c

a,c

a,c

a,c

a,c

a,c

a,c

a,c

a,c

a,c

a,c

a,c

a,c

a,c

a,c

a,c

a,c

a,c

a,c

a,c

a,c

a,c

a,c

C.30 TEST PLAN FOR LOOP TEST CIBAP32

STD-MCE-10-03

a,c

a,c

a,c

a,c

a,c

a,c

a,c

a,c

a,c

a,c

a,c

a,c

a,c

a,c

a,c

a,c

a,c

a,c

a,c

a,c

a,c

a,c

a,c

C.31 TEST PLAN FOR LOOP TEST CIBAP33

STD-MCE-10-04

a,c

a,c

a,c

a,c

a,c

a,c

a,c

a,c

a,c

a,c

a,c

a,c

a,c

a,c

a,c

a,c

a,c

a,c

a,c

a,c

a,c

a,c

a,c

C.32 TEST PLAN FOR LOOP TEST CIBAP34

STD-MCE-10-05

a,c

a,c

a,c

a,c

a,c

a,c

a,c

a,c

a,c

a,c

a,c

a,c

a,c

a,c

a,c

a,c

a,c

a,c

a,c

a,c

a,c

a,c

a,c

C.33 TEST PLAN FOR LOOP TEST CIBAP35

STD-MCE-10-07

a,c

a,c

a,c

a,c

a,c

a,c

a,c

a,c

a,c

a,c

a,c

a,c

a,c

a,c

a,c

a,c

a,c

a,c

a,c

C.34 TEST PLAN FOR LOOP TEST CIBAP36

STD-MCE-10-10

a,c

a,c

a,c

a,c

a,c

a,c

a,c

a,c

a,c

a,c

a,c

a,c

a,c

a,c

a,c

a,c

a,c

a,c

a,c

a,c

a,c

a,c

a,c

C.35 TEST PLAN FOR LOOP TEST CIBAP37

STD-MCE-10-11

a,c

a,c

a,c

a,c

a,c

a,c

a,c

a,c

a,c

a,c

a,c

a,c

a,c

a,c

a,c

a,c

a,c

a,c

a,c

a,c

a,c

a,c

a,c

C.36 TEST PLAN FOR LOOP TEST CIBAP38

STD-MCE-10-13 Revision 1

a,c

a,c

a,c

a,c

a,c

a,c

a,c

a,c

a,c

a,c

a,c

a,c

a,c

a,c

a,c

a,c

a,c

a,c

a,c

a,c

a,c

C.37 TEST PLAN FOR LOOP TEST CIBAP39

STD-MCE-10-15

a,c

a,c

a,c

a,c

a,c

a,c

a,c

a,c

a,c

a,c

a,c

a,c

a,c

a,c

a,c

a,c

a,c

a,c

a,c

APPENDIX D DEBRIS PREPARATION

This Appendix is proprietary in its entirety.

a,c

a,c

a,c

a,c

a,c

a,c

a,c

a,c

a,c

a,c

a,c

a,c

a,c

a,c

a,c

a,c

APPENDIX E TEST FACILITY OVERVIEW

This Appendix is proprietary in its entirety.

a,c

a,c

a,c

a,c

a,c

a,c